FINAL REPORT

June 2008

Investigating Riverbed Hydraulic Conductivity at Several Well Fields along the Great Miami River, Southwest Ohio

Submitted to the Hamilton to New Baltimore Groundwater Consortium, the Miami Conservancy District and the Ohio Water Development Authority

by Dr. Jonathan Levy, Alicja Wojnar and Samuel Mutiti

Table of Contents

Table of Figures

Table of Tables

I. INTRODUCTION

Groundwater and surface water were for a long time treated as separate systems and managed independently. In recent years however, there has been greater understanding that these two systems are interconnected and interact with each one another (Winter et al., 1998).

Knowledge regarding the degree of hydraulic connection between an aquifer and adjacent surface-water bodies is essential due to the increasing demand for clean drinking-water supplies. Drinking-water production wells are frequently placed in close proximity to rivers. Such placement often reverses the natural gaining conditions of the river, inducing surface water to be drawn towards the production well (Hiscock and Grischek, 2002). This induced infiltration increases a well's production capacity but can also potentially increase transport of contaminants, particularly microbial pathogens, from the river to the groundwater system. The rate and direction of movement of water through the porous riverbed is controlled by the vertical hydraulic conductivity (K_v) of the riverbed, the geometry and thickness of the riverbed and the hydraulic gradient between the river and the aquifer (Woessner, 2000; Schubert, 2002; Kalbus et al., 2006; Ryan and Boufadel, 2006). A high riverbed K_v, thin riverbed and a strong downward gradient will all contribute to intensive infiltration of the water from the river into the underlying aquifer.

Given the role of riverbed K_v in controlling the interaction of groundwater and surface water, information about its magnitude, variability and spatial distribution is critical for groundwater managers in addressing questions of both water quality and supply. Determination of riverbed K_v is important when simulating groundwater flow for such uses as accurately delineating source-water protection zones for production wells and predicting groundwater paths and travel times to those wells.

The riverbed K_v is difficult to quantify because it can be hard to directly measure in a fluvial system and because of its high spatial and temporal variability. The spatial variability of the riverbed K_v is dependent on the distribution and degree of heterogeneity of the riverbed sediments. The riverbed K_v can be highly variable both vertically and over relatively small areas in a particular reach of a river (Duwelius, 1996; Calver, 2001; Landon et al., 2001; Chen et al., 2008).

The riverbed K_v can also vary temporally. Such changes are influenced by sediment transport and deposition and scouring of the riverbed (Hiscock and Grischek, 2002; Velickovic, 2005). During periods of low flow, the river energy is low and suspended fine particles will tend to settle. They sometimes settle between coarser-grained riverbed sediment or on the top layer of the riverbed (Schälchli, 1992). Such deposition of fine particles and sometimes also organic matter can create a thin riverbed clogging layer with low K_v (Velickovic, 2005). On the other hand, during period of high flow, particularity during flood events, fine particles may be re-suspended and scour can occur. Erosion of the clogging layer tends to increases the riverbed K_v thereby enhancing infiltration of water from the river to the underlying aquifer (Doppler et al., 2007).

II. RESEARCH OBJECTIVIES

The Miami Conservancy District and the Hamilton to New Baltimore Ground Water Consortium are working in conjunction with local communities to develop source-area protection programs for well fields that are located in the close proximity to the Great Miami River in Butler and Hamilton counties in southwest Ohio. They therefore need to know more about the Great Miami River riverbed K_v. Appropriate K_v values for the Great Miami River

riverbed are largely unknown. The overall goal of this project was to investigate the riverbed K_v and its variability at four locations along the Great Miami River between Hamilton and New Baltimore, communities in southwest Ohio. We approached this project using several techniques at different measurement scales. Three major techniques were applied: seepage metering, slug testing and heat-transport modeling. Concurrently, the US Geological Survey in Columbus, Ohio conducted geophysical surveys of the riverbed using continuous seismic profiling, continuous resistivity profiling and continuous multi-frequency electromagnetic profiling. These surveys were conducted in areas encompassing three of our field sites and provided riverbed stratigraphic information. In the upcoming months, our results will be compared to the USGS results to test whether the stratigraphic information is helpful in predicting the riverbed K_v.

Specific research objectives of this study were to perform the following investigations at each of our four field sites:

1) Make direct point measurements of the riverbed K_v using different types of seepage meters, slug tests and laboratory permeameter analyses
2) Assess the performance of the different types of seepage meters in the various sediment types that were encountered
3) Estimate the riverbed K_v on an intermediate scale through modeling of the heat and water transport between the river and groundwater
4) Compare hydraulic conductivity values obtained using the various methods
5) Compare estimated K_v values to the riverbed stratigraphic data obtained from geophysical profiling conducted by the USGS, Columbus. In so doing, assess the usefulness of the geophysics in predicting K_v values. If successful, devise a scheme for translating the stratigraphic information into K_v values.

III. BACKGROUND: QUANTIFICATION OF RIVERBED K_V

A. Previous Field Studies

Previous studies have demonstrated the highly variable nature of riverbed K_v. Duwelius (1996) conducted in-situ permeameter and slug tests to measure K_v of the east Branch Grand Calumet River. Values ranged from 0.09 to 22.3 m/d within the river channel with the highest values occurring near the center of the river. Calver (2001) summarized 41 investigations on the hydraulic conductivities and concluded the riverbed K_v values can vary over four orders of magnitude, from 0.0086 to 86.4 m/d for the silt-clay and sandy sediments, respectively. Landon et al. (2001) intensively measured K_v in sandy streambeds at seven locations along the Platte River and its five tributaries, in Nevada, applying various measurements techniques – in-situ permeameters, slug tests, seepage meters and grain-size analyses. They found K_v to be highly variable across the stream channels, from site to site and with depth. The river deposits deeper than 0.3 had generally lower K_v values than the upper 0.3 m. Average values of the vertical hydraulic conductivity for the investigated sites ranged from 10 to 170 m/d. Their comparison of the K_v values obtained from different methods suggests that to obtain a good estimate of the spatial variability of K_v in the riverbed, an intensive measurement network rather than method matters. They also noted that seepage meters often fail in high-energy waters and that the permeameter tests are only good to measure this first 0.3 m of the riverbed. They found the slug tests to be the most practical in-stream methods. Finally, Chen (2004) used in-situ permeameters and measured K_v across transects in the Platte, Republican, and Little Blue Rivers, south-central Nebraska. Averages values of the K_v for this study ranged from 15 to 47 m/d for sand sediment and 1.6 m/d for the silty/clayey sediment in the top 0.4 m of the riverbeds.

B. Overview of Techniques

The riverbed K_v can be estimated in the laboratory and in the field and at many scales. Sediment samples can be taken to the laboratory for permeameter tests and grain-size analyses (Kalubus et al., 2006). Falling and constant permeameter tests can give a good approximation of the riverbed K_v only when it is possible to maintain the natural structure of the sediment sample. Grain-size analyses can also provide estimates of hydraulic conductivity in lieu of other information (Fetter, 2001). Measurements of the riverbed K_v in the field can be conducted with minimal disturbance of the natural sediment structure. Methods that are currently applied to quantify hydraulic conductivity of the riverbed are; in-situ falling head permeameter tests (Landon et al., 2001; Fox, 2003; Chen, 2000 and 2004), constant head injection tests (Cardenas and Zlotnik, 2003), slug tests (Landon et al., 2001; Rus et al., 2001), seepage meters (Lee, 1977; Rosenberry, 2005) and modeling of heat and flow transport (Constantz et al., 2003; Anderson, 2005).

C. In-situ Permeameters and Slug Tests

In-situ permeameter tests allow measurements of the vertical hydraulic conductivity over an area of typically 5 to 90 cm in diameter and to depths of about 0.4 m (Landon et al., 2001; Chen, 2004). For these tests, an open pipe is inserted into the riverbed and treated like a conventional permeameter. Water is poured into the top and the rate at which the water falls back to equilibrium (at or near river level) is recorded. Darcy's law is used to calculate the K_v. The advantage of this method is that it is not dependent on the natural gradient; tests can be conducted more quickly than with seepage meters.

As with in-situ permeameters, slug tests are conducted by instantaneously raising or lowering the water-level in a well and measuring the rate at which the water level returns to

equilibrium as water leaves or enters the well through the well screen. Because the water movement into or out of the riverbed is horizontal, slug tests yield values of the horizontal hydraulic conductivity at the depth of the screen over the screen length (typically 0.30 to 1.52 m). K_v values can then be estimated from K_h based on the assumed a K_v-to-K_h anisotropy ratio (Rus et al., 2001).

D. Seepage Meters

A direct measurement of the riverbed K_v is with the use of seepage meters (Israelson and Reeve, 1944; Lee, 1977), typically covering an area with a diameter of 0.30 to 0.58 m. Seepage meters have been widely applied in a variety of hydrologic environments to estimate groundwater seepage flux to lakes and estuaries (Lee and Cheery, 1978; Taniguchi and Fukuo, 1993; Boyle, 1994; Isiorho et al., 1996; Sebestyen and Schneider, 2001; Rosenberry, 2005), creeks (Dumouchelle, 2001; Kelly and Murdoch, 2003), marine environments (Cable et al., 1997a; Paulsen et al., 2001, Taniguchi et al., 2003, Stieglitz et al., 2007), streams (Cey et al., 1998; Alexander and Caissie, 2003) and rivers (Libelo and MacIntyre, 1994; Landon et al., 2001). A conventional seepage meter (Lee, 1977) consists of an open, cut-off bucket or steel drum with a barbed port at the top of bucket or drum (Figure 1). The seepage bucket is pressed into the riverbed and a bag is connected to it that has been pre-filled with a known volume of water. The bag floats in the river so that the hydraulic head inside the bag is the same as in the river. When the hydraulic head in the aquifer is higher than in the river, water will seep into the bucket and into the bag. When the hydraulic head is greater in the river than in the aquifer, water will seep out of the bag, into the bucket and through the riverbed. In either case, the volumetric flux across the river bed through the seepage meter can be calculated. Riverbed K_v is estimated according to Darcy's law by also measuring the hydraulic gradient across the riverbed. The

gradient is measured by installing mini-piezometers (Lee and Cherry, 1978) near the seepage meter.

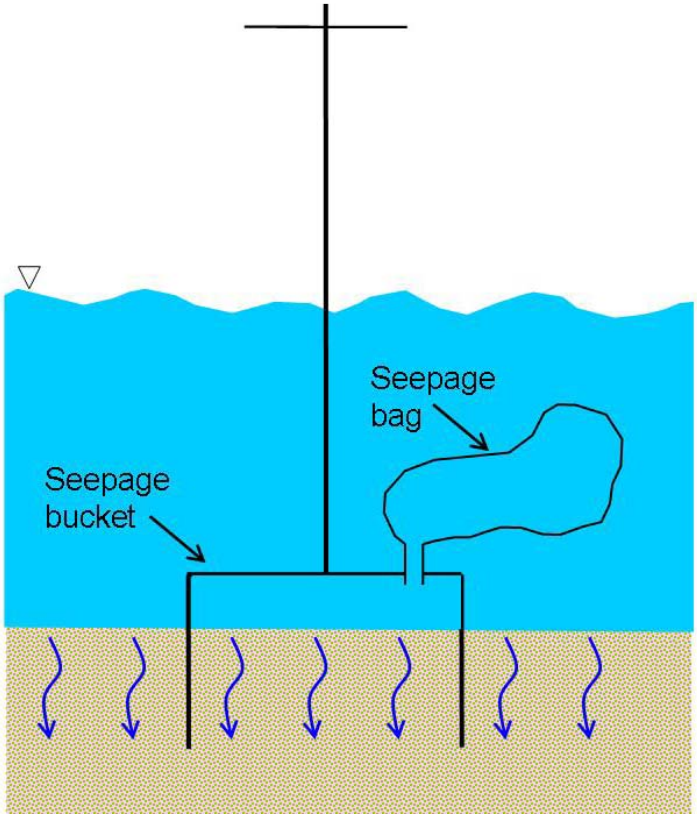

Figure 1. The Idaho seepage meter (after ANCID, 2004)

Various seepage-meter designs and techniques have been tested to ensure the effectiveness of the method and minimize potential measurement errors. Errors can arise from having an appropriate bag type, bag size or tubing diameter (Belanger and Montgomery, 1992; Isiorho and Meyer, 1999; Schincariol and McNeil, 2002). Potential measurement errors are associated with operational issues including: leakage around the seepage bucket caused by inappropriate seepage installation (Libelo and MacIntyre, 1994; Cey et al., 1998), anomalous seepage flux caused by the gas accumulation within the system (Shaw and Prepas, 1989; Sebestyen and Schneider,

2001), head loss and anomalous short-term influx into the empty bags (Shaw and Prepas, 1989, Cable et al 1997b) and unrepresentative inflow into the bag, even in areas of downward gradients caused by river current (Libelo and MacIntyre, 1994; Cable et al., 1997b; Murdoch and Kelly, 2003; Brodie et al., 2005).

The system of tubing and bag associated with seepage metering can lead to frictional losses of head, lessened flow and underestimation of hydraulic conductivity. Studies have been conducted in controlled conditions to determine the accuracy of seepage metering and suggest appropriate adjustments to seepage-meter values based on these issues. Belanger & Montgomery (1992) in comparing seepage-meter results from the field with those in a controlled environmental tank showed seepage meter-to-tank ratios between 0.55 and 0.77. Levy et al. (2007) similarly compared seepage-meter values to pre-determined values of K_v in a large sand tank using the same set of equipment as applied in this study. The seepage meter-to-tank ratio for this equipment was 0.47 suggesting that seepage-meter values should be corrected by multiplying by a factor of 2.1

Modifications to the conventional seepage meter have been developed to avoid many of the problems listed above. One such redesign is the "piezo-seep" (Kelly and Murdoch, 2003) which is not dependent on the natural gradient and does not require collecting water in a bag. The piezo-seep combines the mini-piezometer and seepage bucket into a single device (Figure 2). When the seepage meter is pressed into the riverbed, the piezometer extends below the riverbed. An upward seepage flux is artificially generated by pumping water at a constant rate out of the seepage bucket through an additional port. This creates a hydraulic gradient between the inside of the bucket and below the riverbed that is measured by comparing the hydraulic head in the bucket and the head inside the piezometer. These heads are compared by applying the same

suction to each to bring them both above river level. Riverbed K_v is then calculated according to Darcy's law.

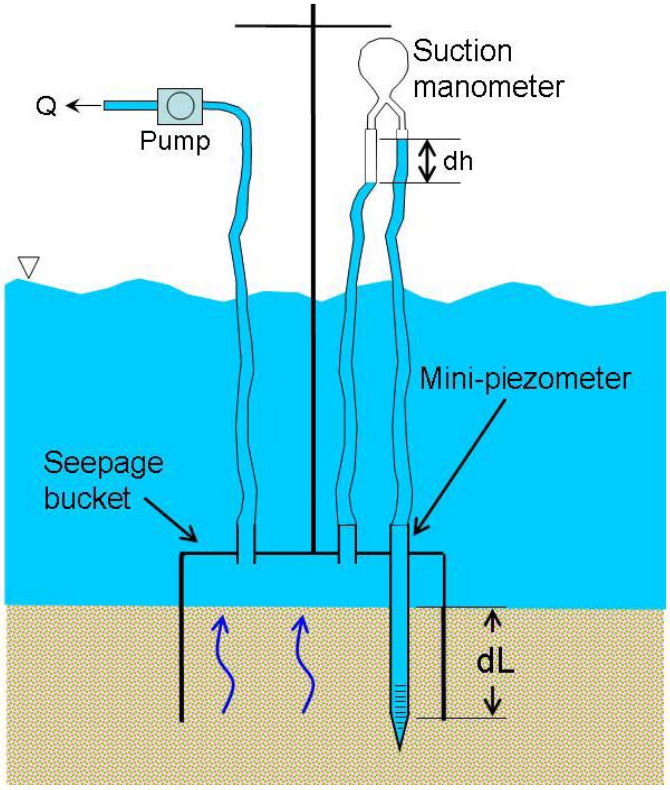

Figure 2. Piezo-seep meter (modified after Murdoch and Kelly, 2003)

Other seepage meters that do not include bags in their design include the dye-dilution meter (Sholkovitz et al., 2003), the ultrasonic seepage meter (Paulsen et al., 2001), and a seepage meter based on the heat-pulse system (Taniguchi and Fukuo, 1993; Krupa et al., 1998). They can automatically collect data over long periods and so are well suited for estimation of the temporal variability of the seepage flux.

E. Heat-flow modeling

Riverbed hydraulic conductivity can be estimated indirectly by simulating heat flow through the system. River temperature is influenced by air temperature, solar radiation, evaporation, snowmelt and precipitation, and undergoes much greater diurnal temperature fluctuation than does groundwater (Constantz et al., 1994, Ronan et al., 1998). The temperature within the riverbed is affected by the river temperature, the underlying groundwater temperature and the movement of water through the system. In gaining river reaches, where groundwater is discharging into a river, the riverbed temperature is heavily influenced by the relatively stable groundwater temperature and therefore fluctuations in the temperature beneath the river are much less than the fluctuations in the river (Figure 3A). In losing river reaches, where water moves from the river to the groundwater system, the riverbed temperature undergoes substantial fluctuations that lag behind and are attenuated compared to the fluctuations in the river (Figure 3B) (Lapham, 1989; Silliman et al., 1995; Constantz, 1998; Stonerstrom and Constantz, 2003).

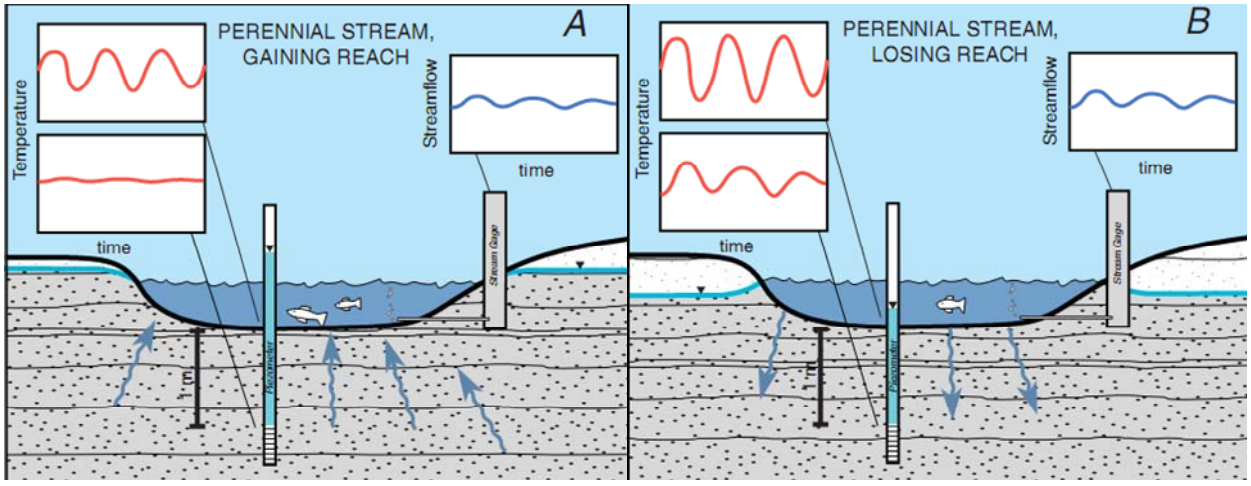

Figure 3. Stream flow and temperature patterns for gaining (*A*) and losing (*B*) stream (after Constantz and Stonerstrom, 2003)

Changes in temperature beneath the riverbed result from heat transport in subsurface which occurs due to the flow of water (advective heat flow), and by heat conduction through the solid and fluid phase (conductive heat flow) (Constantz and Stonestrom, 2003). Conduction is driven by the existing temperature gradient. Assuming one-dimensional flow and heat transport, the governing equation proposed by Stallman (1965) is:

$$K_t \frac{\partial^2 T}{\partial z^2} - qC_w \frac{\partial T}{\partial z} = C_S \frac{\partial T}{\partial t} \quad (1)$$

where:

z is depth below the river-riverbed interface [m],

t is time [s]

K_t is thermal conductivity of the bulk streambed sediments [W/m°C]

T is temperature [°C]

q is volumetric flux per unit area through the sediment [m/s]

C_W, C_S is volumetric heat capacity of water and sediment, respectively [J/m^3°C]

The heat transport theory has been widely applied in many hydrological settings to identify the direction and rate of the vertical flow between surface water and underlying aquifers (Lapham, 1989; Constantz et al., 1994; Silliman et al., 1995; Constantz, 1998; Bartolino and Niswonger; 1999, Constantz et al; 2002, Cox et al., 2002; Cox and Hatch; 2003, Dowman et al., 2003; Stonerstrom and Constantz, 2003; Becker et al., 2006;Hatch et al., 2006; Skinner, 2006; Cox et al., 2007; Keery et al., 2007; Schmidt et al., 2007) and estimate the riverbed K_v (Lapham, 1989; Constantz et al., 2003; Su et al., 2004; Niswonger et al., 2005). The riverbed K_v can be estimated through calibration of the heat transport model. During calibration, boundary conditions are specified and simulated temperatures at a chosen depth are simulated. Riverbed K_v values are adjusted until the simulated temperatures match the observed temperatures.

Computer programs to aid in this process and solve the heat-flow equation numerically include VS2DH (Healy and Ronan, 1996), SUTRA (Voss, 1984) and HYDROTHERM 3 (Kipp et al., 2008). Computer programs have also been developed that solve the heat-flow equation analytically (Lapham, 1989; Arriaga and Leap, 2006).

The USGS heat and flow transport computer program, VS2DH (Healy and Ronan, 1996; Hsieh et al., 2000) is widely used. It is a two-dimensional, finite-difference model that solves the form of the advection-dispersion equation that accounts for conductive, dispersive and advective heat transport through porous media (Healy and Ronan, 1996):

$$\frac{\partial[\theta C_w + (1-\Phi)C_s]T}{\partial t} = \nabla \times K_t(\theta)\nabla T + \nabla \times \theta C_w D_h \nabla T - \nabla \theta C_w v T + q C_w T^* \quad (2)$$

$$D_h = \alpha_T |v| \delta_{i,j} + \frac{(\alpha_1 - \alpha_t) v_i v_j}{v} \quad (3)$$

where

t is time (s);

T is temperature (°C);

T^* is temperature of fluid source (°C);

θ is the volumetric water content;

v is water velocity;

Φ is sediment porosity;

q is the water flux (m s^{-1}), product of the hydraulic conductivity, K (m s^{-1}), and the total head gradient;

K_t is thermal conductivity of the streambed sediments (J s^{-1} m^{-1} °C^{-1});

C_w and C_s are the specific heat capacities of water and sediment, respectively (J m^{-3} °C^{-1});

D_h is the thermo-mechanical dispersion tensor ($m^2\ s^{-1}$);

Q is the flow rate of the fluid source (m^3/s);

α_l is the longitudinal dispersivity (m);

α_t is the transverse dispersivity (m);

$\delta_{i,j}$ is the Kronecker delta function;

ν_i and ν_j are the ith and jth component of the velocity vector, respectively ($m\ s^{-1}$); and

$|\nu|$ is the magnitude of the velocity vector ($m\ s^{-1}$).

F. Geophysical Profiling of the Riverbed

Geophysical surveys are commonly used to gather information about marine, estuarine and riverine lithostratigraphy and geologic structures (Haeni, 1986; USEPA, 1993, Lewelling, 1998; Loke, 2000; Cunningham et al., 2001; Dawson et al., 2002; Kindinger, 2002; Belaval et al., 2003; Kress et al., 2004) as well detect groundwater contamination (USEPA, 1993) and salt-water intrusion (Zohdy et al 1974). The most popular methods used to interpret the riverbed stratigraphy are continuous seismic profiling (CSP), continuous resistivity profiling (CRP) and continuous multi-frequency electromagnetic profiling (CEM). Geophysical methods are advantageous in that they are non-invasive and relatively quick and easy to conduct. The profiling equipment is located behind a small boat and measurements are simultaneously recorded in a laptop computer on board the boat. A fathometer survey and a global positional system (GPS) are usually conducted simultaneously with geophysical surveys to provide information about the location and the depth of water (Placzek and Haeni 1995; Snyder, 1997, Snyder and Wightman, 2002; USEPA, 1993; Snyder, 1997; Powers et al., 1999).

F1. Continuous seismic profiling

During continuous seismic profiling (Figure 4), an acoustic wave, typically from 0.2 to 14 kHz, is transmitted into the subsurface from a transducer suspended just below the water surface (Powers et al., 1999). Acoustic energy transmitted by transducer passes through the water column and into the subbottom (Kindinger, 2002). Where there is a change in acoustic impedance across the interface, such as at the water/bottom interface or changes in lithology or structure, part of the seismic energy is reflected back to the water surface and received by transducers or hydrophones (Figure 4) (McGee, 1995; Dawson et al., 2002). The amount of energy that is reflected by an interface is determined by the reflection coefficient of that interface which is dependent upon the acoustic impedance of the material above and below the interface (McGee, 1995; Placzek and Haeni, 1995; Haeni, 1996; Dawson et al., 2002; Kearey et al., 2002; Kress et al., 2004).

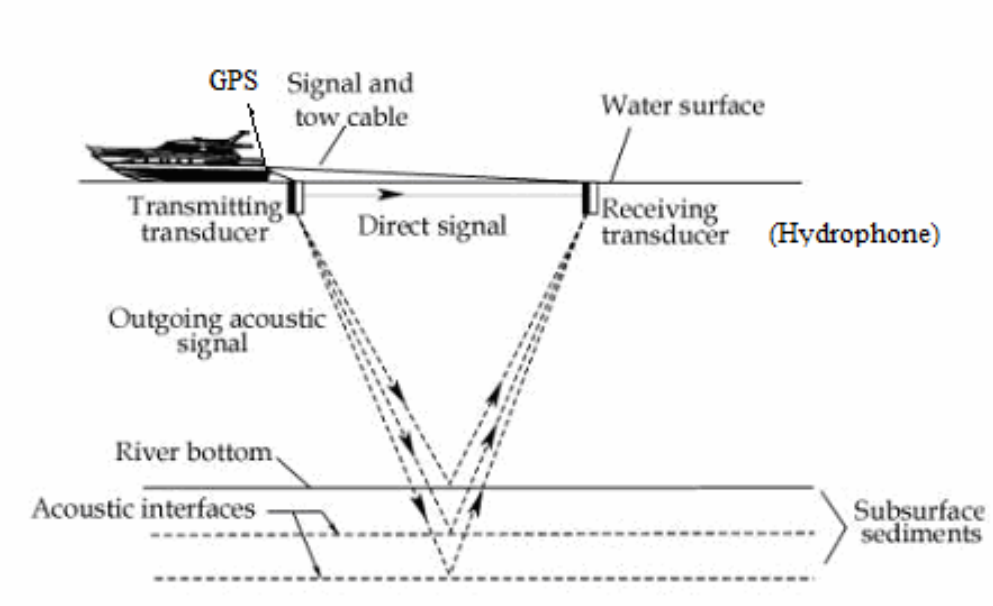

Figure 4. Typical seismic reflection ray path (after Haeni; 1986 by Sweat et al., 2000)

The reflection coefficient for an interface (R, unitless) is defined by Placzek and Haeni (1995) as:

$$R = \frac{Z_2 - Z_1}{Z_2 + Z_1} = \frac{A_r}{A_i} \quad (4)$$

where:

Z_1 and Z_2 are the acoustic impedance of the material respectively above and below the interface (g/m^2s) and

A_r and A_i are the respective amplitudes of the reflected and incident waves at the interface (m)

The acoustic impedance (Z) is (Placzek and Haeni,1995):

$$Z = \rho \cdot V \quad (5)$$

where:

ρ- density of the material (g/m^3) and

V-velocity of sound through material (m/s)

The reflection coefficient increases with an increasing acoustic impedance (Johnson end White, 2007). Reflection coefficients are generally correlated to the bulk density, porosity and median grain size of sediments (Placzek and Haeni, 1995). Low-amplitude, water-bottom reflections are associated with soft, muddy sediment, whereas high-amplitude reflections are associated with relatively low density, coarse grained sediment (Dawson et al., 2000). Data obtained from seismic continuous survey can be used to create an image of the river bottom and subottom lithostratigraphy (Cunningham et al., 2001) and to study preferential paths of hydraulic connection between the river and the underlying aquifer (Lewelling et al., 1998; Sweat, 2000). However, there are some limitations to this method. It has been suggested by Hubbard and Rubin (2000) that the relationships between hydrogeological and geophysical parameters are not unique

and the interpretation of the seismic data should be performed with caution. Moreover, the multiple reflections and noises can lead to misinterpretation of lithostratigraphic units (Placzek and Haeni, 1995; Kress et al., 2004).

F2. Continuous resistivity profiling (dipole-dipole)

The continuous dipole-dipole resistivity technique (Figure 5) uses an electric current applied into the surrounding water and the subsurface via electrodes connected to a multi-core cable or streamer (Figure 5)(Snyder, 1997; Snyder and Wightman, 2002; Johnson end White, 2007). A laptop microcomputer located on the boat together with an electronic switching unit selects the appropriate two electrodes for each measurement. Measured voltage potentials across the pair of electrodes are recorded and stored on the microcomputer for further data interpretation (Loke, 2000; Belaval et al., 2003).

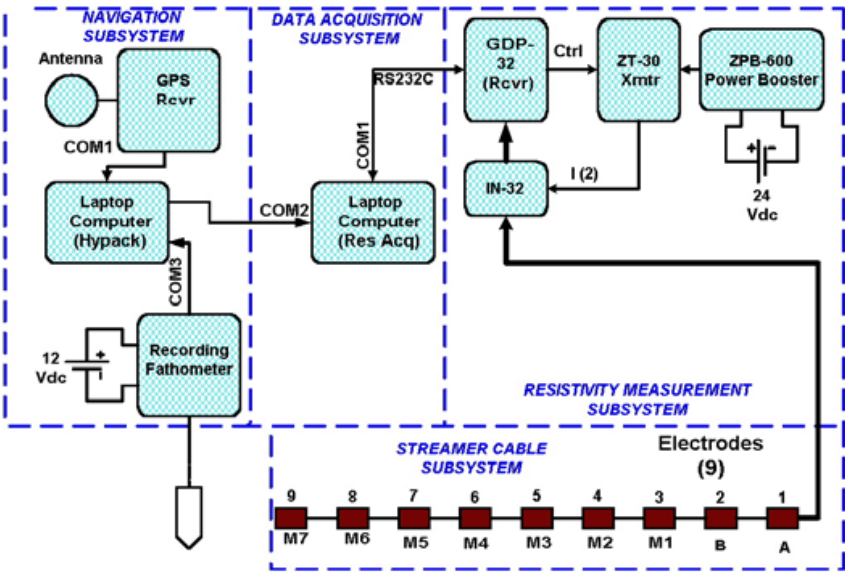

Figure 5. Functional block diagram of marine resistivity (after Snyder et al. 2002)

The apparent resistivity of the water and subsurface is calculated applying Ohm's law (Johnson end White, 2007):

$$\rho_a = k * \Delta V / I \tag{6}$$

where:

ρ_a is the apparent resistivity (Ωm)

k is the geometric factor of the dipole-dipole survey (-)

ΔV is the measured potential difference (V)

I is the applied current (A)

The geometric factor, k, is defined as:

$$k = \pi \times n \times (n+1)(n+2) \times a \tag{7}$$

where:

a is the electrode spacing (m)

n is the ratio of the distance between the current electrodes plus the distance between the current and potential electrodes to the electrode spacing (i.e. if A and B are the current electrodes and M1 and M2 are the potential electrodes in figure 5, then n is the distance between A and B (A-B) plus the distance between M1 and B (M1-B) divided by A-B).

Once collected, the apparent resistivity data are inverted to determine the true subsurface resistivities using such programs as RES2DINV (Loke, 2000; Dawson et al., 2002; Manheim et al., 2002). The subsurface resistivities are affected by hydrogeological characteristics including grain size, mineralogy, fluid content, porosity, degree of water saturation and ionic strength of the pore fluid (Loke; 2000, Belaval et al., 2003; Johnson end White, 2007). The resistivity data, therefore, allow lithostratigraphic characterization of the subsurface (Snyder 1997; Dawson et al., 2002). The most common error associated with this method is inadequate data inversion which can lead to the under or over fitting of the data relative to the actual resistivity (Johnson end White, 2007).

F3. Multi-frequency electromagnetic continuous profiling

The electromagnetic profiling method (Figure 6) is based on the response of the subsurface to the propagation of electromagnetic fields (Kearey et al., 2002). Transmitter coils generate electromagnetic fields which induce electrical currents (eddy currents) in the near subsurface (USPEA, 1993). The induced current then generates a secondary electromagnetic field that is detected by a receiver coil. The amount of current that is being induced by the secondary electromagnetic field is proportional to the electrical conductivity of the subsurface material (Burger, 1992; Kearey et al., 2002).

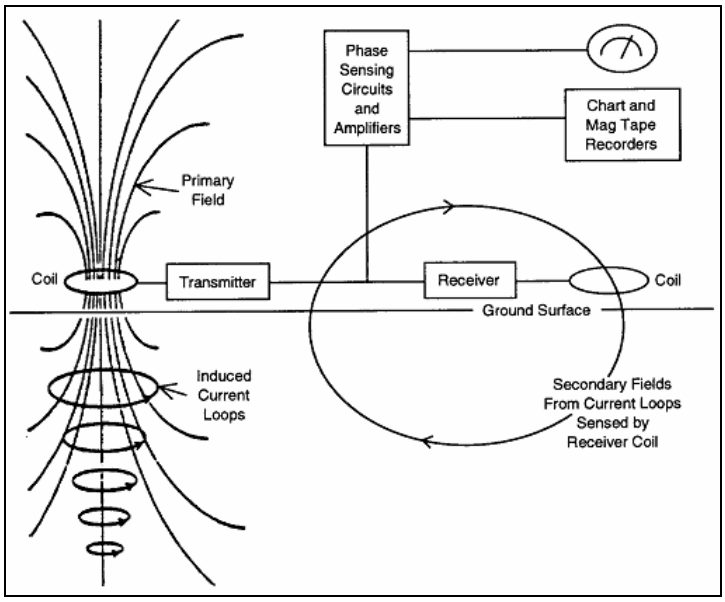

Figure 6. Schematic for electromagnetic induction method (after UPEPA, 1993)

GEM-2 multi-frequency digital sensor developed by GEOPHEX is the most common equipment used for purpose of the subsurface lithostratigraphy identification (http://www.geophex.com). GEM-2 operates in multi-frequency levels with frequencies ranging from 90 Hz to 22 kHz (Won et al., 1996). The depth of the penetration of an electromagnetic field through the subsurface is determined based on the operating frequency and ground

conductivity (Won et al., 1996). Low frequency signals travel further than high frequency signals through conductive materials whereas high frequencies are better than low frequencies at detecting shallow features (Won et al., 1996; Huang and Won, 2000). Continuous multi-frequency electromagnetic surveys can differentiate between materials of different conductivities. One problem associated with using this method on the water bodies are distortions generated by the boat engine that can interfere with true subsurface conductivity (Sambuelli et al., 2007).

IV. DESCRIPTION OF RESEARCH SITES

A. Hydrogeological Setting

The Great Miami Buried Valley Aquifer (GMBVA) system (Figure 7) consists of highly permeable sand-and-gravel glacial outwash deposited during the Wisconsin glaciations (Spieker, 1968a). The GMBVA has been designated by the US Environmental Protection Agency as a sole-source aquifer that serves as a major source of drinking water for communities between Dayton and Cincinnati, Ohio. The GMBVA is mostly unconfined; however, in some places discontinuous lenses of clay and till can be present (Spieker, 1968a; Sheets and Bossenbroek 2005). A sample cross section of the GMBVA with lenses of glacial till is presented for our North Hamilton study site (Figure 8, Sheets and Bossenbroek, 2005). Many municipal production wells are placed within close proximity to the Great Miami River. The GMBVA is 3.2-to 4-km wide and 24-to 56-m deep, bounded on its sides with steeply sloping Ordovician bedrock consisting of low-permeability interbedded limestone and shale (Watkins and Spieker, 1971). Depth to ground water in most parts of the GMBVA system is about 3 to 12 m and fluctuates seasonally (Spieker, 1968; Watkins and Spieker, 1971). The generally high water

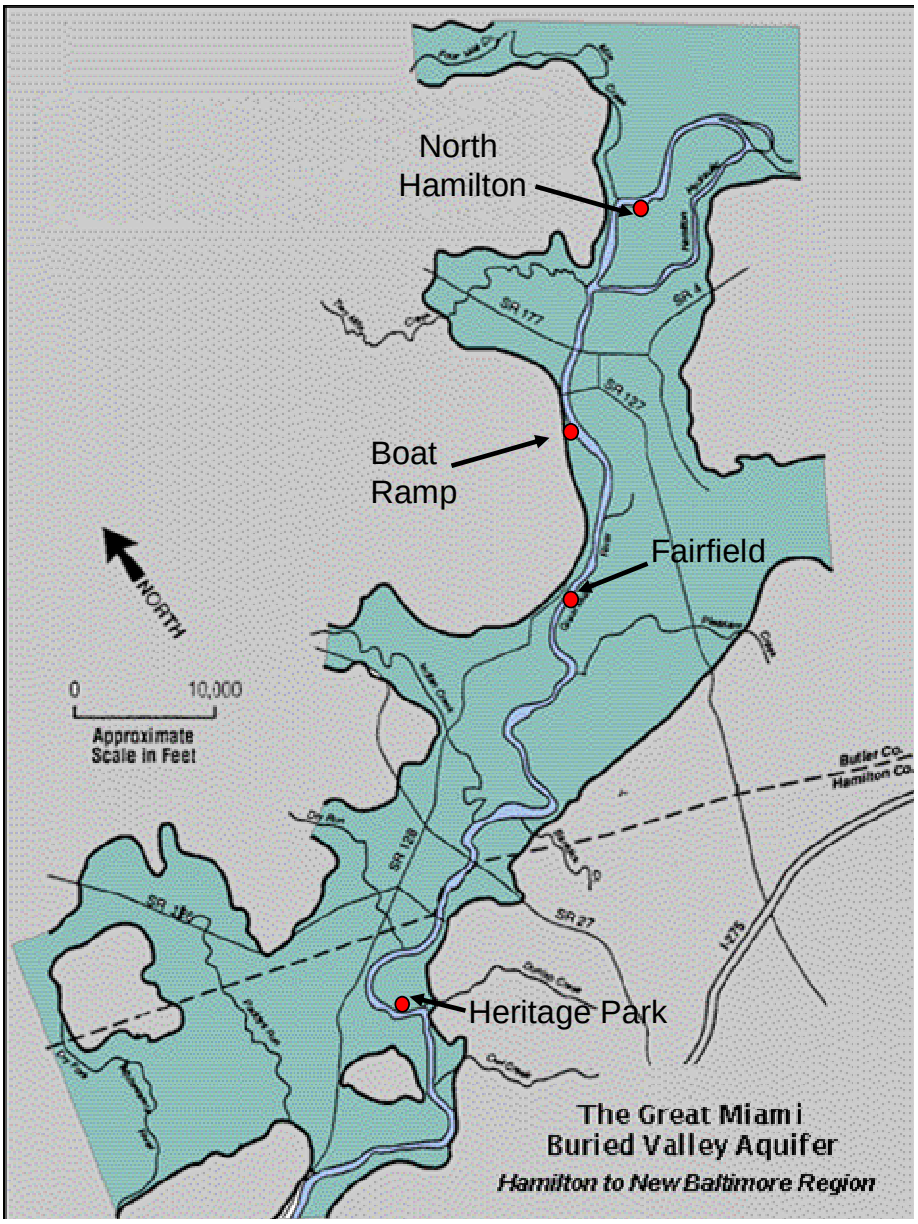

Figure 7: The Great Miami Buried Valley Aquifer System shown with the 4 study sites (map modified after http://www.gwconsortium.org/mapsframes.htm)

table makes the aquifer highly susceptible to contamination especially in the parts where GMBVA is unconfined. Aquifer hydraulic conductivities generally range from 60 to 145 m/d (Sheets and Bossenbroek 2005). Hydraulic conductivities previously measured at and around the Charles M. Bolton well field ranged from 6.9 to 363 m/d (Levy et al., 2007). The river itself

originates just above Indian Lake in Logan County, Ohio and flows generally south-southwest draining an area of 13,947 km^2 and discharging into the Ohio River (MCD, 2004) just west of Cincinnati, Ohio.

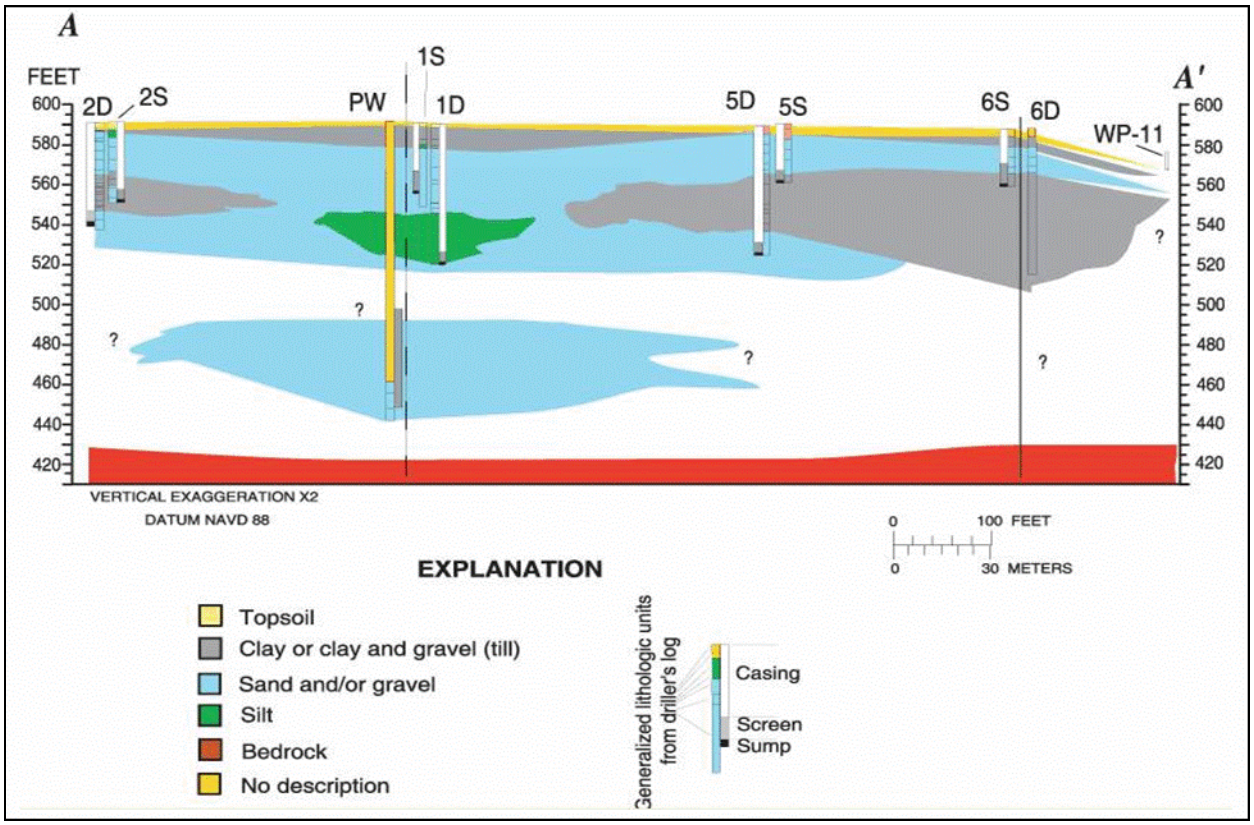

Figure 8: Cross section of the GMBVA at the North Hamilton well field site (after Sheets and Bossenbroek, 2005)

The Lower Great Miami River flows predominantly through agricultural areas that comprise approximately 73% of the land use in the Great Miami River drainage basin (MCD, 2004). The Great Miami River sustains generally high baseflow throughout the year due to high storage capacity and high permeability of the aquifer sediments that underlie the Great Miami River (Spieker, 1968a).

B. Site Selection

Investigation of the riverbed hydraulic conductivity was conducted at four study sites. Field sites were chosen in conjunction with the Miami Conservancy District, the Hamilton to New Baltimore Groundwater Consortium and the USGS. Sites were selected to span a long reach of the Great Miami River and to represent a wide range of sediment types and hydraulic conductivities. The sites were located between Hamilton and New Baltimore, Ohio (Figure 7). Three of them were associated with municipal well fields.

The North Hamilton site was located about 300 m north from the North Hamilton Water Plant in Hamilton (Figure 9). The Hamilton North well field comprises five production wells In addition, during a previous study (Sheets and Bossenbroek, 2005), the North Hamilton was instrumented with a series of monitoring wells between our study site and the production wells (Figure 8). The Fairfield site was located about 250 m north-west of the six production wells that make up the Fairfield well field (Figure 10). The Heritage Park site was located about 800 m south-east of the Southwestern Ohio well field in Ross, Ohio (Figure 11). The Boat Ramp site was located 850 m south of the Columbia Bridge in Hamilton (Figure 12) and was not associated with a well field.

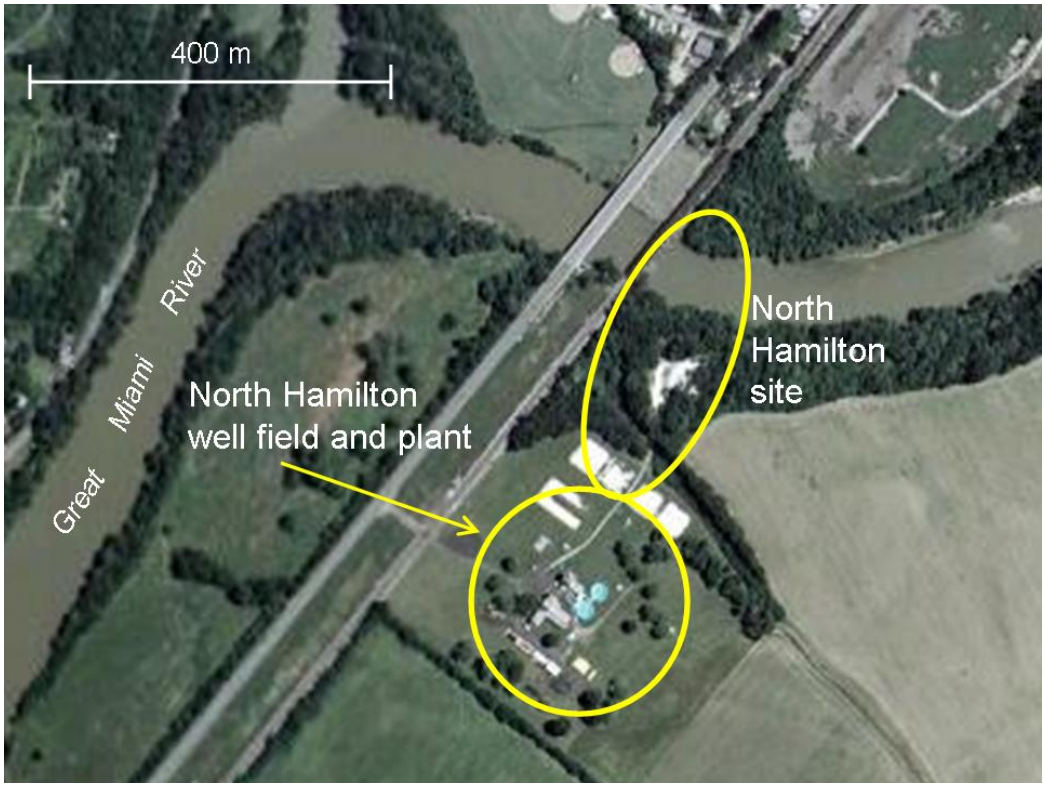

Figure 9. Aerial photograph with localization of North Hamilton site

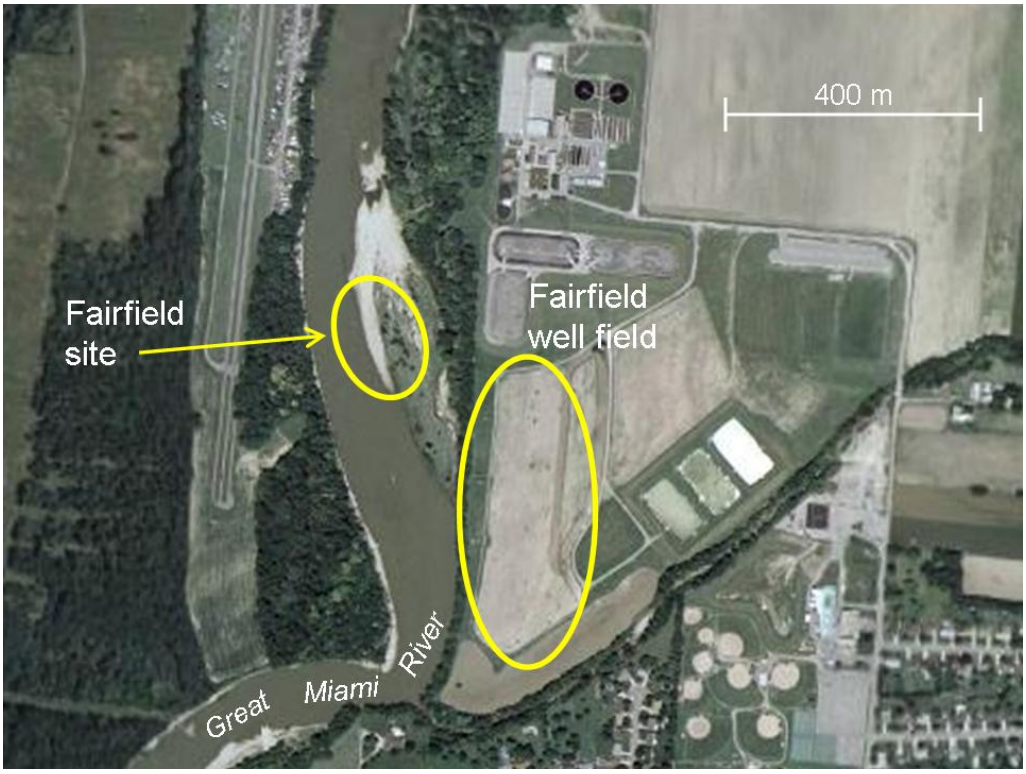

Figure 10. Aerial photograph of the Fairfield site

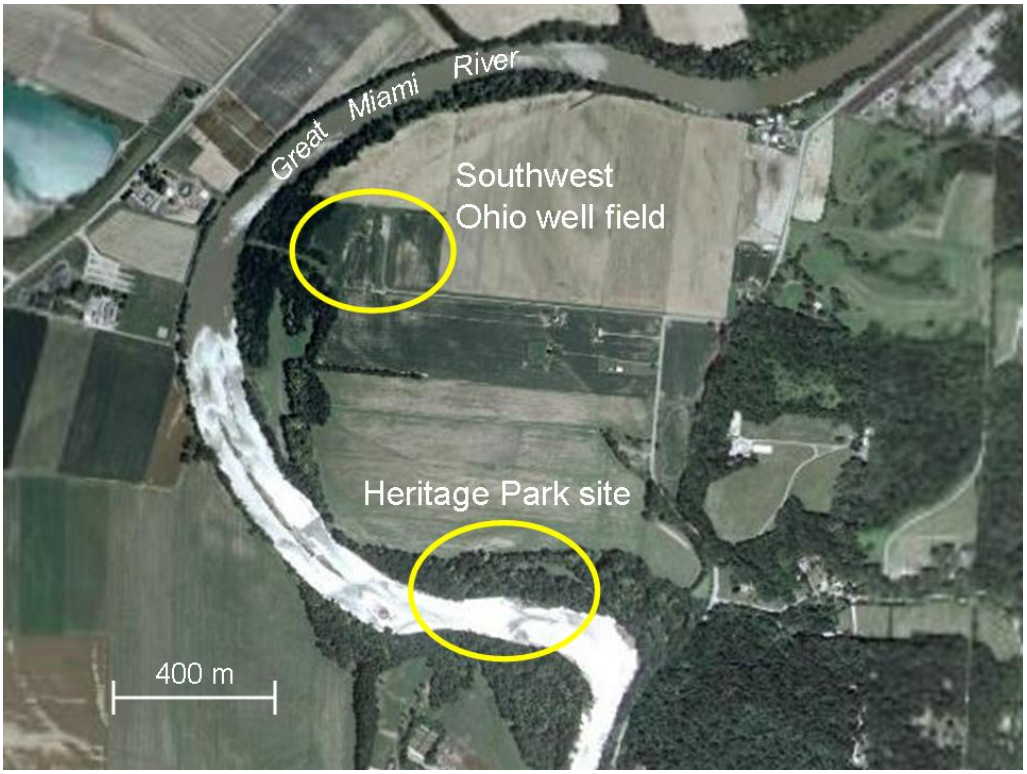

Figure 11. Aerial photograph with localization of Heritage Park site

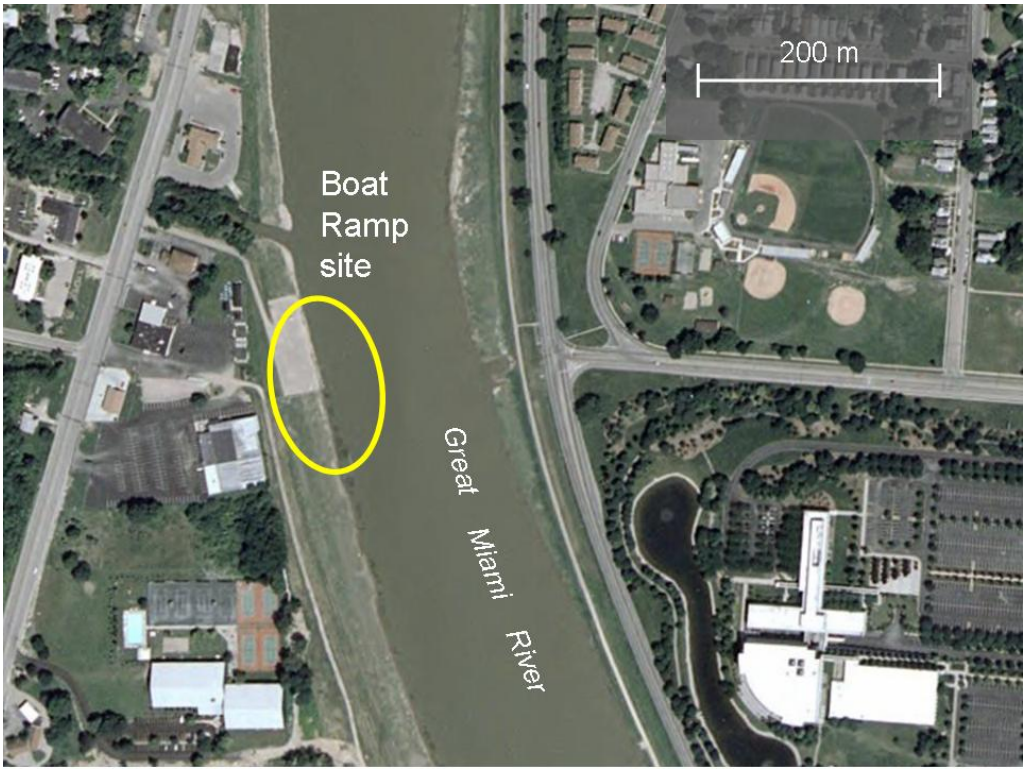

Figure 12. Aerial photograph of the Boat Ramp site

C) Previous Research in the Field Areas

The Lower Great Miami River valley has been previously studied in terms of groundwater resources, the hydrogeologic properties of the Great Miami Buried Valley Aquifer System (Spieker 1968a, Sheets and Bossenbroek, 2005), the interconnection of the river and aquifer (Spieker 1968c) and contamination of both aquifer (Spieker 1968a) and the Great Miami River (MCD, 2004). Research conducted by Spieker (1968a) concentrated mainly on determination of different hydrologic environments existing in the Great Miami Buried Valley Aquifer. He assigned different hydrologic environments based on the type and thickness of the aquifer material and its production capacity. Spieker (1968a) concluded that the most favorable sites for placement of new well fields were parts of the aquifer that were located in the Hamilton – New Baltimore area in close proximity to the Great Miami River. He also conducted electric analog modeling to investigate the effects of increased pumping on groundwater – surface water interactions in the Fairfield and New Baltimore area (Spieker 1968c). He predicted that a new Cincinnati well field that was located just few miles south of the Fairfield (the present day Charles M. Bolton well field) could sustain pumping of 40 million gallons per day. He estimated aquifer recharge by induced river infiltration under low-flow conditions to potentially be 325,000 gallons per day per acre of riverbed. Sheets and Bossenbroek (2005) investigated groundwater flow direction, aquifer properties and the effects on the discontinuous clay/till layers present beneath the riverbed on the connection between GMBVA and the Great Miami River at the North Hamilton well field. Based on aquifer-pumping tests, hydraulic conductivities of the aquifer material ranged from 60 to 137 m/day. The lenses of clay/till beneath the Great Miami River diminished the aquifer/river connection; however, in places where the clay/till layers were not present there was a strong evidence of the interactions between these systems. Groundwater

elevations were strongly influenced by the Great Miami River stage. Brick (2006) measured riverbed K_v at the Charles M. Bolton well field (half-way between our Fairfield and Heritage Park sites) and investigated riverbed K_v and the impact of high river stage on the riverbed K_v using seepage meters in conjunction with mini-piezometers. The riverbed K_v for the Bolton site ranged from 0.0080 to 0.82 m/d despite a riverbed that was visually filled with pebbles and cobbles. He hypothesized that the low K_v values were the result of riverbed clogging, increased by the pumping-induced strong downward hydraulic gradients. Birck (2006) found no significant difference for the measured K_v values for the pre and post flood time periods.

V. METHODS

A. Site Instrumentation

Each site was instrumented with equipment to measure temperature and water level in the river, beneath the riverbed and at points in the groundwater system (on-shore) between the river and the municipal wells. Several 4-cm diameter drive-point wells with 0.45-m long screens were hammered beneath the riverbed to various depths at each site (Figure 13a). On-shore piezometers were installed using a truck-mounted hollow-stem auger rig at depths between 4.8 and 12.2 m (Figure 13b). When possible during drilling, sediment cores were taken with a 0.6-m long, 5-cm diameter split-spoon sampler. Piezometer information is summarized in Table 1.

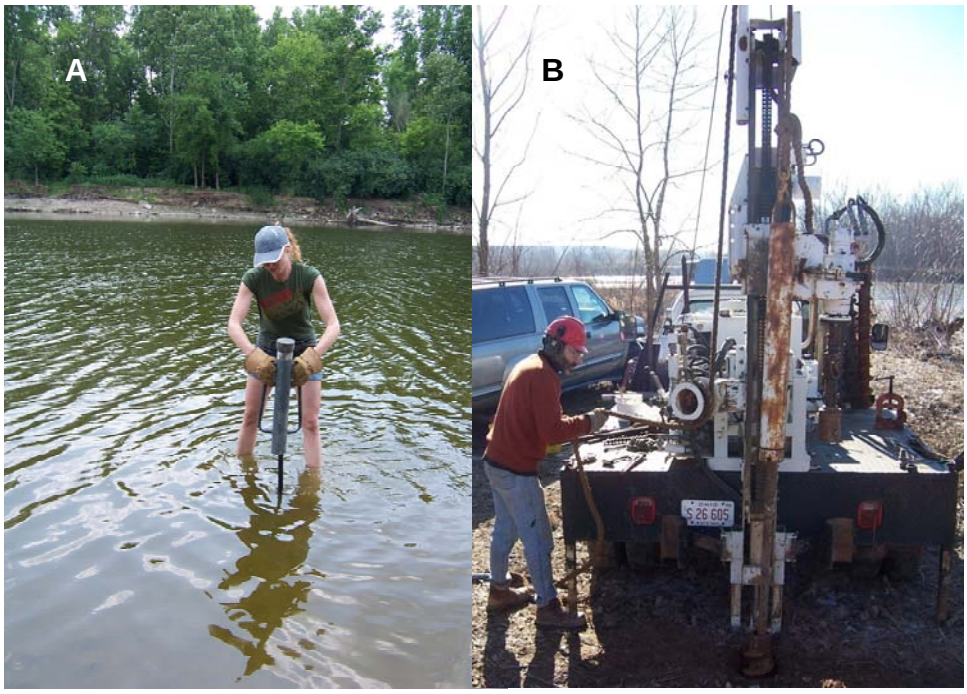

Figure 13. Installation of the A) a drive point piezometer in the riverbed and B) an on-shore monitoring well

Table 1. Piezometer information

ID number	*Well depth (m)*	*Well diameter (m)*	*Screen Length (m)*	*Elevation of top of casing (m amsl)*
NH-W 5D[a,b]	19.8	0.05	1.52	179.8
NH-W 6S	8.8	0.05	3.05	179.3
NH-DP 1[c]	3.1	0.04	0.46	175.3
F-W 1[d]	11.3	0.05	0.30	170.3
F-DP 2	3.6	0.04	0.46	166.7
HP-W 1[e]	12.8	0.05	0.61	161.8
HP-DP 1	1.8	0.04	0.46	156.7
BR-W 1[f]	9.1	0.05	0.30	172.7
BR-DP 1	2.3	0.04	0.46	170.8

[a]NH is the North Hamilton site (wells 5D and 6S were installed by USGS in 2005)
[b]W denotes an on-shore monitoring well
[c]DP denotes a drive-point piezometer into the riverbed
[d]F is the Fairfield site
[e]HP is the Heritage Park site
[f]BR is the Boat Ramp site

At each site, temperature loggers (thermistors) and pressure transducers were placed in the river (attached to fence posts) and in the piezometers to collect temperature and water-levels measurement every 15 minutes over a period of several months (Table 2). These data were used as boundary-input and model-calibration data for the heat-flow simulations. In many piezometers, temperatures and pressures were measured with In-Situ® LevelTroll 300s. The LevelTrolls had a nominal temperature range of -5°C to +50 C and applied pressure range from 7 to 30 PSI. To obtain the water elevations, all piezometers and transducers were surveyed to establish relative elevations. The measured pressures were adjusted using the barometric pressure recorded by an In Situ® BaroTroll. When temperature was measured at more than one depth within the same piezometer, Stowaway Tidbit® thermistors were also employed. These thermistors measured temperature in the range of -20°C to 50°C with an accuracy of +/- 0.2°C.

Table 2. Summary of the temperature and water levels measurement periods

Site	***Collection period***
North Hamilton[a]	July-August, 2007; January-May, 2008
Fairfield	July- October 2007
Heritage Park	July 2007 – October 20078
Boat Ramp[b]	February - May 2008

[a] Equipment stolen around September, 2007 and later replaced

[b] No thermistors in drive-point piezometer from February to March 2008. In April, two thermistors were installed at depths of 0.91 and 1.22 m below riverbed, but W1 became damaged in a high-flow event.

The general setup of all the sites is shown in Figure 14. Individual site schematic profiles are displayed in Figures 15-18 (not to scale). Plan views of instrumentation are displayed in Figures 19-22 (shown to scale).

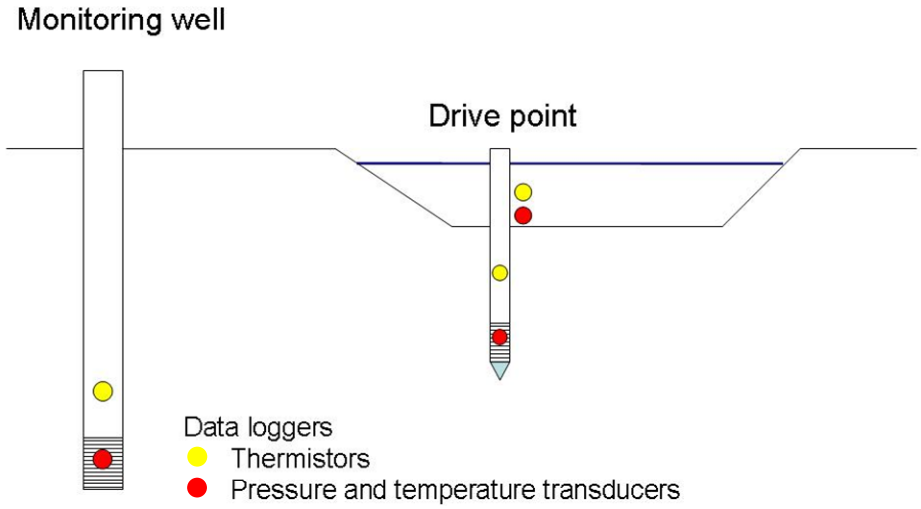

Figure 14. General schematic of temperature and water level monitoring network

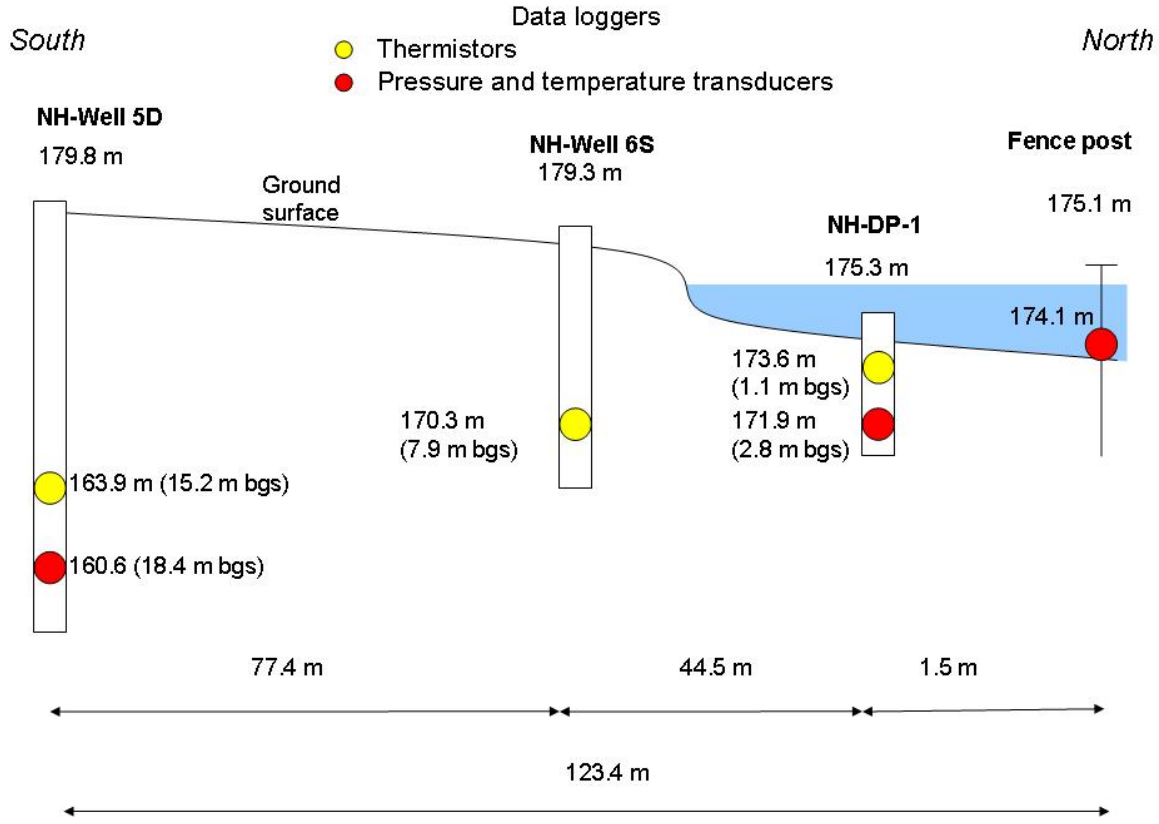

Figure 15. Temperature and water level monitoring network at the North Hamilton site. bgs is below ground surface

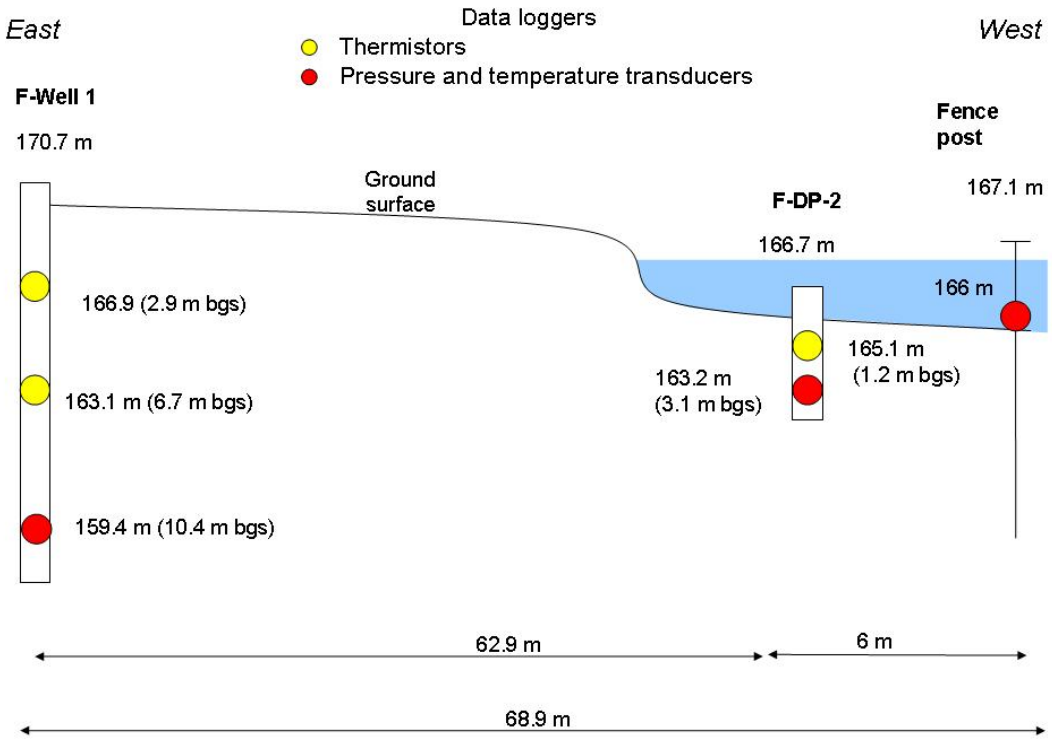

Figure 16. Temperature and water level monitoring network at the Fairfield site. bgs is below ground surface.

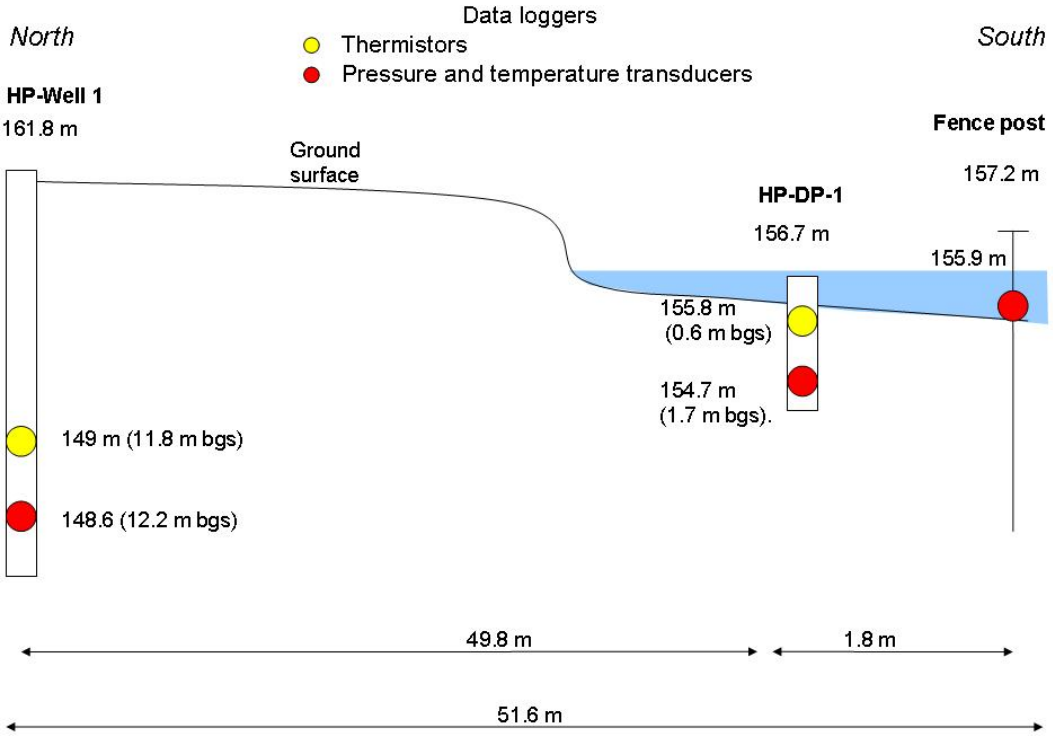

Figure 17. Temperature and water level monitoring network at the Heritage Park site. bgs is below ground surface.

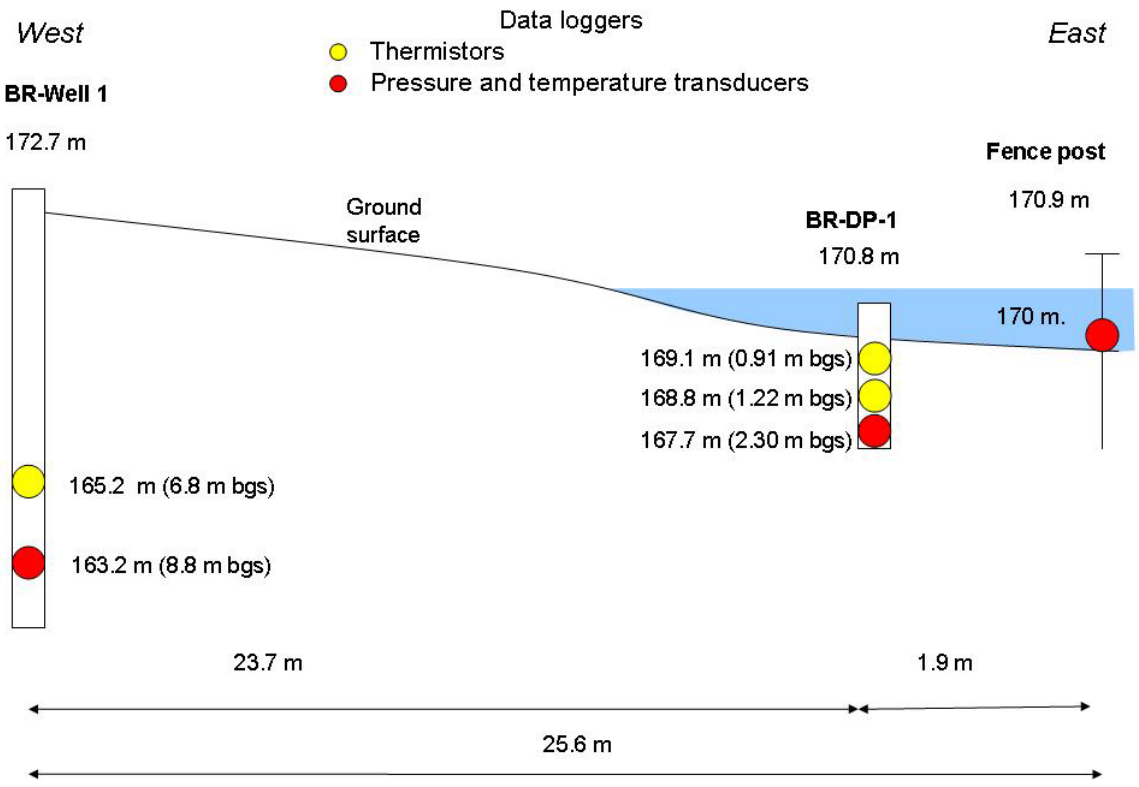

Figure 18. Temperature and water level monitoring network at the Boat Ramp site

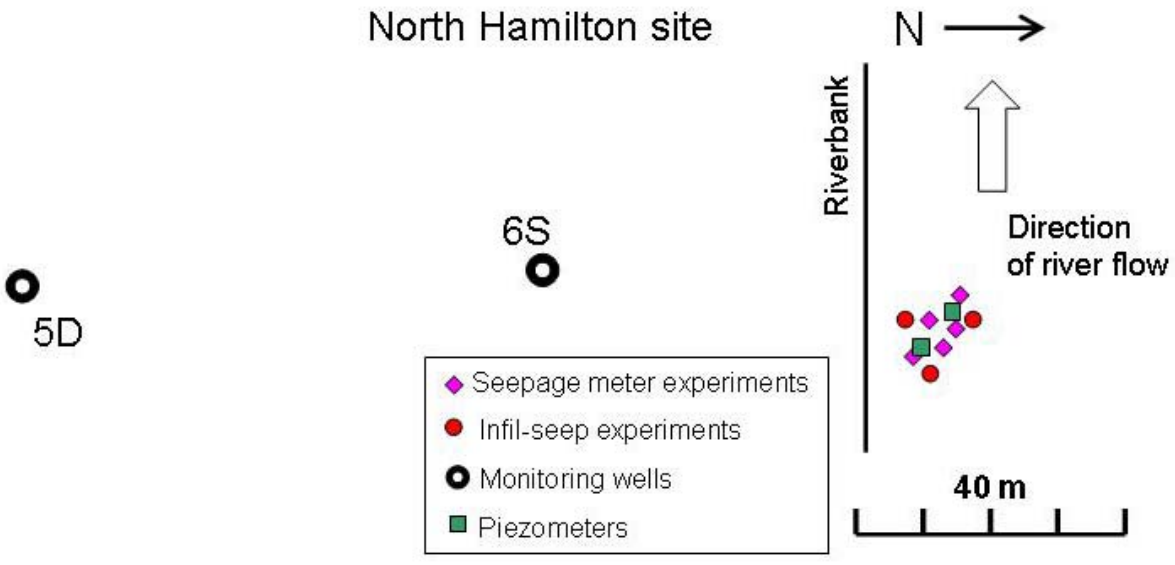

Figure 19. Instrumentation at the North Hamilton site

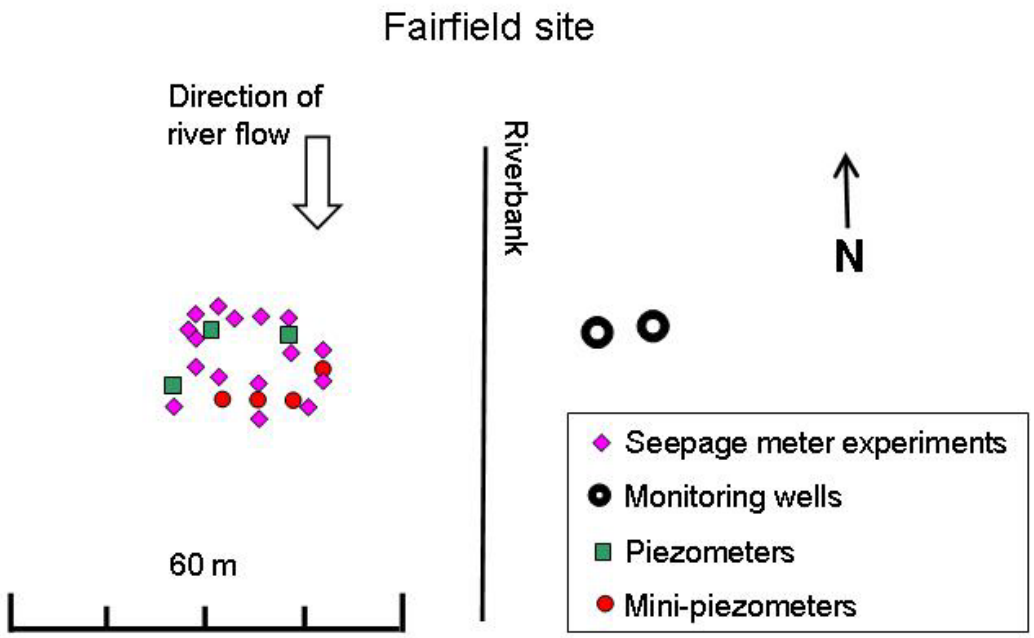

Figure 20. Instrumentation at the Fairfield site

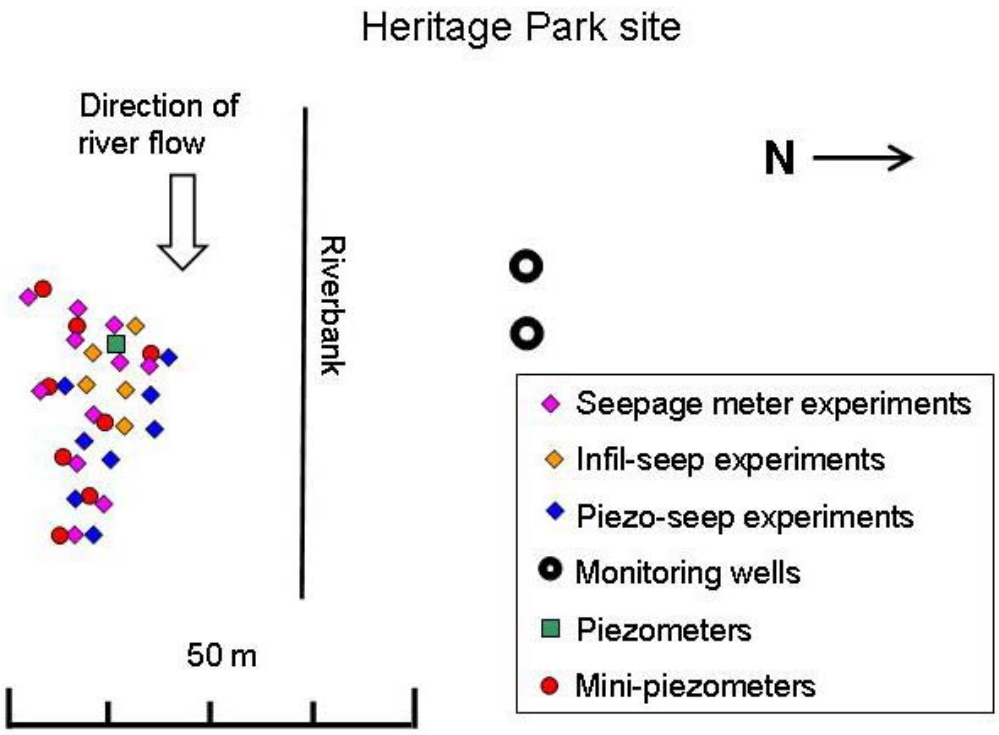

Figure 21. Instrumentation at the Heritage Park site

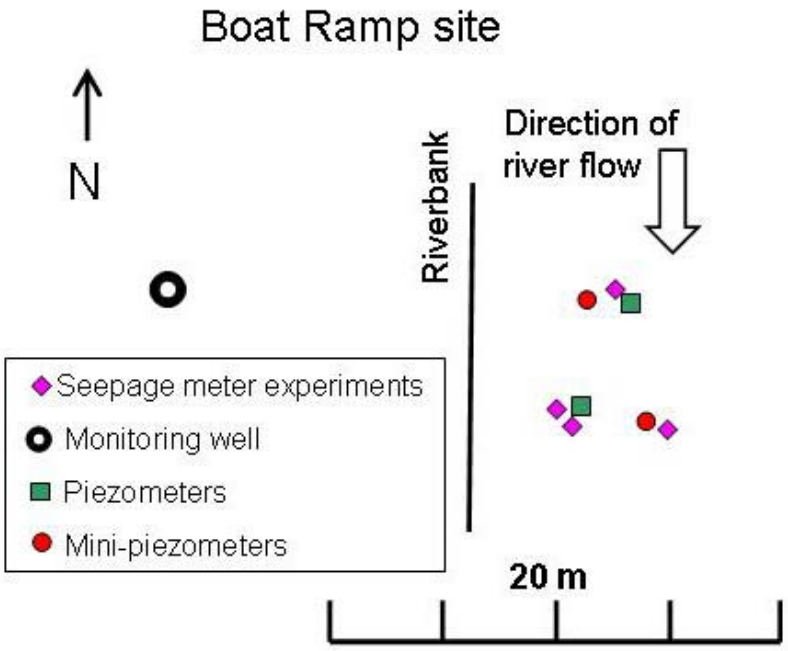

Figure 22. Instrumentation at the Boat Ramp site

B. Grain size analysis

For site characterization, wet-sieve grain-size analyses were conducted on split-spoon core samples obtained during installation of the monitoring wells at three of the four study sites. At the North Hamilton site, we did not install monitoring wells but used those installed by the USGS, Columbus (Sheets and Bossenbroek, 2005). In addition, sediment samples from the riverbed were taken by shovel at all four of the study sites and analyzed for grain-size distribution. All samples were oven dried for 24 hours at 105°C. After oven drying all samples were weighed and a 5%-by-weight solution of sodium metaphosphate ($Na(PO_3)_6$) was added to each sample as a dispersant. The samples were then washed through a series of sieves ranging from 200 to 0.063 mm while being continuously shaken with a mechanical shaker. The sediment caught in the sieves was then dried in the oven and weighed. Sediment finer than 0.063 mm, that passed through the smallest sieve was also measured and represented the combined fraction of

silt and clay. Grain size distribution curves were used to estimate the median grain size (d_{50}) and uniformity coefficient (C_u) defined as:

$$C_u = d_{60}/d_{10} \quad (8)$$

where d_{60} and d_{10} are the grain sizes for which 60 and 10% of the sediment by weight, respectively, are finer than those sizes (Fetter, 2001).

Several empirical equations can be applied to estimate the hydraulic conductivity from the grain size distribution curves (e.g., Hazen, 1892; Terzaghi and Peck, 1964; Shepherd, 1989). Perhaps the most common empirical approximation of K used is the Hazen method (Fetter, 2001):

$$K = C^*(d_{10})^2 \quad (9)$$

where C is an estimated coefficient that depends on grain size and sorting (Fetter, 2001). Coefficients of 80 and 120 are recommended for poorly-sorted, coarse grained sediment and well-sorted, fine sediment respectively (Fetter, 2001). The Hazen approximation was originally derived for uniformly graded sands, but it can provide fairly useful estimates for sediments ranging from sand to gravel (Freeze and Cherry, 1979). The hydraulic conductivity of the sediment samples was calculated using the empirical Hazen method.

C. Laboratory Permeameter Tests

Falling-head permeameter tests were conducted on intact riverbed sediment samples taken from three study sites (Boat Ramp, North Hamilton and Heritage Park). Samples were collected with 3.5-cm diameter plastic tubes opened at both sides. The tubes were slowly pushed into the riverbed so that the structure of sediment sample was minimally disturbed. The sediment cores were then incorporated into a falling-head permeameter and hydraulic conductivities were

measured based on the Darcy's law. The riverbed sediment at the Fairfield site was too coarse to allow sample collection using this method.

D. Slug Tests

Rising- and falling-head slug tests were performed on all piezometers to estimate horizontal hydraulic conductivity. Falling-head slug tests were performed on drive points screened at depths from 0.45 to 3.6 m beneath the riverbed by pouring water into the piezometers. Rising- and falling-slug tests were performed on on-shore piezometers, screened at depths from 4.5 to 10 m, by rapidly lowering and removing solid slugs into the wells. For all slug tests an In-Situ 700® pressure transducer was used to monitor water levels. Data were entered into the software program AQTESOLV® (HydroSOLVE Inc., 2000) and the Bouwer-Rice method (Bouwer and Rice, 1976; Bouwer, 1989) was used to estimate horizontal hydraulic conductivity.

E. Seepage Meters

Direct measurements of the riverbed K_v were made with seepage meters. Three types of seepage meters constructed by the Miami University Instrumentation Laboratory were tested and applied: a conventional seepage meter, a piezo-seep and an infil-seep.

E1. Conventional seepage meter

Measurements of the riverbed K_v with conventional seepage meters were performed at many locations at each of the study sites (Figures 19-22). Conventional seepage meters were modeled after the Idaho seepage meter (ANCID, 2004) and constructed by Miami University's Instrumentation Laboratory. Each of these seepage meters had a 30-cm diameter, stainless steel bottomless seepage meter bucket with sharpened edges and a removable center rod with crossbar to facilitate penetration into coarse-grained riverbeds. The conventional seepage meters were

used in combination with mini-piezometers placed in close proximity to the seepage meters for measuring the vertical hydraulic gradient immediately below the riverbed. Mini-piezometers were made of either 1.27-cm diameter polyethylene semi-rigid tubing or 4.4-cm diameter steel drive points. After the seepage-meter bucket was pressed into the riverbed, the bucket was left for 10 to 15 minutes for equilibration after which time a plastic bag was attached with a known volume of water. A Camelbak® bladder was used as the bag to facilitate removing of all air from the system prior to attaching the bags to the tubing. The bag was left in place for one to several hours, depending on the type of the riverbed sediment (Landon et al., 2001). The bag was then collected and the change of water volume in the bag was measured. Riverbed K_v was calculated according to Darcy's law.

The seepage-meter measurements were conducted with caution in order to avoid potential errors cited by previous researchers. A major potential problem arises with using the conventional seepage meter in a river. The river current can create low pressure around the bag inducing unrepresentative inflow into the bag, even in areas of downward gradients (Bernoulli's effect) (Libelo and MacIntyre, 1994; Cable et al., 1997b; Murdoch and Kelly, 2003; Brodie et al., 2005). To overcome this problem, the bags were placed in semi-enclosed separate plastic bins to maintain the same head as in the river and yet shield the bags from the effects of stream flow. Leakage around the seepage chamber (Libelo and MacIntyre, 1994; Cey et al., 1998) was minimized by providing an effective seal and installation depth to prevent void spaces around the chamber especially while installing seepage meter in coarse-grained sediment. Anomalous seepage flux caused by the gas accumulation within the system (Shaw and Prepas, 1989; Sebestyen and Schneider, 2001) was reduced by removing the air that was trapped in the riverbed sediment while sealing the seepage chamber and with use of the Camelbak® bladders.

Moreover, to avoid miscalculation associated with the head loss and anomalous short-term influx (Shaw and Prepas, 1989, Cable et al 1997b), the bags were pre-filled with water prior to connecting them by snap-connectors to the seepage meters. The Camelbak® bladders were flexible but did not undergo much mechanical relaxation, a tendency that can produce anomalous results (Belanger and Montgomery, 1992; Schincariol and McNeil, 2002).

The seepage meter measurements were assumed to be valid only when the water volume change in the bag was at least 150 ml. This value of water volume change was reported by Cable et al. (1997b) as the minimal volume that should be collected to consider the seepage measurements reliable, as the flux rates generally stabilize after these first 150 ml of volume change.

Based on a previous study conducted in a controlled sand-tank environment (Levy et al., 2007), K_v values derived from conventional seepage meters were multiplied by a factor of 2.1 to correct for bag friction and head-loss through tubing.

E2. Piezo-seep meter

A piezo-seep meter(described in section III D) (Kelly and Murdoch, 2003) is a variation on a conventional seepage meter that generates its own hydraulic gradient to induce flow through the riverbed. The Miami University Instrumentation Laboratory modified the top of one of the seepage buckets according the design by Kelly and Murdoch (2003), with a port for the pump, one for the mini-piezometer and one open to the inside of the bucket (Figure 2). Once the piezo-seep was installed in the riverbed, so that the piezometer was pressed into the riverbed, the appropriate tubes and equipment were attached to the barbed ports (Figure 2). Water was pumped at a constant, measured rate from the inside of the bucket until the heads in the mini-

piezometer the inside of the bucket reached equilibrium. Darcy's law was then applied using the measured gradient and flow rate to calculate the riverbed K_v.

E3. Infil-seep meter

For this study, we designed and tested a new type of seepage meter that we have named an infil-seep meter. The infil-seep meter is simply an in-situ permeameter modified to cover a larger area of riverbed with a relatively small input of water. As for the piezo-seep, flow across the riverbed surface is induced artificially. The infil-seep meter has a 1-m long, 4-cm diameter PVC pipe attached to the top of the bucket (Figure 15). To perform a test, the infil-seep was pressed into the riverbed, and the hydraulic gradient inside of the seepage bucket was induced by pouring water into the PVC pipe. The changing head in the pipe was monitored with an In- Situ® LevelTroll 700 until the water level fell back to equilibrium conditions. Darcy's law was applied with the height of the water column above equilibrium being the instantaneous difference in head (dh in Figure 23). It was assumed the distance across which the head gradient was measured corresponded to the depth below the river bed to which the bucket was inserted (dL in Figure 23).

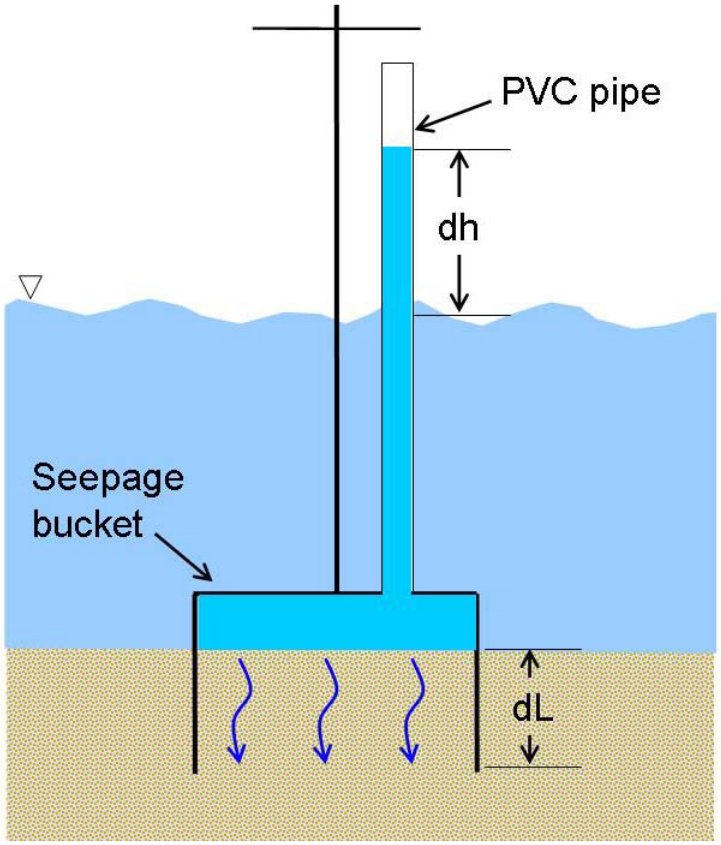

Figure 23. Infil-seep meter

F. Estimation of Riverbed K_v Using Heat and Flow Transport Simulations

Using the VS2DH program (see Section III E, equations 2 and 3), simulated temperatures were fitted to the observed sediment temperatures, by assigning a value of the riverbed K_v and running the simulation until a minimal difference between simulated and observed temperatures was achieved. Two dimensional modeling approaches were adopted to construct models for each site (general schematic in Figure 24). One-dimensional models were also created for the Fairfield, Heritage Park and Boat Ramp sites. For the two-dimensional temperature models, boundary conditions corresponded to specified, variable total head and temperature as observed in the river and the deeper monitoring wells. VS2DH observation points corresponded to the

depths of the temperature sensors. For each textural unit created in the simulations, the sediment thermal conductivity, volumetric heat capacity of the water and sediment, dispersivity and anisotropy ratios were assigned according to values obtained from the literature (Table 3).

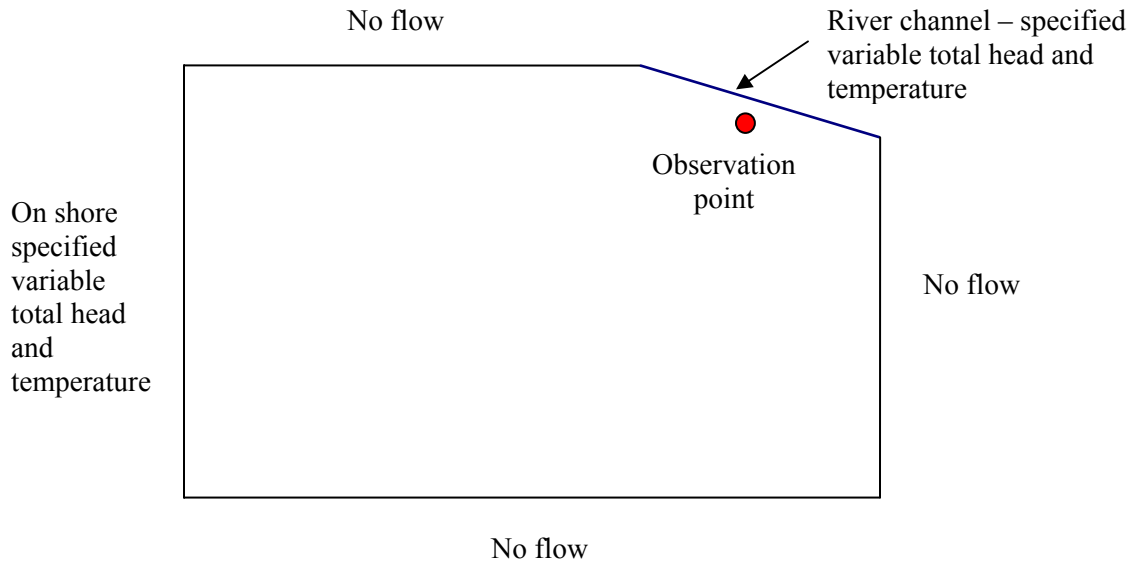

Figure 24. General schematic of a model domain for two-dimensional modeling approach

Table 3. Hydraulic properties used in the the VS2DH simulations, most of them are default values already existing in VSH2D for similar materials

Parameter	***Riverbed***	***Aquifer***	***Source(s)***
Porosity	0.2 to 0.3	0.24	Fetter, 2001; Niswonger & Prudic, 2003)
Anisotropy ratio (K_v/K_h)	0.1	0.1	Estimate
Dispersivity (m)	0.1	0.1	Constantz et al., 2003 Niswonger and Prudic, 2003
C_s (J m^{-3} °C^{-1})	$1.2*10^6$	$1.2*10^6$	Su et al., 2004
K_{Ts} (W m^{-1} °C^{-1})	2.1	2.1	Niswonger and Prudic, 2003
K_{Tr} (W m^{-1} °C^{-1})	2.3	2.3	Niswonger and Prudic, 2003
C_w (J m^{-3} °C^{-1})	$4.18*10^6$	$4.18*10^6$	Cox et al., 2007

For the one dimensional simulations, we assumed that heat and flow transport was only in vertical direction from or to the river. The upper boundary conditions were specified, variable temperatures and total heads observed in the river; the lower boundary conditions were the specified, variable temperatures and total heads observed at the bottom of the deepest drive point that was installed in the riverbed. Each 1D model domain had a unit width of 2 m, the unit length was the depth of the deeper observation point in the piezometer installed in the riverbed.

G. Geophysical investigation of riverbed characteristics conducted by USGS

Continuous seismic reflection profiling (CSP), continuous resistivity profiling (CRP), and multi-frequency continuous electromagnetic profiling (CEP) were performed at three of the sites (North Hamilton, Fairfield and the Boat Ramp) by the U.S. Geological Survey (USGS), Columbus, Ohio to investigate the riverbed lithostratigraphy. EdgeTech® SB-216S swept-frequency towfish and EdgeTech® X-STAR topside unit were employed with a shooting rate of 250 ms and recoding rate of 40, 50 or 100 ms. For CRP Advanced Geosciences Inc. ® Super Sting, R81P-8-channel dipole-dipole array was used with1-m spacing for electrodes on streamer. CEP surveys were conducted at three frequencies 750, 3,150 and 15,030 Hertz using a Geophex, Inc.® GEM-2 sensor (Sheets and Dumouchelle, 2008).

VI. Results

A. Grain-size analyses

The grain-size analyses conducted on the riverbed samples (about 0.8 to 3 kg via shovel) from the Great Miami riverbed verified that the sediment varied significantly from site-to-site ranging from predominantly silt and clay to cobbles (Table 4, Figure 25). Two samples were taken from the riverbed at the Fairfield site. Both samples were very poorly sorted (Table 4). One sample comprised about 38% cobble-sized sediment (> 64 mm) with about 88% greater than

sand-sized and about 1% silt and clay. The second sample had no cobbles, but still contained 85% greater than sand-sized. Two samples were also taken from about the same location at the Heritage Park site, but one was from before a large storm event in January 2008 and one was after. The sample before the event, in contrast to the Fairfield site, was very well-sorted coarse sand. It also comprised only a small amount (2%) of silt and clay, but had < 25% greater than sand size and nothing larger than medium pebbles. The sample taken after the high-flow event was more like the Fairfield samples with 11.5% cobbles and 82% greater than sand-sized. The North Hamilton site riverbed sample was medium-well sorted with a median grain size corresponding to a medium sand and <2% greater than sand size. No riverbed sediment sampled at the North Hamilton site was larger than fine pebbles, and the riverbed sample comprised about 7% silt and clay. The riverbed site with the finest sediment was the Boat Ramp with a median grain size corresponding to very fine sand. In spite of the relatively small median grain size, about 15% was greater than sand size. The Boat Ramp site had the highest proportion of silt and clay by far, making up about 48% of the riverbed sediment. Because we did not break down size classifications below 0.063 mm, we could not compute a d_{10} for this sample.

Hydraulic conductivities calculated based on the grain size distributions using the Hazen method (Fetter, 2001) ranged from 0.85 m/d for one of the Fairfield samples to 10.36 m/d for the North Hamilton site (Table 4).

Grain-size analyses were also performed on many split-soon samples obtained during installation of the monitoring wells. Those results and Hazen calculations are presented in Appendix 1. Split-spoon samples indicated that at the Fairfield site, sediment was very heterogeneous, with medium grain sizes ranging from medium sand to pebbles and uniformity coefficients from 3.6 to 60. At the Heritage Park site, sediment was more homogeneous and

usually well-sorted, ranging from fine sand to very fine pebbles. Only two split-spoon samples were recovered from the Boat Ramp, and they both comprised poorly-sorted very coarse sand.

Table 4. Sediment median grain size, sorting and hydraulic-conductivity (K) estimation.

	Fairfield-1	***Fairfield-2***	***Heritage Park-before flood***	***Heritage Park-after flood***	***North Hamilton***	***Boat Ramp***
Classification[a]	Poorly-sorted medium pebble	Poorly-sorted coarse pebble	Well-sorted very coarse sand	Poorly-sorted medium pebble	Medium-well-sorted medium sand	Very fine sand
Sample mass (g)	1761	2923	859	2008	629	820
d_{50}[b] ***(mm)***	8.6	50.0	1.6	13	0.4	0.07
% cobbles (64-256 mm)	0	38.1	0	11.5	0	0
% pebbles (2-64 mm)	84.7	49.6	24.1	70.1	1.5	14.7
% sand (0.063-2 mm)	13.5	11.9	73.7	17.9	91.5	36.8
% silt + clay (<0.63 mm)	1.86	0.430	2.1	0.48	7.1	48.4
C_u[c]	30.9	54.6	2.66	20.9	5.6	NA[d]
K (m/d)[e]	0.85	8.4	3.4	8.4	10.36	NA

[a]Classification is based on the scales given by Fetter (2001)
[b]d_{50} is the median grain size
[c]C_u is the uniformity coefficient
[d]Not calculated due to lack of information distribution of sizes < 0.063 mm preventing estimation of the d_{10}
[e]K is estimated from the grain size results using the Hazen method

B. Falling head permeameter test

Falling head permeameter tests were conducted on riverbed samples taken from three study sites to a depth of approximately 15 cm. Collection of the riverbed sediment at the Fairfield site for permeameter tests was not possible due to the coarse character of the riverbed. The riverbed K_v values were calculated from the solution of Darcy's law applied to a falling-head test (Fetter, 2001). The riverbed K_v obtained from the falling-head test was the lowest for the Boat Ramp

site and the highest for the Heritage Site, with geometric means of 0.00293 m/d and 51.2 m/d, respectively (Table 5). K_v obtained for the North Hamilton site was intermediate at 9.03 m/d.

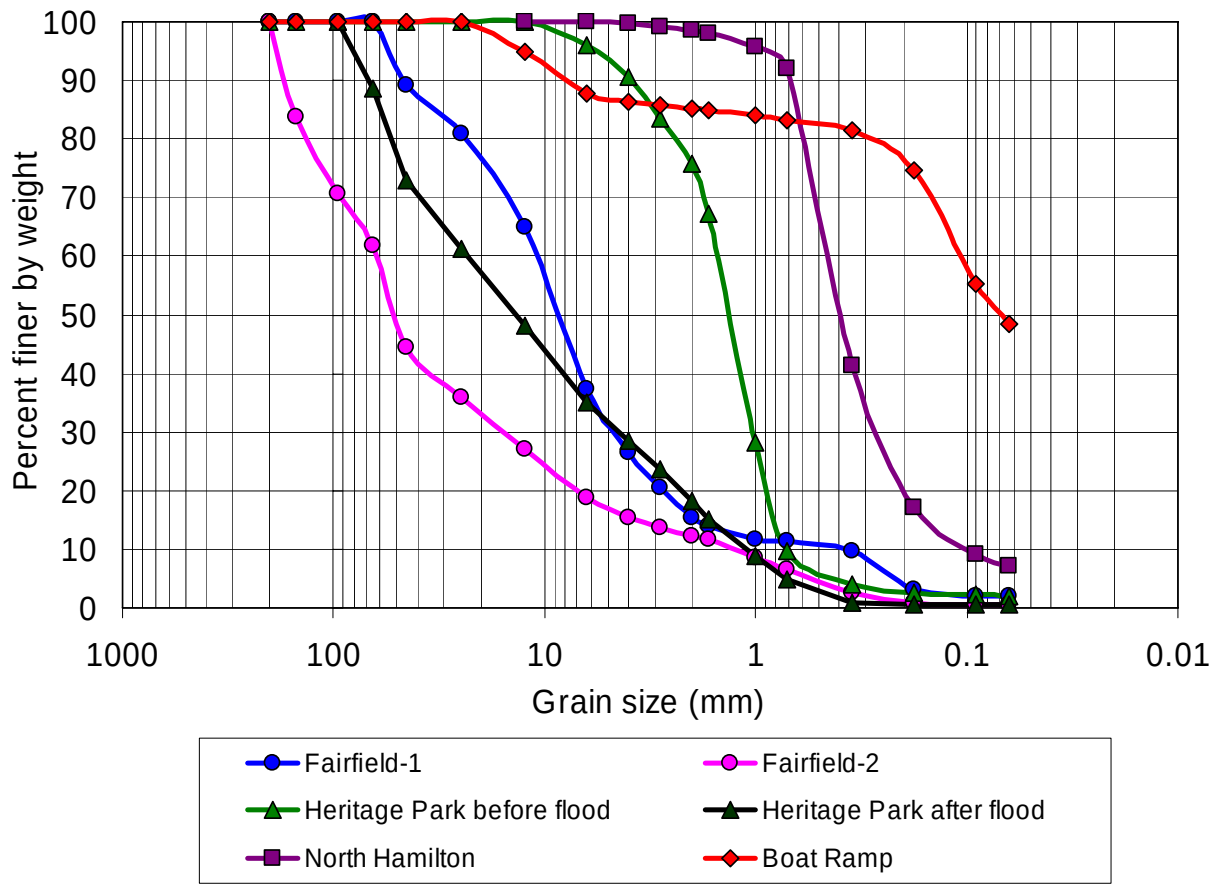

Figure 25. Grain size distribution curves of riverbed samples from four study sites

Table 5. Riverbed K_v values obtained from falling head permeameter tests

Site	*# of samples*	*Sediment length (cm)*	*K_v (m/d)*
North Hamilton	1	17.8	9.03
Heritage Park	3	13.8	52.5
		11.1	47.5
		14.2	53.7
Boat Ramp	1	12.1	0.00293

C. Slug tests

Falling- and rising-head slug tests conducted in the riverbed piezometers and in piezometers on shore were used to calculate horizontal hydraulic conductivity (K_h) values via the Bouwer and Rice method (Bouwer and Rice, 1976; Bouwer, 1989) applied using AQTESOLV® (HydroSOLVE Inc., 2000). For these analyses, we assumed a vertical to horizontal hydraulic conductivity anisotropy ratio of 0.1. This value of the K_v/K_h anisotropy ratio is a typical value derived from the pumping tests in alluvium (Freeze and Cherry, 1979).

Slug tests in drive-point wells in the riverbed yielded K_h values at depths between 0.36 and 1.52 m below the river. K_h at the Fairfield site, at a depth of 1.52 m, was relatively low, with a value of 1.11 m/d. K_h values at the other sites were all more than an order of magnitude greater (Table 6). Two measurements made at different locations but at the same depth at the Heritage Park site gave some indication of the horizontal spatial variability with values differing by a factor of two (Table 5). This difference corresponds to the observation that there was more resistance to the hammering associated with the installation of DP-4 suggesting coarser sediment than at DP-3.

Table 6. Falling head slug tests results for drive-point piezometers located in the riverbed

Site	*Piezometer*	*# of tests*	*Below river or onshore*	*Depth of mid-screen (m)*	*Screen length (m)*	*K (m/d)*
Fairfield	DP-3	3	Riverbed	1.52	0.46	1.11
Fairfield	W-1	7	On shore	11.2	0.30	94.6
Heritage Park	DP-2	4	Riverbed	0.357	0.085	78.0
Heritage Park	DP-3	2	Riverbed	0.737	0.085	45.8
Heritage Park	DP-4	3	Riverbed	0.737	0.085	24.3
Heritage Park	W-1	3	On shore	12.5	0.60	24.8
Heritage Park	W-2	2	On shore	4.61	0.60	42.0
Boat Ramp	DP-2	2	Riverbed	1.17	0.46	30.6

Falling- and rising-head slug tests were also conducted on monitoring wells located on shore (Table 6). The K_h values generally corresponded to previously reported values ranging from 6.9 to 363 m/d (Levy et al., 2007) for wells at the Charles M. Bolton well field. Note that at the Fairfield site, the K_h value below the riverbed was much smaller than the value derived on-shore. At the Heritage site the riverbed and on-shore values were much more comparable. Slug tests have yet to be performed for on-shore wells at the North Hamilton and Boat Ramp sites. These tests will be performed by August 2008.

D. Conventional Seepage Meter

All conventional seepage meter results were corrected (as described in the Methods) by multiplying by a factor of 2.1. At the Fairfield site, the hydraulic gradient was always strongly downward (Table 7), averaging -0.258, presumably due to pumping at the Fairfield well field. The riverbed K_v values obtained from ten seepage meter measurements, were highly variable (Table 7, Figure 26) ranging from 0.37 to 9.1 m/d with a geometric mean of 1.9 m/d.

At the Heritage Park site, hydraulic gradients were almost always upward (indicating a gaining reach of the river) and averaged 0.023. The Southwestern Ohio well field is far enough away so as not to induce infiltration from this part of the river. Eight seepage-meters tests were conducted in the sandy riverbed sediment in the northern, shallower part of the river. Riverbed K_v was relatively homogeneous and higher on average than at any other site. Values ranged from 2.3 to 7.9 m/d with a geometric mean of 5.3 m/d (Table 7, Figure 26).

Table 7. Riverbed seepage meter results with accompanying measured parameters.

ID	*Hydraulic gradient*	*Water volume change (ml)*	*Time (min)*	*Corrected[b] Kv (m/d)*
F-S1	-0.179[a]	430	25	4.30
F-S2	-0.179	654	18	9.06
F-S3	-0.464	675	57	1.14
F-S4	-0.227	308	44	1.38
F-S5	-0.354	208	60	0.436
F-S6	-0.242	509	55	1.71
F-S7	-0.051	277	61	4.00
F-S8	-0.051	389	59	5.81
F-S9	-0.065	330	139	1.63
F-S10	-0.256	283	134	0.368
HP-S1	0.0324	745	154	6.66
HP-S2	0.0514	402	154	2.26
HP-S3	0.0427	668	118	5.91
HP-S4	0.0427	389	55	7.38
HP-S5	0.00673	166	140	7.85
HP-S6	0.0340	507	144	4.62
HP-S7	-0.0217	280	117	4.94
HP-S8	0.0120	173	125	5.15
NH-S1	-0.0792	160	56	1.61
BR-S1	-0.538	184	108	0.141
BR-S2	-0.437	171	145	0.120
BR-S3	-0.556	153	129	0.095
BR-S4	-0.750	309	122	0.151
Geometric mean for Fairfield				**1.91**
Geometric mean for Heritage Park				**5.28**
Geometric mean for North Hamilton				**1.61**
Geometric mean for Boat Ramp				**0.125**

[a]Negative gradients are downward, indicating a losing reach.

[b]Values are corrected by multiplying by a factor of 2.1 (see Methods)

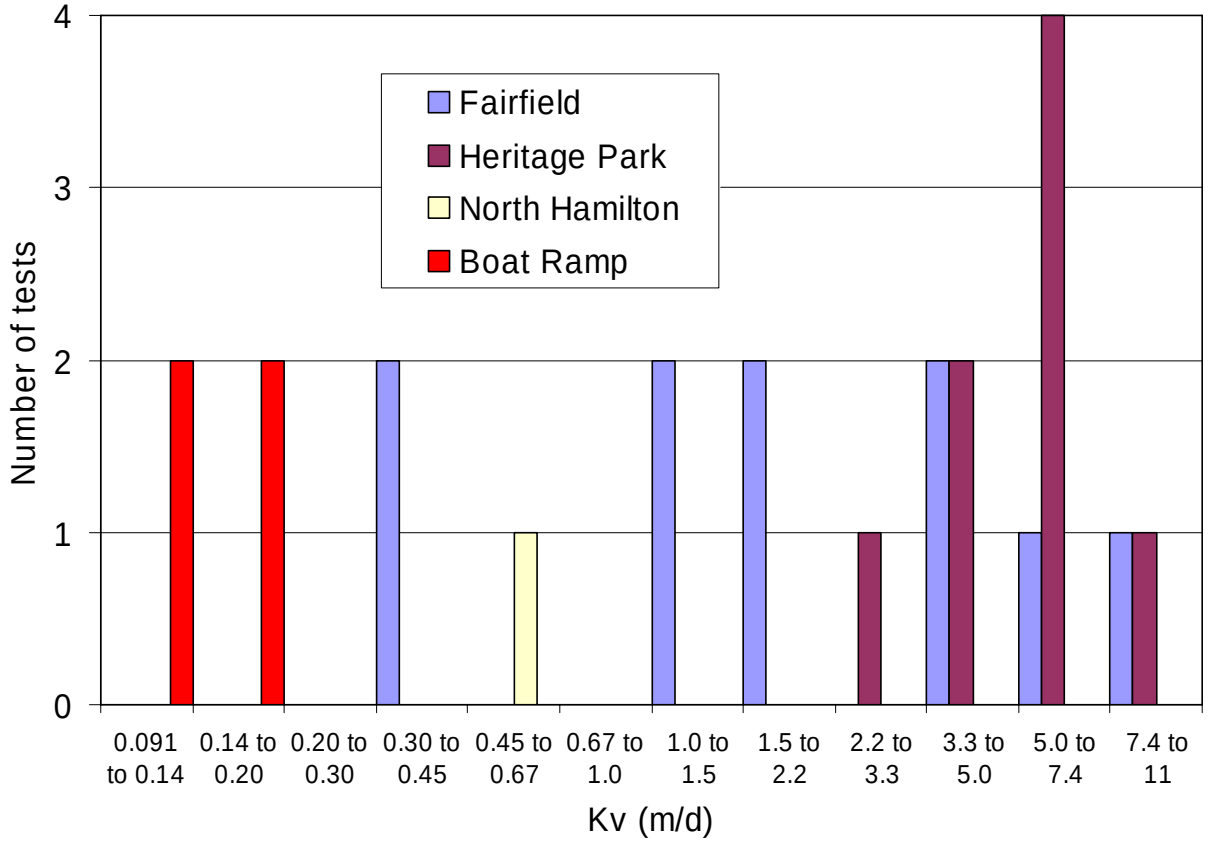

Figure 26: Conventional seepage-meter derived riverbed K_v distribution at the four sites. Ranges are logarithmically distributed assuming a log-normal distribution of values.

At the North Hamilton site, gradients were downward, presumably due to pumping at the North Hamilton well field and a power plant to the south of the North Hamilton water plant. The gradient magnitudes, however, were much smaller than at the other sites (averaging -0.0554). The small gradients combined with low-permeability sediment produced very small seepage fluxes. At the time of this writing, therefore, only one valid seepage test (i.e., losing > 150 mL of water) was obtained for the North Hamilton site which yielded a riverbed K_v value of 0.1.6 m/d (Table 7). We plan to conduct several more tests before the end of August 2008 leaving seepage meters on site for at least 24 hours.

Hydraulic gradients at the Boat Ramp site were strongly downward, averaging -0.512, despite the fact that there is no nearby municipal well field. The downward gradients could result from a dam situated about 1 km downstream. Four seepage-meter measurements were made in the western, shallower part of the river. Riverbed K_v values were lower than at any other sites and ranged from 0.095 to 0.15 m/d, with geometric mean of 0.12 m/d (Table 7, Figure 26).

E Piezo-seep meter

The piezo-seep meter was applied successfully only at the Heritage Park site. The riverbed sediment was too cobbly to press in the mini-piezometer at the Fairfield site. At the Boat Ramp and North Hamilton sites, the mini-piezometer became plugged with fine sediment. The sandy sediment at the Heritage Park site was well-suited to the piezo-seep meter.

Ten tests were performed at eight locations (Table 8). Piezo-seep riverbed K_v values ranged from 64 to 173 m/d with a geometric mean of 101 m/d (Table 8, Figure 27). These values are approximately 40 times greater than the values derived from conventional seepage metering.

Table 8. Piezo-seep meter results from the Heritage Park site.

Date	***ID and Location***	***run***	***Q (mL/sec)***	***Induced gradient***	***K (m/d)***
4/17/2008	PS-1	1	14.0	0.103	173
4/17/2008	PS-2 8 ft from PS-1	1	14.2	0.156	115
4/17/2008	PS-4 next to MP-2	1	13.8	0.152	115
4/18/2008	PS-1 next to MP-4	1	14.3	0.224	80.9
4/18/2008	PS-2	1	12.0	0.132	115
4/18/2008	PS-3 next to MP-1	1	12.2	0.242	64.0
4/18/2008	PS-4 next to MP-5	1	9.52	0.129	93.1
4/24/2008	PS-1 next to MP-8	1	10.4	0.150	88.0
4/24/2008	PS-1 next to MP-8	2	6.51	0.100	82.3
4/24/2008	PS-1 next to MP-8	3	7.84	0.125	79.4
4/24/2008	Mean of 3 runs at PS-1	Mean			83.2
	Geometric mean				**101**

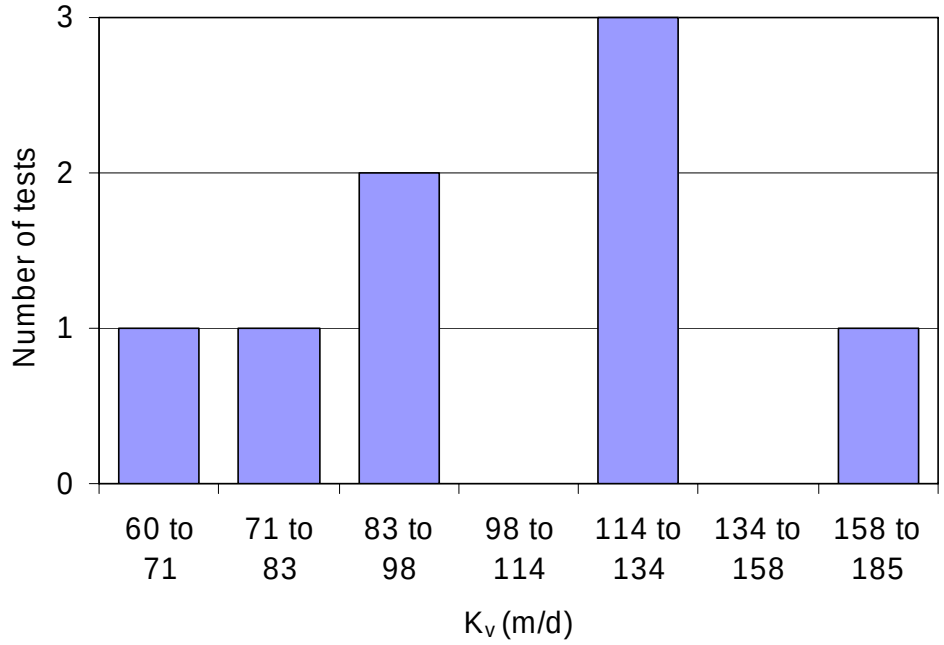

Figure 27: Piezo-seep derived riverbed K_v distribution at the Heritage Park site. Bin ranges are logarithmically distributed assuming a log-normal distribution of values.

F. Infil-seep meter

The infil-seep meter method has been tested at three study sites: Fairfield, North Hamilton and Heritage Park. Complications arose when applying the infil-seep method in the field. At the Fairfield site, the riverbed was too coarse to obtain a good enough seal with the infil-seep meter. At all the sites, when water was poured into the pipe, the pressure inside the seepage cylinder would start to push the instrument out of the riverbed. Several apparently valid tests at the North Hamilton and Heritage Park sites were run while holding the cylinder in place, but the compared to the conventional seepage results, infil-seep K_v values obtained from the infill-seep method were much higher. Infil-seep-derived riverbed K_v values at North Hamilton ranged from 53 to 187 m/d, with geometric mean of 101 m/d (Figure 28). These results are approximately two orders of magnitude higher than those derived from the conventional seepage metering. At the

Heritage Park site, six apparently valid tests were performed. Infil-seep K_v values ranged from 282 to 470 m/d with geometric mean of 347 m/d, again, approximately two orders of magnitude higher than those derived from the conventional seepage metering (Figure 28).

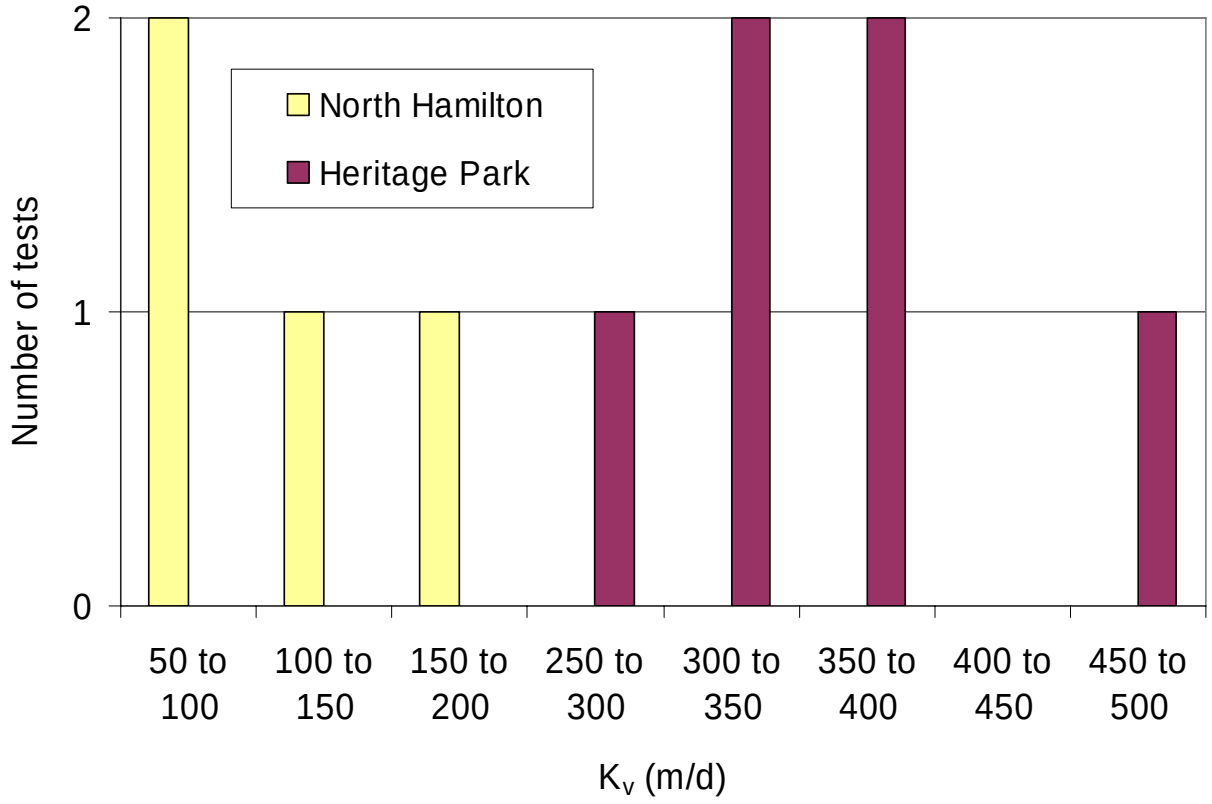

Figure 28. Riverbed hydraulic conductivity distribution at the North Hamilton site based on the infil-seep measurements.

G. Temperature and Water-Level Patterns

Temperatures and water levels were monitored for a period of several months at each study site in piezometers on shore, in piezometers below the river and in the river. Water levels in the observation wells and river stage for each study sites are presented in Appendix 2. At the Fairfield site, data were collected from June to October, 2007 (Figure 29). The river temperature apparently experienced dramatic diurnal fluctuations during this time. In addition, the river temperature dropped each time there was a rain event as can be seen by the relation of the

temperature to the river stage (Figure 29). Temperature fluctuations below the river were indicative of downward gradients and substantial heat transport from the river to the underlying sediment. At the depth of 1.15 m below the river, temperature fluctuated following river weekly fluctuations, with a time lag of about four days. At a depth of 2.98 m, the time lag was about 8 days and the fluctuations were much smaller than those observed at the 1.15-m depth (Figure 29). Being the warmest part of the year, temperatures observed in the on-shore piezometer, F-W1, were substantially lower than those observed in the river and the drive-point wells. Temperatures in F-W1 during this period rose as part of a lagged-seasonal fluctuation.

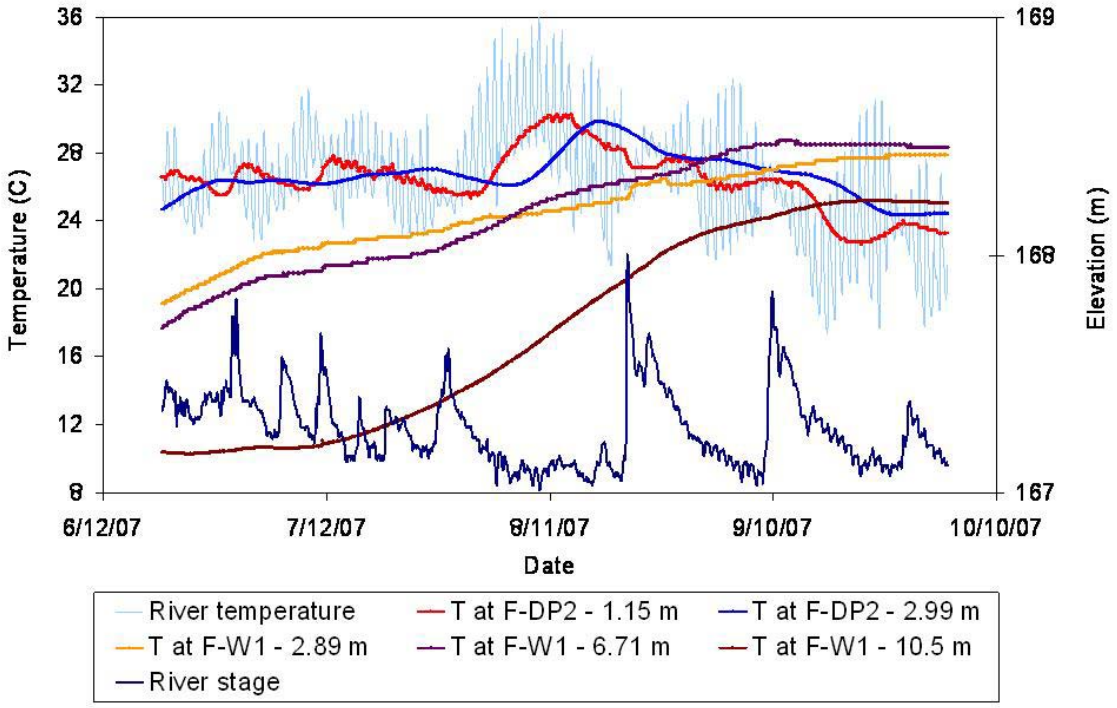

Figure 29: Observed temperatures and river stage at the Fairfield site

At the North Hamilton site data were collected from June to August 2007 and from January to May 2008. Similarly to the Fairfield site, at the North Hamilton site, fluctuations of the subsurface temperatures reflected the downward flow of water from the river (Figure 30). At a depth of 1.16 m, temperature fluctuations lagged behind those of the river by about 2 days. At

the depth of 1.98 m below the river the response to the river-temperature fluctuations was observable, but greatly attenuated. In addition, the temperatures followed the general trend of rising during summer months. Generally constant temperatures were observed in on-shore wells NH-5D and NH-6S indicating that the temperatures had not been affected by the river temperature. Interestingly, temperatures were higher in the deeper well NH-5D than they were in NH-6S despite the greater depth of NH-5D. Temperatures at NH-5D were also constant throughout the observation period. Both these facts could be an artifact of the location of NH-5D in a clayey, low permeability lens. Temperatures in NH-5D probably simply reflect the yearly average while those in NH-6S were still reflecting winter recharge and were steadily rising through the observation period.

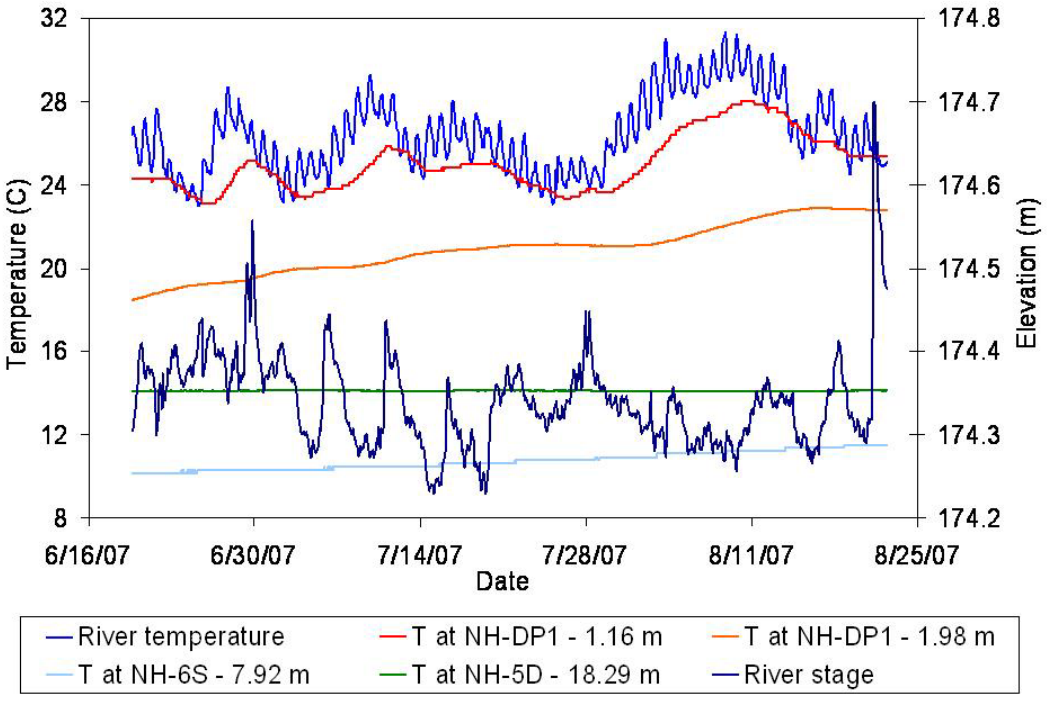

Figure 30. Observed temperatures and river stage at the North Hamilton site

At the Heritage Park site data were collected from July 2007 to February 2008 (Figure 31). Water-level data indicated gaining-stream conditions; heads in HP-DP1 were higher than the

river levels. Due to the lack of downward flow, subsurface temperatures recorded at 0.61 and 1.71 m below the river were much lower (about 10°C) than those in the river. The more dramatic temperature increases in HP-DP1 corresponded to periods of higher river stage (Figure 31). Temperatures observed in the wells HP-W1 and HP-W2 were fairly constant, with slight rising seasonal trend.

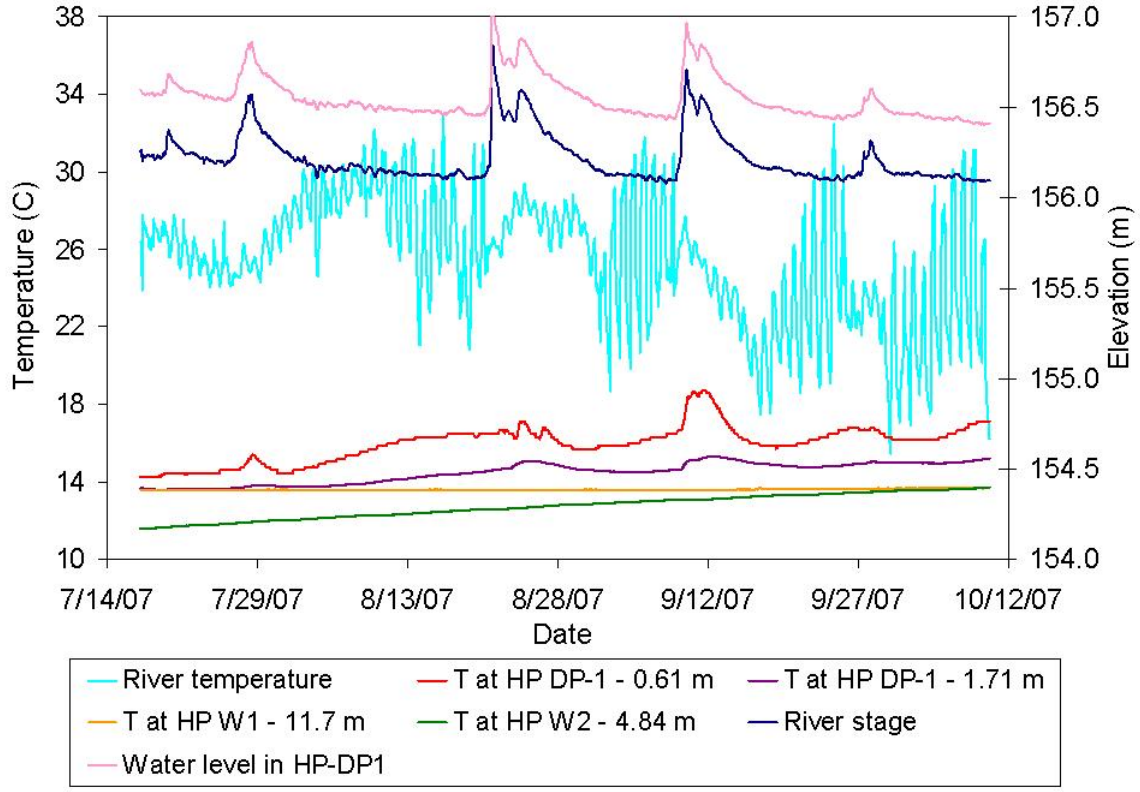

Figure 31. Observed temperatures and water levels at Heritage Park

At the Boat Ramp site, data were collected from February through March 2008 and from April to May 2008. Data in the on-shore well were lost after the flood events in March 2008 and are therefore shown only through March 4. Water levels in BR-DP1, at a depth of 2.29 m, were consistently lower than the river elevation, indicating losing-stream conditions. Yet, the subsurface temperatures exhibited only slight fluctuations compared to river-temperature fluctuations. Water levels at depth and on shore were sometimes higher and sometimes lower

than river level. Temperatures recorded in the well BR-W1 were much higher than those in the river, probably reflecting yearly averages or even a long-lagged summertime influence. For a period of time from April to May 2008, the river temperature steadily rose as did the temperatures in BR-W1.

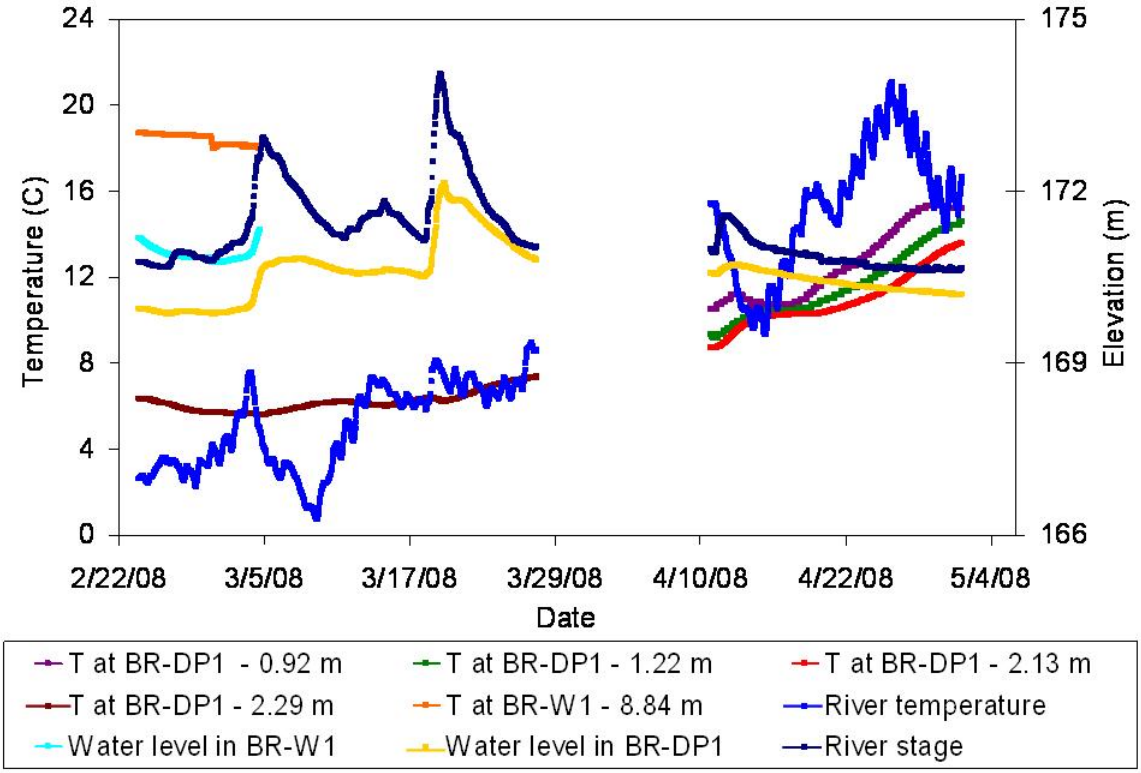

Figure 32. Observed temperature and water levels at Boat Ramp site

H. Heat-flow simulations

Heat-flow simulations were made of each site to make independent estimates of riverbed K_v. Using the VS2DH computer program, two dimensional models were created for each study site and one–dimensional models were created for the Fairfield, Heritage Park and Boat Ramp sites. Transport of heat and water was simulated to generate sets of model-predicted temperature changes over time for observation points located below the river.

H1. Fairfield site

For the Fairfield site, temperature changes over time were simulated in F-DP2, at the depths of 1.15 and 2.98 m for the period between June and October, 2007. The two-dimensional model was discretized with a uniform grid of 120 columns and 100 rows. The top of the model domain occupied by the river was modeled as a specified variable-head boundary, the middle of the river and the bottom of the model were modeled as no-flow boundaries (as shown for the general case in Figure 24). Flow was assumed to be mainly horizontal at depth and, therefore, a no-flow boundary was used at a depth of 60 m. The water level measured in F-DP2 on the first day of sampling was used as the initial water-table elevation. Initial temperatures were interpolated from measurements taken in the first 30 minutes of sampling from the river, both measurement depths in F-DP2 and from the monitoring well F-W1.

The 1D model was discretized with a uniform grid of 50 columns and 50 rows . The top and bottom boundaries were specified as the variable-head boundaries. The same hydraulic properties were used as for the 2D model (Table 3).

Actual and simulated temperatures at piezometer F-DP2 at a depth of 1.15 m are shown in Figures 33 and 34 for the 2D and 1D simulations, respectively. Each figure shows the simulated temperatures with a range of K_v values representing the top 1 m (the riverbed) of the model domain. The rest of the model domain was assumed to comprise material with a K_h of 100 m/d (Sheets and Bossenbroek 2005). Both simulations indicated that values between 0.073 and 0.26 m/d provided realistic fits to the observed data. A K_v of 0.073 m/d provided the best fit for the 2D model while a value of 1.5 m/d provided the best fit of the 1D model.

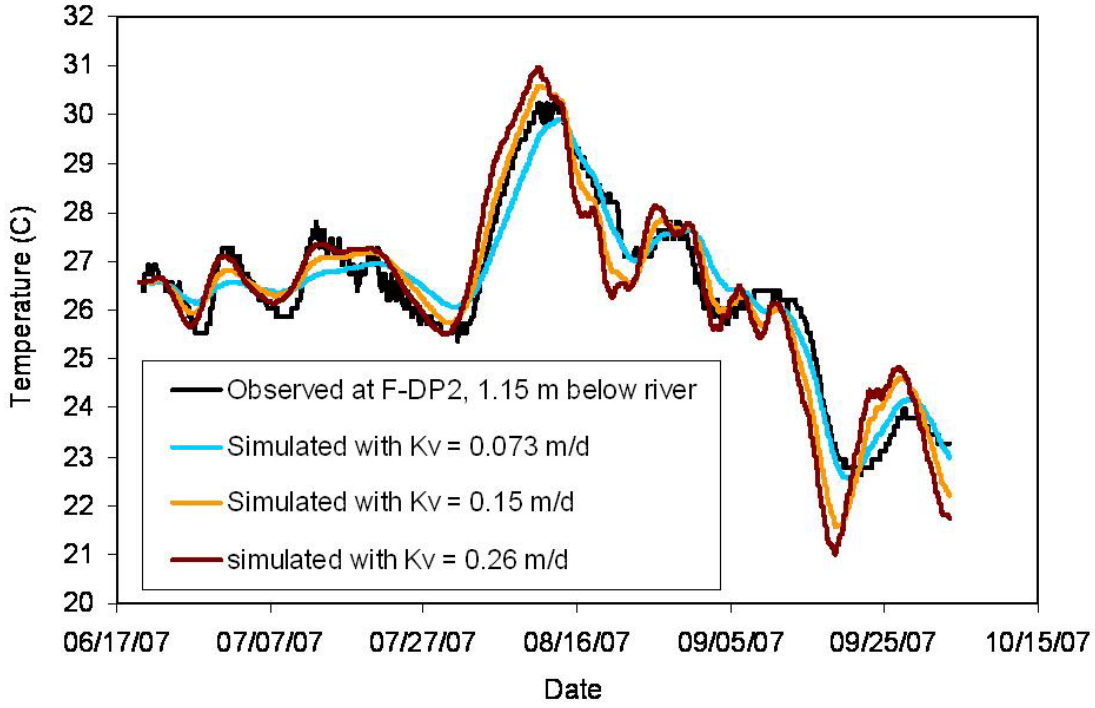

Figure 33. Two-dimensional VS2DHI-simulated and observed riverbed temperatures at the Fairfield site at a depth of 1.15 m with a range of K_v values.

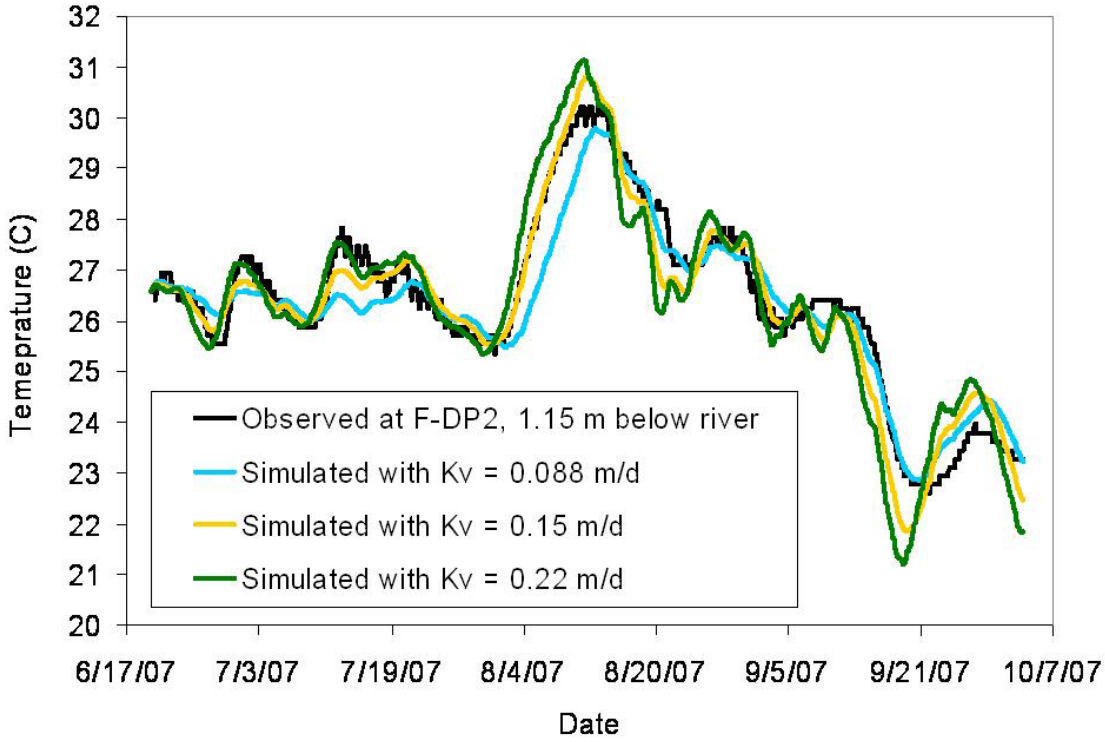

Figure 34. One-dimensional VS2DHI-simulated and observed riverbed temperatures at the Fairfield site at a depth of 1.15 m with a range of K_v values.

The simulations indicated that there might have been some temporal variability of K_v as might be expected with storm-related scour and deposition. For example, a value of 0.26 m/d provided a better fit to the observed temperatures from June 19 to July 30, 2007, whereas the K_v values of 0.15 and 0.073 m/d provided better fits from July 30 to August 20 and from August 8 to October 3, 2007, respectively.

For the observation depth of 2.98 m (also in F-DP2), the 2D model was used and the best K_v values ranged from 0.051 to 0.15 m/d (Figure 35). From June 19 to October 3, 2007, the K_v value that provided the best fit varied temporally from 0.15 to 0.073 m/d and finally to 0.051 m/d. There was good agreement between the best-fit values for the 1.15 m and 2.98 m depths.

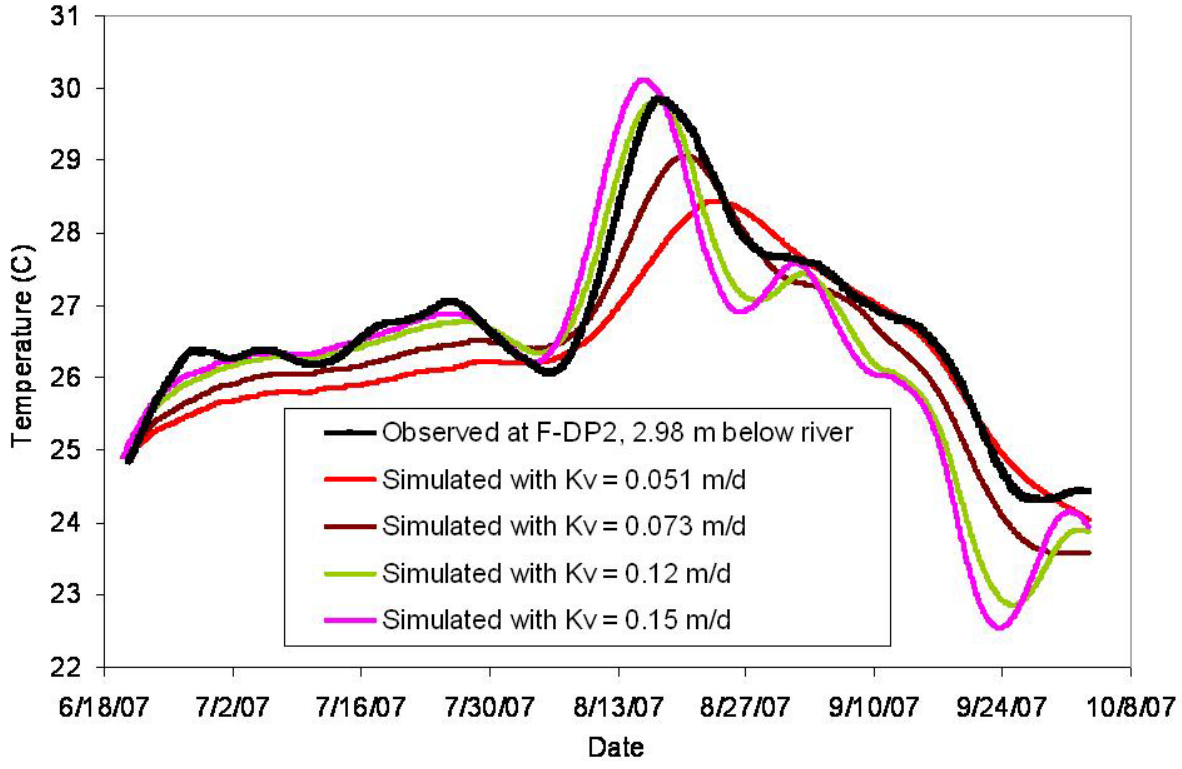

Figure 35. Two-dimensional VS2DHI-simulated and observed riverbed temperatures at the Fairfield site at a depth of 2.98 m with a range of K_v values.

H2. North Hamilton site

At the North Hamilton site, temperature changes were simulated over time in NH-DP1, at a depth of 1.16 m below the river for the period of June to August 2007 using the two-dimensional approach. The 2D model was discretized with a uniform grid of 150 columns and 120 rows. As with the Fairfield model, the top of the model domain that was occupied by the river was modeled as a specified, variable-head boundary; the middle of the river and the bottom of the model were modeled as no-flow boundaries. The rest of the model domain was created based on the cross section of the GMBVA at the North Hamilton well field site (Figure 8, Sheet and Bossenbroek, 2005). The measured water level in NH-DP1 on the first day of sampling was used as the initial water-table elevation. Initial temperatures were interpolated from measurements taken in the first 30 minutes of sampling from the river, both measurements depths in NH-DP1 and from the monitoring wells NH-5D and NH-6S (Figure 15). Temperatures at piezometer NH-DP1 were simulated using a variety of K_v values representing the top 1 m (riverbed) of the model domain (Figure 36). The match of simulated to observed values was not as good as at the Fairfield site. Higher values of K_v produced the right amount of fluctuation but with temperatures a bit too high. Alternatively, lower values simulated the observed average temperature but underestimated the degree of observed temperature fluctuation. Based on the simulations, it appears that the best values are between 0.0037 and 0.037 m/d with the median value of 0.024 m/d (Figure 36).

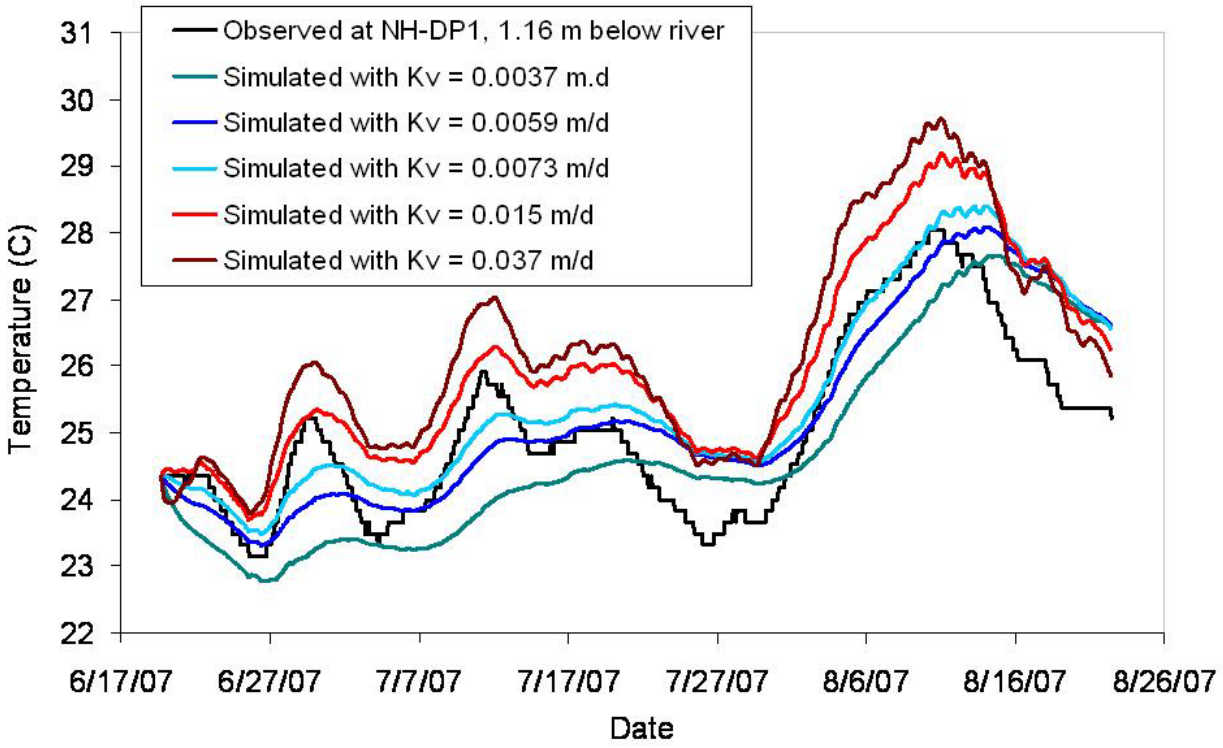

Figure 36. Two-dimensional VS2DHI-simulated and observed riverbed temperatures at the North Hamilton site at a depth of 1.1 m with a range of K_v values.

H3. Heritage Park

At the Heritage Park site, temperature changes over time were simulated in HP-DP1, at a depth of 0.61 m below the river for the period between July to October 2007. A one-dimensional model was used, discretized with a uniform grid of 50 columns and 50 rows. The top of and the bottom boundaries were specified as variable-head boundaries. The water level measured in HP-DP1 on the first day of sampling was used as the initial water-table elevation. Initial temperatures were interpolated from measurements taken in the first 30 minutes of sampling from the river and from HP-DP1 at two measurements depths. Simulated temperatures at piezometer HP-DP1 did not fit the observed data well (Figure 37). A K_v value of about 3.7 to 5.9 m/d matched the observed magnitude of temperature fluctuations, but all simulated K values

underestimated the observed overall temperature. More investigation is needed to determine why the simulations did not work as well at this site.

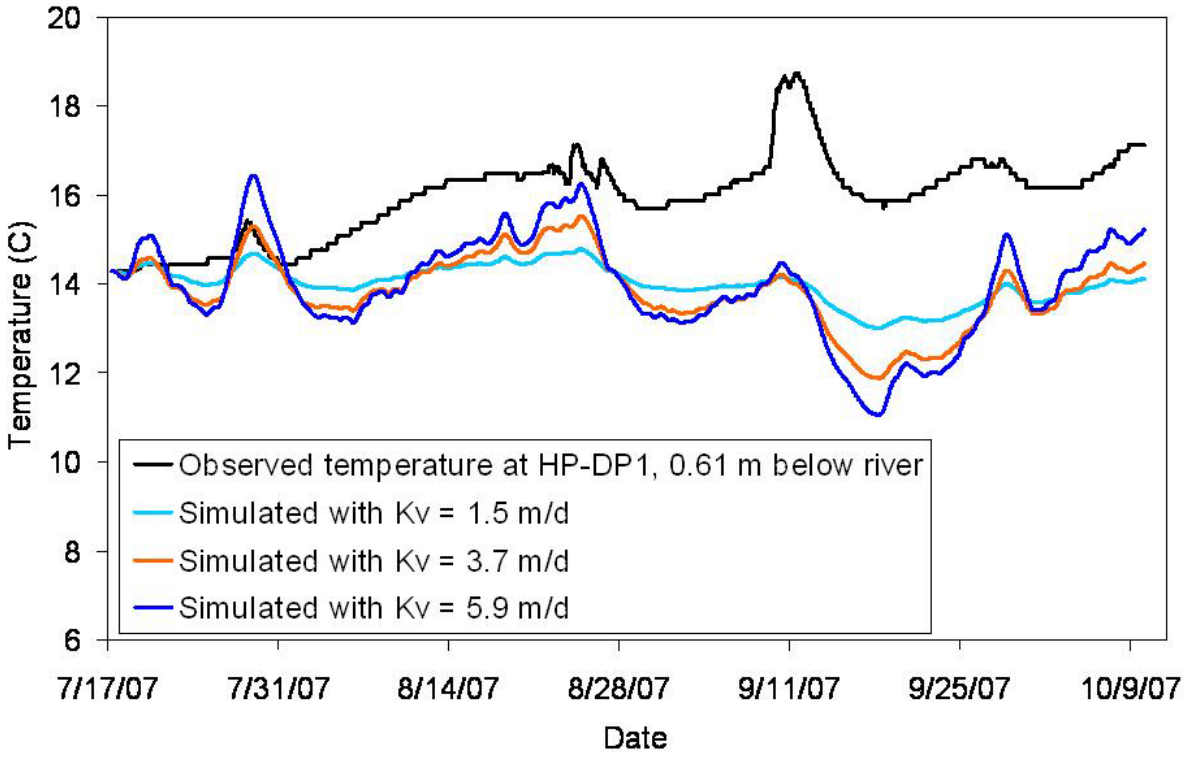

Figure 37. One-dimensional VS2DHI-simulated and observed riverbed temperatures at the Heritage Park site at a depth of 0.61 m with a range of K_v values.

H4. Boat Ramp site

At the Boat Ramp site, temperature changes over time were simulated in BR-DP1, at a depth of 1.22 m below the river for the relatively short period between April and May 2008. (Equipment and data were lost in the floods in March 2008; equipment was replaced in April.) A one-dimensional model was used, discretized with a uniform grid of 50 columns and 50 rows. The top of and the bottom boundaries were specified as variable-head boundaries. The water level measured in BR-DP1 on the first day of sampling was used as the initial water-table elevation. Initial temperatures were interpolated from measurements taken in the first 30 minutes of sampling from the river and from the three measurements depths in BR-DP1.

Simulated temperatures at piezometer BR-DP1 fit the observed data best with K_v values 0.59 to 0.73 m/d (Figure 38).

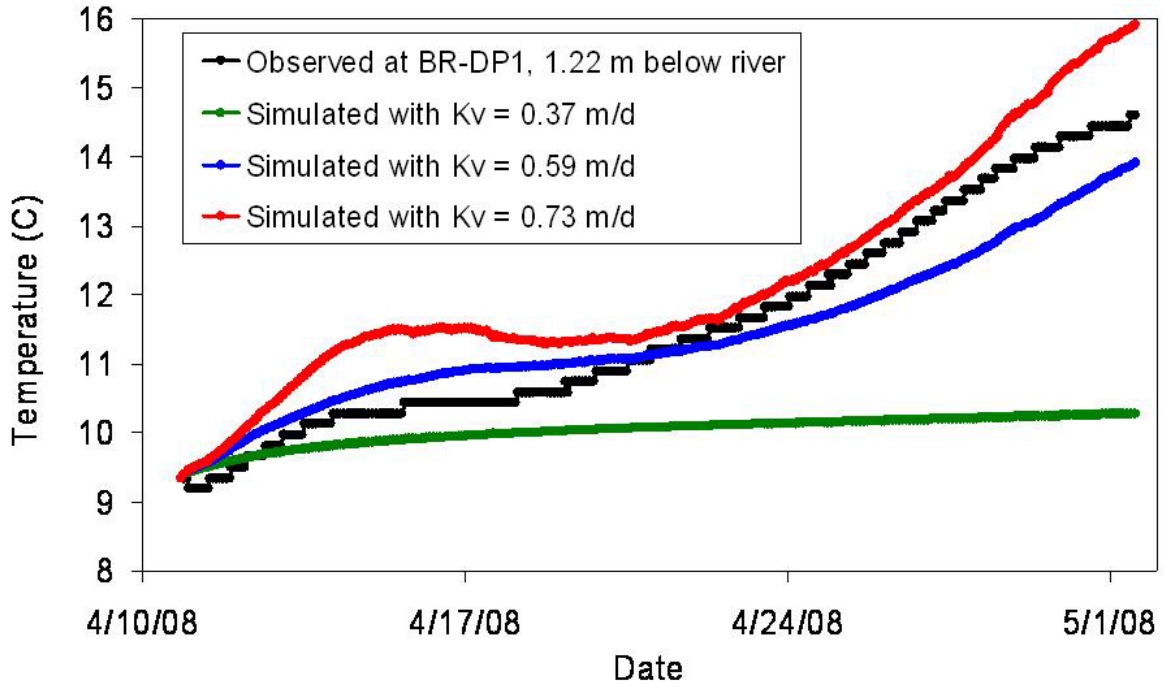

Figure 38. One-dimensional VS2DHI-simulated and observed riverbed temperatures at the Boat Ramp site at a depth of 1.22 m with a range of K_v values.

I. Geophysical Surveys

All data from the geophysical surveys have been collected by the USGS, Columbus and are currently being processed and analyzed. The results of these analyses, once available, will be utilized to determine the geometry and thickness of the riverbed along portions the Great Miami River corresponding to the Fairfield, North Hamilton and Boat Ramp sites. Results from the seismic surveys will help in the identification of stratigraphic boundaries in the subsurface immediately below the Great Miami River. The velocities of the seismic waves will provide an insight into the composition of the different stratigraphic layers. Resistivity and conductivity results will be used to identify the presence or absence of an external colmation layer on the

riverbed. The external colmation layer is expected to comprise saturated fine-sediments with very low resistivity values. In cases where the riverbed contains an internal colmation layer (coarse sediments clogged mixed with fines), the resistivity values are expected to be relatively higher than those for the external colmation layers but lower than either the sand and gravel aquifer or bedrock.

J. Summary of Results

Seven methods were applied to measure the riverbed hydraulic conductivity. Some methods measured K_v and some measured K_h (Table 9). For those that measured K_h, a rough approximation would be to divide the value by 10 to compare to the K_v values. There were large discrepancies between the various methods applied. These will be discussed further in the next section.

Table 9. Summary of results. Except for the heat-flow simulations, values represent geometric means. For the heat-flow simulations, ranges are given. The values in parentheses indicate the number of tests performed.

	Fairfield	***North Hamilton***	***Heritage Park***	***Boat Ramp***
Grain-size/Hazen: Kh	2.66 (2)	10.4 (1)	5.32 (2)	-
Laboratory Permeameter: Kv	-	9.03 (1)	51.2 (3)	0.00293 (1)
Slug test: Kh	1.11 (1)	-	44.3 (3)	30.6 (1)
Conventional seepage meter: Kv	1.91 (10)	1.61 (1)	5.28 (8)	0.125 (4)
Piezo-seep meter: Kv	-	-	101 (8)	-
Infil-seep meter: Kv	-	101 (4)	347 (6)	-
Heat flow simulations: Kv	0.051 - 0.15	0.0073 - 0.037	1.5 -5.9	0.59 -0.73

VII. Analysis and Discussion

A. Variability of the Riverbed K_v

A major objective of this study was to provide water-managing agencies with values of the riverbed K_v that could be applied in large-scale groundwater-flow models. This task is challenging not only because of the difficulty of the methods, but because of the inherent

variability of the parameter of interest. Four sites were chosen that spanned an 18-km reach of the Great Miami River and represented a variety of grain sizes. Yet, at each site, there was substantial variability. For example, while the range is much less at the other sites, conventional seepage metering results at the Fairfield site span more than an order of magnitude (0.37 to 5.8 m/d, Table 7). In contrast, the eight seepage meter results from Heritage Park varied by only a factor of three. On the other hand, the two grain-size analyses taken at Heritage Park before and after a major storm event demonstrated the temporal variability of these systems. If the grain sizes can change so dramatically, the river K_v could be changing as well. In the end, what we should expect from an investigation such as this one is a reasonable range of values associated with each site. The spatial and temporal variability need to be taken into account when assessing the various methods. There are some methods for which we were only able to do one or two tests to date. Extreme caution should be used making assessments based on these methods. One or even a few samples may be insufficient to properly characterize the system.

B. Comparison and Assessment of Methods

B1. Heat-flow simulations

Of all the methods applied, there are several advantages to using the heat-flow simulations. First, the simulations are perhaps the most representative of the applied methods in that they are based on in-situ information and they provide estimates of K_v with possibly the least disturbance to the natural riverbed. The only disturbance associated with the method is the initial installation of the piezometers. Second, data are collected over a relatively long period of time. This provides an opportunity to estimate riverbed K_v under a variety of conditions and even get some idea regarding the temporal variability of the system. Third, the estimates represent a larger area than the estimates derived from other methods. All the other methods are point measurements.

The seepage meters covered an area of only about 0.068 m^2. Temperature fluctuations below the riverbed are affected by water moving through a presumably larger area due to what are bound to be constantly shifting groundwater flow directions. The deeper the observation point, the larger the area represented. There are, of course, many model parameters to estimate and for each of these parameters, there is additional uncertainty. We intend to do detailed sensitivity analyses to explore the impacts of those uncertainties. In addition, the modeling outcomes are only as good as the input temperature and hydraulic head data that we have gathered. Obviously, the better the fits of the simulated temperatures to the observed temperatures, the more confidence we can have in the results. In spite of the uncertainty associated with the modeling, we feel that the temperature modeling provides the best estimates we have at this time of riverbed K_v. In the following sections, therefore, results from other methods are compared to those from the temperature-modeling as some measure of their performance. Various methods are also compared to each other.

We have done the most modeling and achieved the best fits for the Fairfield site. The one- and two- dimensional modeling results are very consistent with each other, and the results derived from using observations at different depths are also very consistent. The range of values spanned a factor of 2, but this might actually represent the temporal variability of the system. The temperature fits were also fairly good for the North Hamilton site and the fitted K_v values again spanned a range of about a factor of five. The K_v values, however, were surprisingly low and much lower than observed with any other method. We will continue to investigate this site with more tests of the various methods. The model calibration for the Boat Ramp site was good, but covered a much shorter period of time. As a result, the range of values presented was very small. Finally the temperature simulations at the Heritage Park site did not fit the observed data

as well as at other sites. This was probably due to the fact that the site was within a gaining reach of the river. Temperature fluctuations within the riverbed in gaining reaches are much less than in losing reaches, making model calibration more difficult.

B2. Conventional Seepage Meters

Conventional seepage meters were successfully applied at all sites, although more tests with longer time periods are necessary, especially at the North Hamilton site. Results were reproducible and it seemed that we had good seals even in the coarse-textured riverbed at the Fairfield site.

Riverbed K_v values derived from the conventional seepage meters were generally closer to those derived from the temperature modeling than those of the other methods. Only the conventional seepage metering yielded values that were consistently as low as the model-predicted values. Still, some large discrepancies existed. The values at the Heritage Park site were in excellent agreement to the temperature modeling values, although it should be noted that the simulated temperatures were not matched well to the observed data. At the Fairfield site, however, the conventional seepage-meter results were greater than the temperature modeling estimates by approximately an order of magnitude. At the North Hamilton site, the discrepancy was even greater, but no conclusion should be drawn due to only one seepage measurement there thus far. At the Boat Ramp site, conventional seepage meter K_v values were lower than the temperature model-derived values by about a factor of 5.

Conventional seepage meter results were generally self-consistent. Substantial variability in the seepage meter data existed at the Fairfield site, but not more than might be expected from this cobbly site. Results from the Heritage Park and Boat Ramp sites were surprisingly consistent.

B3. Hazen method and Laboratory Permeameters

The Hazen method and the laboratory permeameter tests were applied to small riverbed-surface samples brought back to the laboratory. The field methods test larger areas and represent what is happening as water moves vertically through a greater depth of sediment than was sampled for the laboratory tests. Discrepancies with field data may arise due to vertical heterogeneities in the field that were not present in the small laboratory samples. When taking samples for the permeameter tests we noticed that the riverbed sediment sometimes changed dramatically within several centimeters of the surface. Generally, the riverbed sediment became much coarser with depth, particularly at the North Hamilton and Heritage Park sites. At the Boat Ramp site also there appeared to be more cobbles with depth. Based on these observations we believe that the K_v values obtained from the permeameter tests may not be representative of the entire riverbed. Moreover, the top riverbed layer is probably repeatedly scoured and re-deposited during high-flow events. This transient sediment may not be representative of what is often a more stable, coarser layer underneath.

The Hazen method (Hazen, 1892) is ideally suited to fairly-well sorted sands (Fetter, 2001). The sediments represented here are generally more heterogeneous than sediment should be for application of this method. The Hazen method uses only the d_{10} to estimate hydraulic conductivity; the relative distribution of the coarser sediment is not taken into account. In lieu of all other methods, a method such as the Hazen method provides an initial estimation of hydraulic conductivity, but it is not surprising that values derived using this method were substantially different than those derived from some of the other field methods. At the Fairfield and North Hamilton sites, the Hazen method yielded values that were higher than conventional seepage metering values and much higher than the values derived from temperature modeling (Table 9).

Interestingly, the Hazen derived value for Heritage Park was in close agreement with conventional seepage metering, slug tests and heat-flow simulations.

The most direct comparison possible is between the Hazen method and the laboratory permeameter tests. This comparison was possible only at the North Hamilton and Heritage Park sites. For the North Hamilton site, where the sediment was a well-sorted medium sand, there was very good agreement between these methods (Table 9). For the Heritage Park site, the samples used for the laboratory permeameter tests came from after the January 2008 high-stage event, corresponding to one of the grain-size samples that yielded a Hazen-method estimate of 8.4 m/d. The Hazen method estimate is lower than the laboratory permeameter test by a factor of 6.

B4. Slug tests

Slug tests are a very common hydrogeological method for estimating hydraulic conductivity in the area around a well screen. There were two complications with regard to using them in this study. The first was that we were concentrating our study on the riverbed, approximately the shallowest meter or so underlying the river. Riverbed slug tests were performed in drive-point wells. To consider the tests valid, it was necessary to drive them far enough into the river bed to avoid any direct hydraulic connection with the river. We had to compromise between preventing this connection and keeping the drive-point piezometers shallow to measure the layer of interest. Ultimately we performed slug tests in a deeper part of the system than was studied with the seepage meters, and if the seals were not perfect, the resulting measurement would be an overestimation of hydraulic conductivity.

The second complication with comparing other methods to slug tests was that the slug tests estimated K_h rather than K_v. To compare the values to those from other methods, we needed to

estimate a K_v/K_h anisotropy ratio. The anisotropy ratio is itself highly variable and difficult to measure. We used an estimate of 0.1, but its uncertainty should be considered when comparing these methods.

At the Fairfield site, only one slug tests was performed to date. The K_h derived from this test was in fairly close agreement with other methods, especially with the temperature modeling. The Heritage Park riverbed slug-test mean was 44.3 m/d corresponding to a K_v of approximately 4.4 m/d, a value that compared well to the conventional seepage value and the heat-flow simulation estimation. Only one slug test has been performed thus far at the Boat Ramp site, and the derived hydraulic conductivity was much higher than values from other methods. More slug tests are needed at the Boat Ramp site to better understand the apparent discrepancy. Slug tests also still need to be performed at the North Hamilton site.

B5. Piezo-seep meters

The piezo-seep meters have the advantage of generating their own gradients. They are not depended on the natural inflow or outflow of water through the riverbed. It is possible, therefore, to perform many tests relatively quickly. The disadvantage is that it can be difficult to push the attached mini-piezometer into the riverbed and there is uncertainty associated with not knowing if there is a good enough seal around the mini-piezometer. This is especially true in coarser sediment where the piezo-seep meter is simply not practical. On the other hand, in sediment that is too fine, the mini-piezometer can get plugged, which is what occurred at the North Hamilton and Boat Ramp sites. So far, therefore, we have only been used successfully at the Heritage Park site. It should be possible to use a smaller piezometer screen in fine-sediment settings.

Values were self-consistent, but much higher than the values from conventional seepage meters and the temperature modeling. We had previously performed tests with the piezo-seep in controlled conditions in a large tank filled with a fairly uniform sand. In that setting, the piezo-seep method was in close agreement with other methods. The reasons for the large discrepancies at Heritage Park are unknown and warrant more investigation. One possibility is that there was not a good enough seal around the mini-piezometer. If the mini-piezometer was in direct hydraulic connection to the river, the measure gradient would be too low resulting in an over-estimation of hydraulic conductivity. The solution to this problem might be a longer piezometer.

B6. Infil-seep meters

Infil-seep meters in theory work just like in-situ permeameters (e.g., Landon et al., 2001). We designed the infil-seep meter so that it would have the advantage of a small input tube with larger seepage bucket. This allows us to induce substantial changes in head with relatively little water and still test a relatively large area of the riverbed. Unfortunately, the biggest problem that we encountered was that the pressure inside the bucket would become so great as to push the entire infil-seep up and out of the riverbed. Typically, we had to stand on the bucket to prevent its rising out of the sediment.

All values derived from the infil-seep were very high, ranging from 101 to 347 m/d. We believe that these high values might have resulted from the bucket pushing up and losing connection with the riverbed or that the pressure was great enough in the bucket as to blow sediment out away from the sides of the bucket. In either case, the direct hydraulic connection with the river would result in erroneously high K_v values. In the end, we do not believe that the infil-seep method is viable. The high pressures will continue to raise doubts with the results.

C. Addressing the Low Riverbed K_v values

Based on the conventional seepage metering and temperature modeling, at all four field sites, the riverbed K_v is much lower than the typical K_h of the Great Miami Buried Valley Aquifer. This was found to also be the case in a previous study by Miami University conducted at the Bolton site, adjacent to the Charles M. Bolton well field, about midway between the Fairfield and Heritage Park sites. At the Bolton site, riverbed K_v values derived from conventional seepage metering ranged from 0.0080 to 0.81 m/d with a geometric mean of 0.092 m/d. Temperature modeling at the Bolton site yielded K_v estimates from 0.061 to 0.21 m/d (Levy et. al, 2007). The results were very similar to those from the Fairfield site (Table 9). The low values were in contrast to the visibly-coarse nature of the riverbed at both sites. We present the same hypothesis as we did for the Bolton site (Levy et al., 2007), that there exists a thin clogged or colmation layer comprising a coarse matrix (gravel, pebbles and cobbles) with imbedded fines. Such clogging is especially prevalent where municipal pumping induces downward gradients and the downward movement of fine sediment. In addition, data from the Bolton site suggests that this colmation layer is relatively resistant to scour and is therefore also an armor layer. On top of this layer one can find a mix of sand and gravel that comes and goes depending on the river stage and velocity. It is this transient sediment that we sampled for the laboratory permeameter tests.

The clogged-layer hypothesis is supported by the fact that the riverbed K_v values were lowest at the Fairfield and North Hamilton sites, where municipal pumping occurs. In addition, at the North Hamilton, Heritage Park and Boat Ramp sites, the sediment cores for the laboratory permeameters were collected in plastic tubes which could only be pushed up to 18 cm into the riverbed before encountering a coarser layer that could not be penetrated. In the case of the

North Hamilton, and Heritage Park sites, the laboratory permeameter K_v values were much higher than those from the temperature modeling or conventional seepage metering. We hypothesize that this is because the laboratory permeameters tested the transient sediment overlying a clogged layer. In the case of the Boat Ramp site, it appears as if the overlying sediment was much finer than at the other sites (48 % silt + clay, Table 4) resulting in an extremely low K_v value (based on the laboratory permeameter test). It also appears that underlying the fine sediment at the Boat Ramp site is a coarser layer that is not as clogged as at the other sites. The slug test at the Boat Ramp site was at a mid-screen depth of 1.17 m, probably below the silty/clayey sediment. The heat-transport modeling at the Boat Ramp site matched temperatures at a depth of 1.22 m. It is possible that the K_v value of 0.59 to 0.73 m/d from the modeling reflects a combination of a thin layer of fines overlying a much more conductive layer represented by the slug test.

An important aspect of this study to keep in mind is that we were limited in all our work and at each site to the shallower, point-bar side of the river where one would expect to find the finest riverbed sediment. It is probable that the riverbed K_v is much higher in the thalweg and on the cut-bank side where the current is faster and only coarser sediment would be deposited. In a previous study on the Calumet River, Duwelius (1996) found the highest K_v values occurring near the center of the river. It is probable that all our values are biased toward the low end. Of all the techniques applied in this study, only temperature modeling is practical for covering a larger area of the Great Miami River riverbed. To cover larger areas, thermisters need to be installed in more on-shore and riverbed piezometers at a greater variety of depths to intercept more flow paths from the river to the aquifer.

VIII. Summary and Conclusions

The goal of this study was to estimate appropriate values for riverbed vertical hydraulic conductivity (K_v) of the Great Miami River in a variety of settings between Hamilton and Cincinnati, Ohio. Quantifying the riverbed K_v is important when trying to understand groundwater/surface-water interactions. Such interactions are crucial for making predictions and decisions about local water supply and water quality. Four field sites were chosen representing a variety of riverbed sediments from silt and clay to cobbles. Estimates of riverbed K_v were made applying a variety of methods at a variety of scales including three types of seepage meters, slug tests, laboratory permeameter tests, grain-size analyses and modeling of heat and flow transport between the river and groundwater. Some general conclusions were:

- The various methods yielded some very different riverbed K_v values. It therefore becomes important to know which methods to rely on and which methods are most appropriate in which settings.
- The infil-seep method did not work. The method produces pressures that disturb the seepage bucket and/or the sediment around the bucket. As a result, the method produced K_v values that were much higher than those derived from other methods. We do not consider these data to be trustworthy.
- The piezo-seep meter method was also problematic. It could only practically be applied in relatively uniform sand. Sediment that was either too coarse or too fine prohibited its applicability. At the Heritage Park site it was used with apparent consistency, and yet it yielded values that were higher than other methods by a factor of about 20. The geometric mean K_v was 101 m/d. The high values could have been the result of an insufficient seal around the mini-piezometer.

- Conventional seepage metering, like the previous two seepage-meter methods, measured the riverbed K_v on a fairly small scale: cross sectional areas of 0.068 m^2. Results were consistent and reproducible. Values of K_v were very small compared typical values of horizontal hydraulic conductivity of the glacial outwash. Mean values ranged from 0.13 m/d for the silty Boat Ramp site, 1.61 m/d for the sandy and silty North Hamilton site, 1.91 m/d for the sandy, pebbly and cobbly Fairfield site to 5.28 m/d for the sandy Heritage Park site.
- Heat and flow transport was modeled for time periods of one month to 4 months using the USGS program VS2DH. The temperature modeling method covers larger areas, greater depths and longer time periods than do any of the other methods. The method is therefore more appropriate for the purposes of obtaining K_v values for use in large-scale flow models. Observed temperatures were matched well at the Fairfield and Boat Ramp sites and to a lesser degree at the North Hamilton site. The matches were not good at the Heritage Park site, probably due to the upward gradients there. The modeling yielded K_v values of 0.0073 to 0.037 m/d for the North Hamilton site, 0.051 to 0.15 m/d for the Fairfield site, 0.59 to 0.73 m/d for the Boat Ramp site and 1.5 to 5.9 for the Heritage Park site. K_v values generated from this method were generally lower than the values obtained through the conventional seepage metering or any other method.
- The permeameter laboratory tests provided the K_v values over the very small areas corresponding to the 3.5-cm diameter sampling tubes. Permeameter K_v values averaged 0.00293 m/d for the Boat Ramp, 9.03 m/d for the North Hamilton and 51.2 m/d for Heritage Park site. These values represent only top 12-18 cm of the riverbed sediment, so

their applicability is limited. More samples will be needed from each site to better assess the representativeness the K_v values from this method

- Slug tests conducted in the riverbed resulted in values of K_h at deeper points than for the seepage metering or laboratory permeameter tests. Also, to infer a K_v value, one must estimate a K_v/K_h anisotropy ratio. Using a value of 0.1 the average slug test K_v values were 0.11 m/d at the Fairfield site, 3.06 m/d at the Boat Ramp site and 4.43 m/d at the Heritage Park site. These values agree fairly well with the heat-flow simulation results and to some extent with the conventional seepage-metering results.
- Of all the methods, we have the most confidence in the conventional seepage metering and the temperature modeling due to their reproducibility and appropriateness of scale. While they differ to some extent, both methods result in relatively values of riverbed K_v. Our best estimates would be derived from some combination or averaging of these methods.
- Riverbed K_v values for the sites located next to municipal well fields (North Hamilton, Fairfield) were lower than for other two sites. This is especially surprising given the coarse-textured riverbed at the Fairfield site. We hypothesize that this is due to clogging of a relatively coarse sediment matrix with fine sediment that is pulled into the matrix under the influence of pumping.
- We were unable at this time to incorporate results obtained from the USGS geophysical investigation of the riverbed lithostratigraphy. More coordination with the USGS is needed to compare data. This work will be our main thrust in the next two months.

Intensive investigation on the riverbed hydraulic conductivity yielded in wide ranges of values for different methods. It is difficult to compare them directly and more difficult to give a

single representative K_v value for each site. Estimation is complicated by the high spatial variability of the Great Miami River sediments and the dynamic character of the riverbed. Still, we do believe that the riverbed K_v values are much lower than the K_h values for the aquifer materials. This lower K_v would hamper the volume of water exchange between the river and groundwater and slow down any potential contaminant transport.

One of the limitations of the research in the big rivers is that all the measurements can be conducted only in the shallow water and there is no possible to cover entire reach of river with measurements. Therefore, measured Kv values may not the representative for the entire riverbed. This limitation could be overcome by concentrating on the heat-transport simulation approach with an expanded monitoring network, especially in areas of induced infiltration.

IX. References

Alexander, M.D and Caissie, D, 2003 Variability and comparison of hyporheic water temperatures and seepage fluxes in a small Atlantic salmon stream, Ground Water, 41(1), 72-82

ANCID, 2004, Australian National Committee on Irrigation and Drainage (ANCID): Channel seepage management tool, point measurement: principle, method http://ancid.org.au/seepage/3_3_31_pointMeasPrinc.html

Anderson, M.P., 2005, Heat as a groundwater tracer. Ground Water, 43 (6), 951-968

Arriaga, M.A and Leap, D.I., (2006) Using solver to determine vertical groundwater velocities by temperature variations, Purdue University, Indiana, USA, Hydrogeology Journal 14:253-363

Bartolino, J.R., Niswonger, R.G., 1999 Numerical simulation of vertical ground-water flux of the Rio Grande from ground-water temperature profiles, Central New Mexico U.S. Geological Survey Water-Resources Investigation Report 99-4212

Baxter, C., Hauer, F.R., Woessner, W.W., 2003 Measuring groundwater-stream water exchange: New techniques for installing minipiezometers and estimating hydraulic conductivity. Transactions of the American Fisheries Society 132: 493-502

Becker, M.W., Georgian, T., Ambrose, H., Siniscalchi, J., Frederick, K, 2006 Estimating flow and flux of ground water discharge using water temperature and velocity. Journal of Hydrology, 296, 221-233

Belanger, T.V and Montgomery, M.T., 1992 Seepage meters errors. Limnology and Oceanography, 37(8): 1787-1795

Belaval, M., Lane, J.W., Lesmes, D.P, Kineke, G.C., 2003, Continuous-resistivity profiling from coastal ground-water investigations: three case studies. Symposium on the Application of Geophysics to Engineering and Environmental Problems (SAGEEP), April 6-10, 2003, San Antonio, Texas, Proceedings: Denver, Colorado, Environmental and Engineering Geophysics Society, CD-ROM, 14 pp water.usgs.gov/ogw/bgas/publications/SAGEEP03_Belaval/SAGEEP03_Belaval.pdf

Bouwer, H and Rice, R.C., 1976 A slug test method for determining hydraulic conductivity of unconfined aquifers with completely or partially penetrating wells. Water Resources Research 12 (3): 423-428

Bouwer, H., 1989 The Bouwer and Rice slug test – an update. Ground Water 27, no. 3: 304-309.

Boyle, D.R, 1994 Design of a seepage meter for measuring groundwater fluxes in the nonlittoral zones of lakes- evaluation in a boreal forest lake. Limnology and Oceanography, 39(3): 670-681

Brick, M.D., 2006 Temporal variability of riverbed hydraulic conductivity at an induced infiltration site, southwest Ohio. M.S Thesis, Miami University

Brodie, R.S., Baskran, S., Ransley, T., Spring, J., 2005. The seepage meter: processing a simple method of directly measuring water flow between surface water and groundwater systems, www.connectedwater.gov.au/documents/IAH05_SeepMeter.pdf

Burger, H.R., 1992 Exploration geophysics of the shallow subsurface. Library of Congress Cataloging-in-Publication Data, ISBN 0-13-296773-1

Cable, J.E., Burnett, W.C., Chanton, J.P., Corbett, D.R., and Cable, P.H., 1997a. Field evaluation of seepage meters in the coastal marine environment. Estuarine, Coastal and Shelf Science 45, 367-375

Cable, J.E., Burnett, W.C and Chanton, J.P., 1997b. Magnitude and variations of groundwater seepage along a Florida marine shoreline, Biochemistry 38: 189-205

Cardenas, M.B and Zlotnik, V.A., 2003 A simple constant-head injection test for streambed hydraulic conductivity estimation. Ground Water 41(6): 867-871

Calver, A., 2001 Riverbed permeabilities: Information from pooled data. Ground Water 39(4):546-553

Cey, E.E., Rudolph, D.L., Parkin, G.W., and Aravena, R., 1998 Quantifying groundwater discharge to a small perennial stream in southern Ontario, Canada, Journal of Hydrology 210: 21-37

Chen, X.H., 2000 Measurement of streambed hydraulic conductivity and its anisotropy. Environmental Geology 39(12): 1317-1324

Chen, X.H., 2004 Streambed hydraulic conductivity for rivers in South-Central Nebraska. Journal of the American Resources Association, 561-573

Constantz, J., Thomas, C.J., Zellweger G., 1994. Influence of diurnal variations in stream temperature on stream flow loss and groundwater recharge. Water Resources Research, 30(12): 3253-3264

Constantz, J., 1998. Interaction between stream temperature, stream flow, and groundwater exchanges in alpine streams. Water Resources Research, 34(7): 609-1615

Constantz, J., Stewart, A.E., Niswonger R., Sarma, L., 2002. Analysis of temperature series profiles for investigating stream loses beneath ephemeral channels. Water Resources Research, 38(12), 1316, doi: 10.29/2001WR001221

Constantz, J. Stonestrom, D.A., 2003 Heat as a tracer of water movement near streams. In Heat as a tool for studying the movement of ground water near streams, Stonestrom, D.A., and Constantz, J, US Geological Survey Office of Ground Water and Water Resources. Circular 1260, 96 pp

Constantz, J., Cox, M., Su, G.W., 2003 Comparison of heat and bromide as ground water tracer near streams. Ground Water, 41(5), 647-656

Cox, M., Rosenberry, D., Su, G., Conlon, T., Lee, K., and Constantz, J., 2002. Comparison of methods to estimate streambed seepage rates in Kenny, J.F., ed., Ground Water/Surface

Water Interactions, AWRA 2002 Summer Specialty Conference Proceedings: American Water Resources Association, Middleburg, Virginia, 519-523

Cox, M., and Hatch, Ch., 2003 Water temperature, streamflow and ground-water elevation in and adjacent to the Russian River between Hopland and Guerneville, CA from 1998-2002. U.S. Geological Survey, Open-Report 03-454

Cox, M.H, Su, G.W., Constantz, J., 2007 Heat, chloride, and specific conductance as ground water tracers near streams, Ground Water 45(2): 187-195http://www.google.com/search?hl=en&client=firefox-a&rls=org.mozilla:en-US:official&hs=PKw&q=related:water.usgs.gov/ogw/bgas/publications/SAGEEP03_Belaval/SAGEEP03_Belaval.pdf

Cunningham K.J., Locker S.D., Hine A.C., Bukry D., Barron J.A., Guertin L.A., 2001 Surface-Geophysical characterization of groundwater systems of the Caloosahatchee River Basin, Southern Florida. U.S. Geological Survey Water-Resources Investigations Report 01-4084

Dawson, C.B., Lane, J.W., White, E.A., Belaval, M., 2002 Integrated geophysical characterization of the Winthrop landfill southern flow path, Winthrop, Maine, in Symposium on the Application of Geophysics to Engineering and Environmental Problems, Las Vegas, Nevada, February 10-14, 2002, Proceedings: Denver, Colo., Environmental and Engineering Geophysical Society, CD-ROM, 22p

Doppler, T., Franssen, H.J., Kaiser, H.P., Kuhlman, U., Stauffer, F., 2007 Field evidence of dynamic leakage coefficient for modeling river-aquifer interactions. Journal of Hydrology 347: 177-18

Dumouchelle, D.H., 2001 Evaluation of ground-water/surface water relations, Chapman Creek, West- Central Ohio, by means of multiple methods, U.S. Geological Survey, Water Resources Investigations Report 01-4202

Duwelius, R.F., 1996 Hydraulic conductivity of the streambed, east branch Grand Calumet River, Northern Lake County, Indiana. U.S Geological Survey, water-Resources Investigation report 96-4218

Dowman, Ch.E., Ferre, T.P., Hoffmann, J.P., Rucker, D.F., Callegary, J.B., 2003 quantifying ephemeral streambed infiltration from downhole temperature measurements collected before and after streamflow. Vadose Zone Journal, 2, 595-601Dumouchelle, D.H., 2001 Evaluation of ground-water/surface water relations, Chapman Creek, West- Central Ohio, by means of multiple methods, U.S. Geological Survey, Water Resources Investigations Report 01-4202

Duwelius, R.F., 1996 Hydraulic conductivity of the streambed, east branch Grand Calumet River, Northern Lake County, Indiana. U.S Geological Survey, water-Resources Investigation report 96-4218

Fetter, C.W. 2001 Applied Hydrogeology. Prentice-Hall, Inc. Upper Saddle River, N.J

Fox, G., 2003 Estimating streambed and riverbed aquifer parameters from a stream/aquifer analysis test. Hydrology Days: 68-79

Freeze, R.A and Cherry, J.A., 1979 Groundwater, Prentice Hall Inc Englewood Cliffs, NJ

Haeni, F.P., 1986 Application of continuous-seismic reflection methods to hydrologic studies, Groundwater 24(1):23-31

Hatch, Ch.E., Fisher, A.T., Revenaugh,, J.S., Constantz, J., 2006 Quantifying surface water-groundwater interactions using time series analysis of streambed thermal records: Method development. Water Resources Research 42, W10410, doi: 10.1029/2005WR004787

Hazen, A. 1892 Some physical properties of sands and gravels, with special reference to their use in filtration. 24th Annual Report, Massachusetts State Board of Health, Pub.Doc. No.34, 539-556

Healy, R.W and Ronan, A.D., 1996 Documentation of the computer program VS3DH for simulation of energy transport in variably saturated porous media—modification of the U.S. Geological Survey's Computer Program VS2DT, U.S. Geological Survey Water-Resources Investigation Report 96-4230, 36 pp

Hiscock, K.M., and T. Grischek. 2002. Attenuation of groundwater pollution by bank filtration. Journal of Hydrology 266, 139-144.

Hsieh, P.A., Wingle W., Healy R.W., 2000 VS2DHI—A graphical software package for simulating fluid flow and solute or energy transport in variable saturated porous media. U.S. Geological Survey Water-Resources Investigations Report 9-4130

Huang, H and Won, I.J., 2000 Conductivity and susceptibility mapping. using broadband electromagnetic sensors. Journal of Environmental and Engineering Geophysics 5(4): 31-41

Hubbard, S.S and Rubin, Y., 2000 Hydrogeological parameter estimation using geophysical data: a review of selected techniques. Journal of Hydrogeology 45: 3-34

HydroSOLVE Inc., 2000 AQTESOLV for Windows User's Guide. Reston, Virginia: HydroSOLVE

Isiorho, S.A., Beeching, F.M., Stewart P.M., Whitman R.L., 1996 Seepage measurements from Long Lake, Indiana Dunes National Lakeshore, environmental Geology 28(2): 99-105

Isiorho, S.A and Meyer J.H., 1999 The effects of bag type and meter size on seepage meter measurements. Ground Water 37:411-413

Israelson, O.W and Reeve, R.C, 1994. Canal lining experiments in the Delta Area, Utah. Utah Agricultural Experimental Station, Bulletin 313: 15-35

Johnson, C.D and White, E.A., 2007 Marine geophysical investigation of selected sites in Bridgeport harbor, Connecticut, 2006. U.S Geological Survey, Scientific Investigations Report 2007-5119

Kalbus, E., Reinstorf, F., Schirmer, M., 2006 Measuring methods for groundwater, surface water and their interactions: a review, Hydrology and Earth System Sciences Discussions 3: 1809-1850

Kearey, P., Brooks, M., Hill, I., 2002 An introduction to geophysical exploration. Blackwell Science Ltd ISBN 0-632-04929-4

Keery, J., Binley, A., Crook, N., Smith, J.W.N., 2007 Temporal and spatial variability of groundwater-surface water fluxes: Development and application of an analytical method using temperature time series. Journal of Hydrology 336: 1-16

Kelly, S.E and Murdoch, L.C., 2003 Measuring the hydraulic conductivity of shallow submerged sediments, Ground Water, 41(4): 431-439

Kindinger, J., 2002 Lake Belt study area-high resolution seismic refection survey, Miami-Dade County Florida. U.S. Geological Survey, Center of Coastal and Regional Marine Studies. Open-File Report 02-325

Kipp, K.L., Hsieh, P.A., Charlton, S.R., 2008 Guide to the revised ground-water flow and heat transport simulator: HYDROTHERM – Version 3. US Geological Survey, Techniques and Methods 6-A25

Kress, W.H., Dietsch, B.J., Steele, G.V., Cannia, J.C., 2004 Use of continuous seismic profiling to differentiate geologic deposits underlying selected canals in Central and Western Nebraska, U.S. Geological Survey, Fact Sheet 115-03

Krupa, S.L., Belanger, T.V., Heck, H.H., Brock J.T., Jones, B.J., 1998 Krupaseep – The next generation seepage meter. Journal of Coastal Research 25:210-213

Landon, M.K., Rus, D.L., Harvey, F.E., (2001) Comparison of in stream methods for measuring hydraulic conductivity in sand streambeds. Ground Water, 39(6): 870-885.

Lapham, W.W., 1989 Use of temperature profiles beneath streams to determine rates of vertical ground-water flow and vertical hydraulic conductivity. U.S. Geological Survey Water-Supply Paper 2337

Lee, D.R., 1977 A device for measuring seepage flux in lakes and estuaries. Limnology and Oceanography, 22: 140-147

Lee, D.R., Cherry, J.A., 1978 A field exercise on groundwater flow using seepage meters and mini-piezometers. Journal of Geological Education, 27: 6-9

Levy,J., Kilroy, K., Brick, M.D., Mutiti, S., Windler, B., Idris, O., Allen, L., 2007 Temporal variability of riverbed conductance at the Bolton well field along the Great Miami River, Southwest Ohio. Submitted to the City of Hamilton and the Hamilton to New Baltimore Groundwater Consortium

Lewelling, B.R., Tihansky, A.B., Kindinger, J.L. 1998 Assessment of the hydraulic connection between ground water and the Peace River West-Central Florida. USGS Florida

Libelo, E.L and MacIntyre, W.G., 1994 Effects of surface-water movement on seepage-meter measurements of flow through the sediment-water interface. Applied Hydrogeology 4: 49-54

Loke, M.H., 2000 Electrical imaging surveys for environmental and engineering studies. A practical guide to 2-D and 3-D surveys www.terraplus.com

Manheim, F.T., Krantz, D.E., Snyder, D.S., and Sturgis, B., 2002 Streamer resistivity surveys in Delmarva Coastal Bays. Proceedings Symposium on the Application of Geophysics to Environmental and Engineering Problems (SAGEEP) http://woodshole.er.usgs.gov/staffpages/fmanheim/delmarva.htm

MCD, 2004 Water Quality Assessment in the Lower Great Miami River Watershed. Miami Conservancy District (MCD), www.miamiconservancy.org

McGee, T.M., 1995 High-resolution marine reflection profiling for engineering and environmental purposes, Part A: Acquiring analogue seismic signals. Journal of Applied Geophysics 33, 271-285

Murdoch, L.C and Kelly, S.E., 2003 Factors affecting the performance of conventional seepage meters. Water Resources Research, 39(6), 10 pp

Niswonger, R.G., and Prudic, D.E., Appendix B; Modeling heat as a tracer to estimate streambed seepage and hydraulic conductivity, in Stonerstrom, D.A., Constantz, J (eds.) Heat as a tool for studying the movement of ground water near streams, U.S. Geological Survey Circular, C 1260, pp. 81-89

Niswonger R.C., Prudic, D.E., Pohll, G., Constantz, J., 2005 Incorporating seepage losses into the unsteady streamflow. Equations for simulating intermitted flow along mountain front streams. Water Resources research, 41, doi;10.1029/204WR003677

Paulsen, R.J., Smith, C.F., O'Rourke, D., and Wong, T.F., 2001 Development and evaluation of an ultrasonic ground water seepage meter. Ground Water, 39: 904-911

Placzek, G and Haeni, F.P., 1995 Surface geophysical techniques used to detect existing and infilled scour holes near bridge piers. U.S Geological Survey Water- Resources Investigations report 95-4009

Powers, C.J., Haeni, F.P., Smith, S., 1999 Integrated use of continuous seismic-refection profiling and ground penetrating radar methods at John's Pond, Cape Cod, Massachusetts. Symposium on the Application of Geophysics and Engineering and Environmental Problems, California, Proceedings: Wheat Ridge, Colo., Environmental and Engineering Geophysical Society, p: 359-368

Ronan A.D., Prudic D.E., Thodal C.E., Constantz J., 1998 Field study and simulation of diurnal temperature effects on infiltration and variably saturated flow beneath an ephemeral stream. Water Resources Research, 34, (9): 2137-2153

Rosenberry, D.O., 2005 Integrating seepage heterogeneity with the use of ganged seepage meters, U.S. Limnology and Oceanography: Methods 3: 131-142

Rosenberry, D.O., Menheer, M.A., 2006 A system for calibrating seepage meters used to measure flow between ground water and surface water. U.S. Geological Survey Scientific Investigations Report 2006-5053

Rus, D.L., MCGuire, V.L., Zurbuchen, B.R., Zlotnik, V.A., 2001 Vertical profiles of streambed hydraulic conductivity determined using slug tests in Central and Western Nebraska. U.S. Geological Survey, Water-Resources Investigations Report 01-4212

Ryan, R.J and Boufadel, M.C., 2006 Influence of streambed hydraulic conductivity on solute exchange with the hyporheic zone. Environmental Geology 51:203-210, DOI 10.1007/s00254-006-0319-9

Sambuelli, L., Leggieri, S., Calzoni, C., Porporato, C., 2007 Study of riverine deposits using electromagnetic methods at a low induction number, Geophysics 72(5): 113-120

Schälchli, U., 1992 The clogging of coarse gravel river beds by fine sediment. Hydrobiologia 235/236: 189-197

Schincariol, R.A and McNeil, J.D., 2002 Errors with small volume elastic seepage meter bags. Ground Water 40(6): 649-651

Schmidt, C., Bayer-Raich, M., Schirmer, M., 2006 Characterization of spatial heterogeneity of groundwater-stream water interactions using multiple depth streambed temperature measurements at the reach scale. Hydrol. Earth Syst Sci. Discuss., 3, 1419-1446

Schmidt, Ch., Conant Jr.B., Bayer-Raich, M., Schirmer, M., 2007 Evaluation and field-scale application of an analytical method to quantify groundwater discharge using mapped streambed temperatures. Journal of Hydrology 347: 292-30

Schubert, J., 2002. Hydraulic aspects of river bank filtration—field studies. Journal of Hydrology, 266: 145-161

Sebestyen, S.D and Schneider, R.L., 2001 Dynamic temporal patterns of nearshore seepage flux in a headwater Adirondack Lake. Journal of Hydrology 247:137-150

Shaw, R.D and Prepas, E.E., 1989 Anomalous, short- term influx of water into seepage meters. Limnology and Oceanography, 34 (7): 1343-1351

Sheets, R.A and Bossenbroek, K.E., 2005 Ground – water flow directions add estimation of aquifer hydraulic properties in the lower Great Miami River Buried Valley Aquifer System, Hamilton area, Ohio. US Geological Survey, Scientific Investigations Report 2005-5013

Sheets, R.A., and Dumouchelle D. H., 2008, Geophysical investigation along the Great Miami River, from New Miami to Charles M. Bolton Well Field,Cincinnati, Ohio, U.S. Geological Survey, Scientific Investigations Report,2008-XXXX, [in review

Shepherd, R.G., 1989. Correlations of permeability and grain size. Groundwater 27(5):663-638

Sholkovitz, E., Herbold, C., Charette, M., 2003 An automated dye-dilution based seepage meter for the time-series measurement of submarine groundwater discharge. Limnology and Oceanography: Methods: 16-28

Silliman, S.E., Ramirez J., McCabe R.L., 1995 Quantifying downflow through creek sediments using temperature time series: one—dimensional solution incorporating measured surface temperature. Journal of Hydrology 167: 99-119

Skinner, K.D., 2006 Estimating streambed seepage using heat as a tracer on the Lower Boise River, canyon County, Idaho. U.S. Geological Survey, Scientific Investigations Report 2005-5215

Spieker, A.M., 1968a, Ground- water hydrology and geology of the Lower Great Miami River Valley Ohio. Geological Survey Professional Paper 605-A

Spieker, A.M., 1968c, Effect of Increased pumping of groundwater in the Fairfield – New Baltimore Area, Ohio- A prediction by analog-model study. Geological Survey Professional Paper 605-C

Stallman, R. W., 1963 Computation of groundwater velocity from temperature data. Water Supply Paper U.S. Geological Survey No. 1544-H: 36–46

Stallman, R.W., 1965 Steady one-dimensional fluid flow in a semi-infinite porous medium with sinusoidal surface temperature. Journal of geophysical Research, 70, 2821-2827

Stieglitz, T.C., Rapaglia, J., Krupa, S.C., 2007 An effect of pier pilings on nearshore submarine groundwater discharge from a (partially) confined aquifer, Estuaries and Coasts 30(3):543-550

Stonerstrom, D.A and Constantz, J. 2003 Heat as a tool for studying the movement of ground water near streams: US Geological Survey Office of Ground Water and Water Resources. Circular 1260, 96 pp

Su, G.W., Jaspere, J., Seymour, D., Constantz, J., 2004 Estimation of hydraulic conductivity in an alluvial system using temperature. Ground Water 42(6): 890-901

Snyder, D.D., 1997 Application of continuous resistivity profiling to aquifer characterization. Zone Engineering and Research Organization www.zonge.com/PDF_Papers/IP_MarineAquifer.pdf

Snyder, D.D., MacInnes, S.C., Raymond, M.J., and Zonge, K.L., 2002 Continuous resistivity profiling in shallow marine and fresh water environments: Symposium on the Application of Geophysics to Engineering and Environmental Problems (SAGEEP), 13GSL4

Snyder, D.D and Wightman E., 2002 Application of continuous resistivity profiling to aquifer characterization: Symposium on Application of Geophysics to environmental and Engineering Problems (SAGEEP), 13GSL10

Sweat, M.J., 2000 Continuous seismic reflection profiling near Grassy Island, Wyandotte Unit of Shiawassee National Wildlife Refuge Wyandotte, Michigan. U.S. Geological Survey Administrative Completion Report for WRD

Taniguchi, M and Fukuo, Y., 1993 Continuous measurements of ground-water seepage using an automatic seepage meter. Ground Water, 31: 675-679

Taniguchi, M., Burnett, W.C., Smith, Ch.F., Paulsen, R.J., O'Rourke, D., Krupa, S.L., Christoff, J.L., 2003 Spatial and temporal distributions of submarine groundwater discharge rates obtained from various types of seepage meters at site in the Northeastern Gulf of Mexico. Biogeochemistry 66: 35–53

Terzaghi, K and Peck, R. B. 1964 Soil mechanics in engineering practice. Wiley, New York

United States Environmental Protection Agency (USEPA), 1993 Use of airborne, surface and borehole geophysical techniques at contaminated Sites. A Reference Guide- EPAI625/R-92/007

Velickovic, B., 2005 Colmation as one of the processes in interaction between the groundwater and surface water. Facta Universitatis, Architecture and Civil Engineering 3(2): 165-172

Voss C.I., 1984 SUTRA: a finite element simulation model for saturated-unsaturated, fluid-density dependent ground-water flow with energy transport or chemically reactive single species solute transport. US Geological Survey, Report 84-4369

Watkins, J.S and Spieker, A.M., 1971 Seismic refraction survey of Pleistocene drainage channels in the Lower Great Miami River Valley, Ohio. Geological Survey Professional Paper 605-B

Winter, T.C., Harvey, J.W., Franke, O.L., Alley, W.M., 1998 Ground water and surface water, a single resource. U.S. Geological Survey Circular 1139

Woessner, W.W., 2000 Stream and fluvial plain ground water interactions: rescaling hydrogeologic thought. Ground Water 38(3): 423-429

Won, I.J., Keiswetter, D.A., Fields, G.R.A., Sutton, L.C., 1996 GEM-2: A new multi-frequency electromagnetic sensor. Journal of Environmental and Engeenering Geophysics, 1(2): 129-137

Zohdy, A.A.R., Eaton. G.P., Mabey, D.R., 1974 Application of geophysics to ground-water investigations. U.S Geological Survey Techniques for Water –Resources Investigations

APPENDIX 1. Grain size distribution curves and the hydraulic conductivity for sediments from the core samples obtained while installing monitoring wells

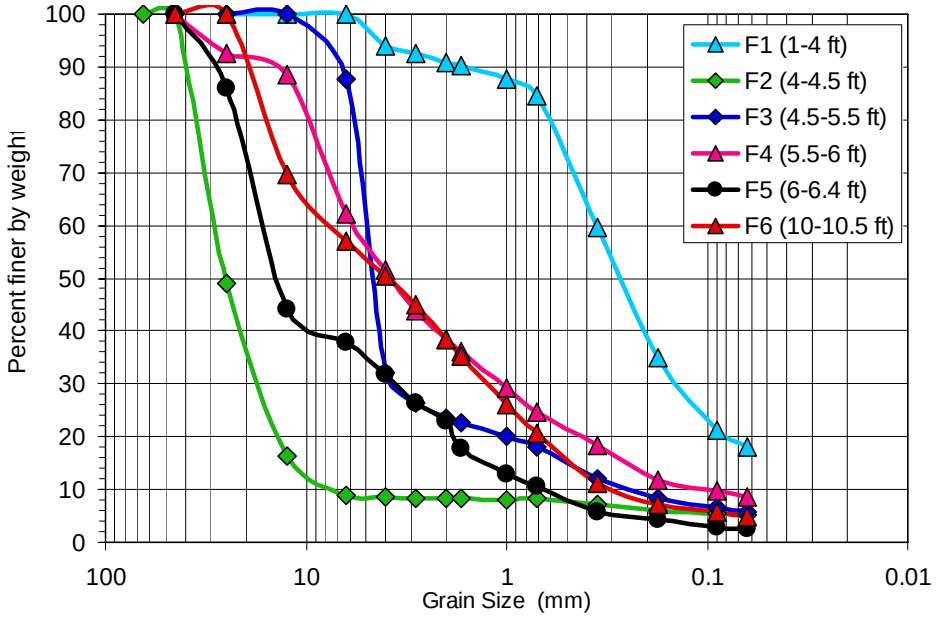

Figure A1. Grain size distribution curves for sediments from F-W1 (total depth 37.22 ft) at the Fairfield site

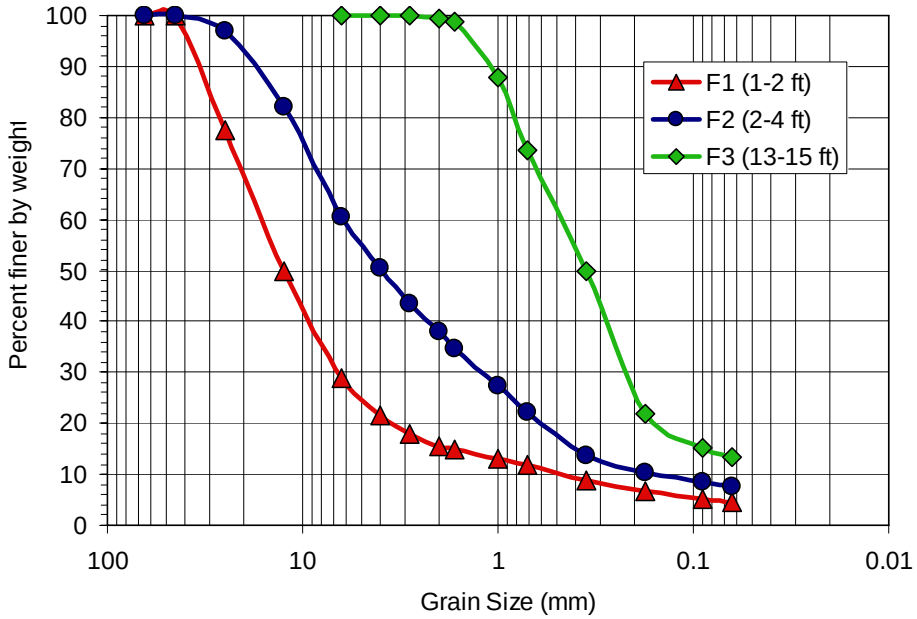

Figure A2. Grain size distribution curves for sediments from F-W2 (total depth 14.5 ft) at the Fairfield site

Table A1. Sediment sorting and hydraulic conductivity estimation from Hazen equation for sediments from Wells 1 and 2 (W1 and W2) at Fairfield site

Sample and depth (ft)	***d_{50}[a] (mm)***	***% Silt + Clay***	***C_u[b]***	***Classification[c]***	***K[d] (ft/d)***
F W1-1 (1-4 ft)	0.25	18	---	Fine to medium sand	----
F W1-2 (4-4.5 ft)	24	5.2	3.6	Well-sorted coarse pebbles	2200
F W1-3 (4.5-5.5 ft)	4.7	5.8	2.13	Well-sorted fine pebbles	2.7
F W1-4 (5.5-6 ft)	3.9	8.7	60.0	Poorly sorted very fine pebbles	0.34
F W1-5 (6-6.4 ft)	13	2.7	24.6	Poorly-sorted medium pebbles	16.2
F W1-6 (10-10.5 ft)	3.9	4.9	26	Poorly sorted very fine pebbles	3.1
F W2-1 (1-2 ft)	11.7	4.6	36	Poorly-sorted medium pebbles	----
F W2-2 (2-4 ft)	4.0	7.6	33.9	Poorly-sorted medium pebbles	2200
F W2-3 (13- 15 ft)	0.35	13	NA[e]	Medium sand	2.7

[a]d_{50} is the median grain size

[b]C_u is the uniformity coefficient

[c]Classification is based on the scales given by Fetter (2001)

[d]K is estimated from the grain size results using the Hazen method

[e]Not calculated due to lack of information distribution of sizes < 0.063 mm,

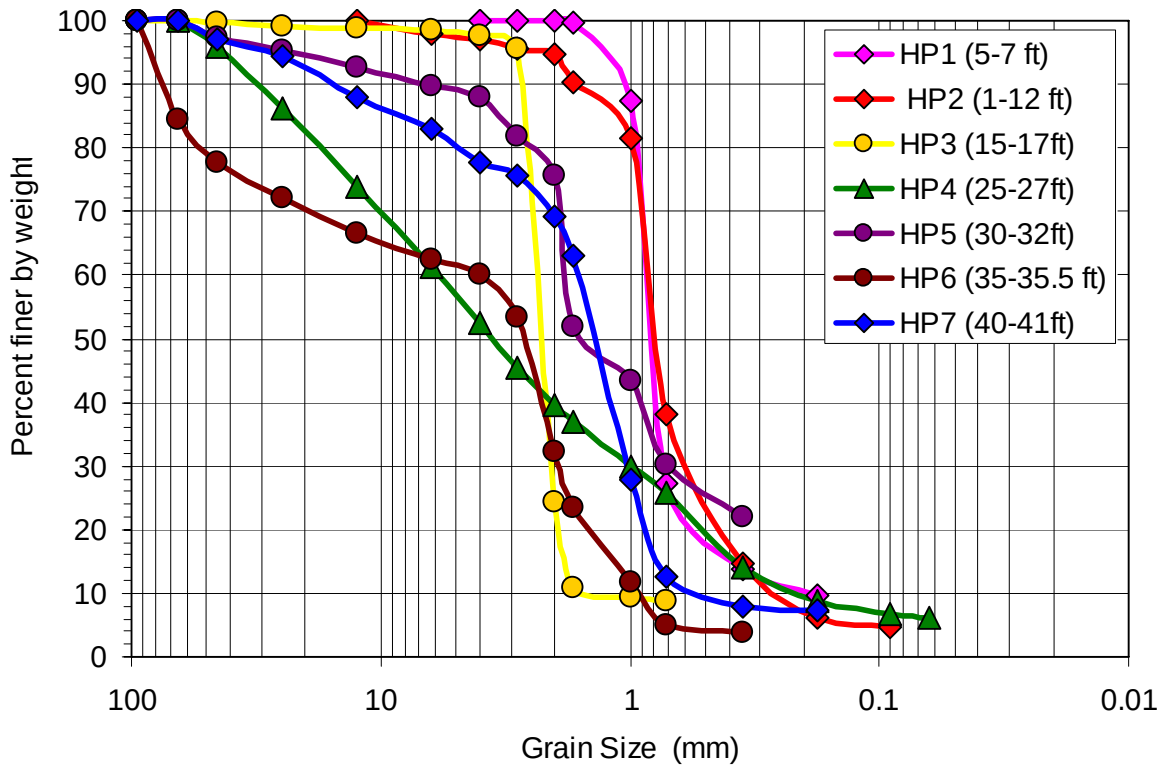

FigureA3. Grain size distribution curves for sediments from Well 1 (total depth 41.93 ft) at the Heritage Park site

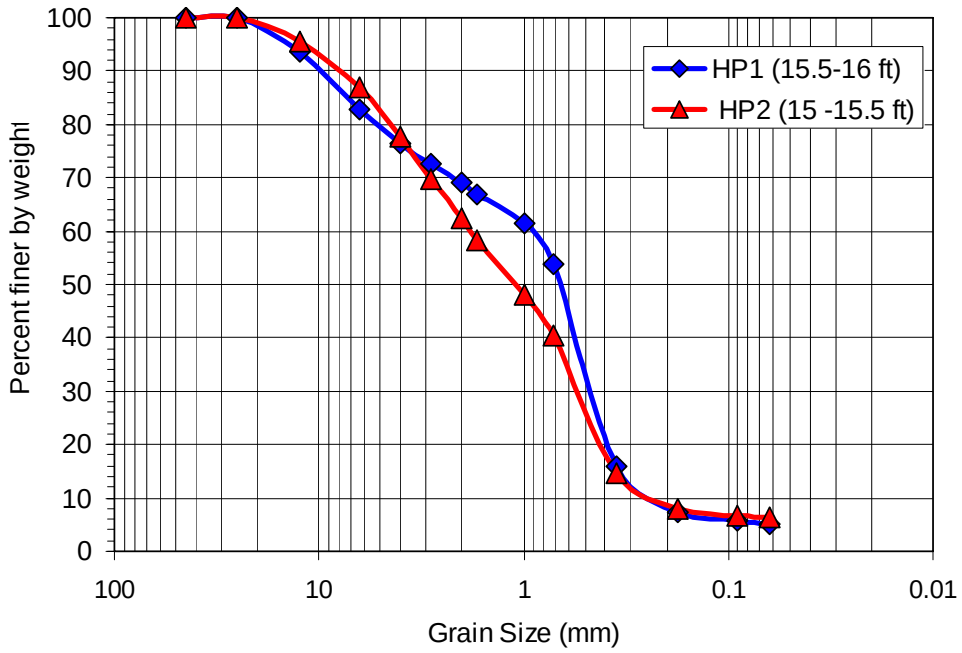

Figure A4. Grain size distribution curves for sediments from well 2 (total depth 16.11 ft) at the Heritage Park site

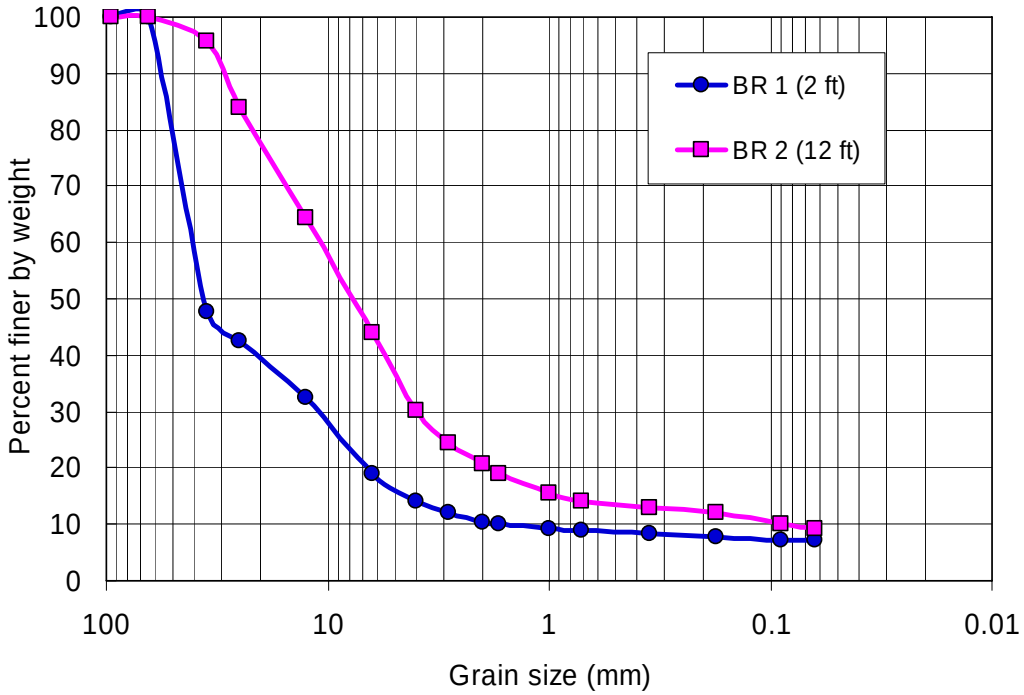

Figure A5. Grain size distribution curves for sediments from Well 1 (total depth 30 ft) at the Boat Ramp site

Table A2. Sediment sorting and hydraulic conductivity estimation from Hazen equation for sediments from wells 1 and 2 (W1 and W2) at Heritage Park site

Sample and depth (ft)	***d_{50}[a] (mm)***	***% Silt + Clay***	***C_u[b]***	***Classification[c]***	***K[d] (ft/d)***
HP W1-1 (5-7ft)	0.81	9.7	0.4	Well-sorted coarse sand	90.69
HP W1-2 (1-12 ft)	0.42	4.6	4.2	Well-sorted medium sand	0.33
HP W1-3 (15-17 ft)	0.48	8.8	3.1	Well-sorted medium sand	0.58
HP W1-4 (25- 27 ft)	3.8	6.0	28.6	Poorly sorted very fine pebbles	1.5
HP W1-5 (30-32 ft)	0.15	21	NA[e]	Fine sand	NA
HP W1-6 (35-35.5ft)	2.8	3.9	4.4	Well-sorted very fine pebbles	18.36
HP W1-7 (40-41 ft)	1.3	7.3	3	Well-sorted very coarse sand	6.37
HP W2-1 (15 -15.5 ft)	0.57	5.2	3.3	Well-sorted coarse sand	1.59
HP W2-2 (15.5 -16 ft)	1.05	6.4	7.17	Poorly-sorted very coarse sand	1.59

[a]d_{50} is the median grain size

[b]C_u is the uniformity coefficient

[c]Classification is based on the scales given by Fetter (2001)

[d]K is estimated from the grain size results using the Hazen method

[e]Not calculated due to lack of information distribution of sizes < 0.063 mm

Table A3. Sediment sorting and hydraulic conductivity estimation from Hazen equation for sediments from well 1 at Boat Ramp site

Sample and depth (ft)	***d_{50}[a] (mm)***	***% Silt + Clay***	***C_u[b]***	***Classification[c]***	***K[d] (ft/d)***
BR 1 (2 ft)	0.7	7.1	7.9	Poorly-sorted coarse sand	16.6
BR 2 (12 ft)	1.3	9.3	38	Poorly-sorted very coarse sand	57.5

[a]d_{50} is the median grain size

[b]C_u is the uniformity coefficient

[c]Classification is based on the scales given by Fetter (2001)

[d]K is estimated from the grainsize results using the Hazen method

APPENDIX 2. Water levels in the monitoring wells and river stage for each study site

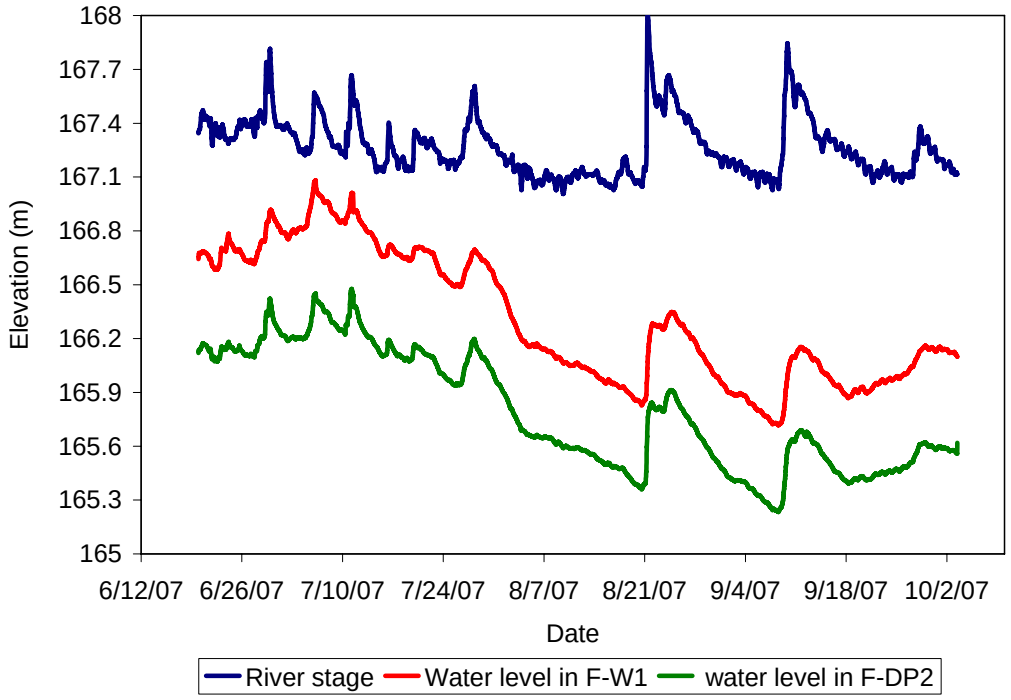

Figure B1: Water levels and river stage at the Fairfield site

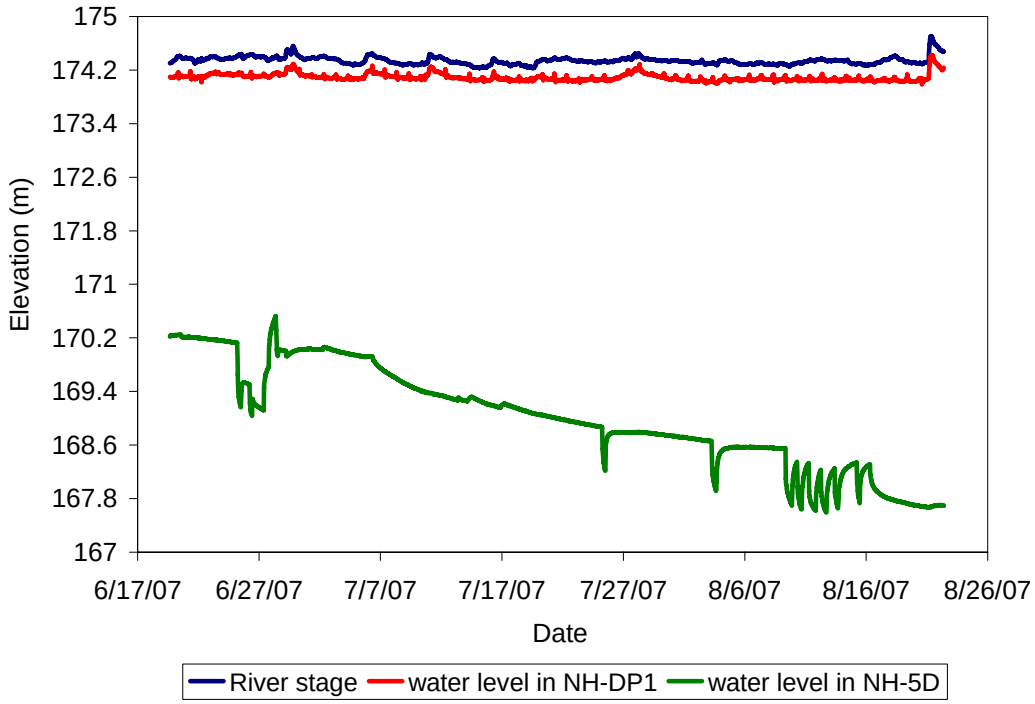

Figure B2: Water levels and river stage at the North Hamilton site

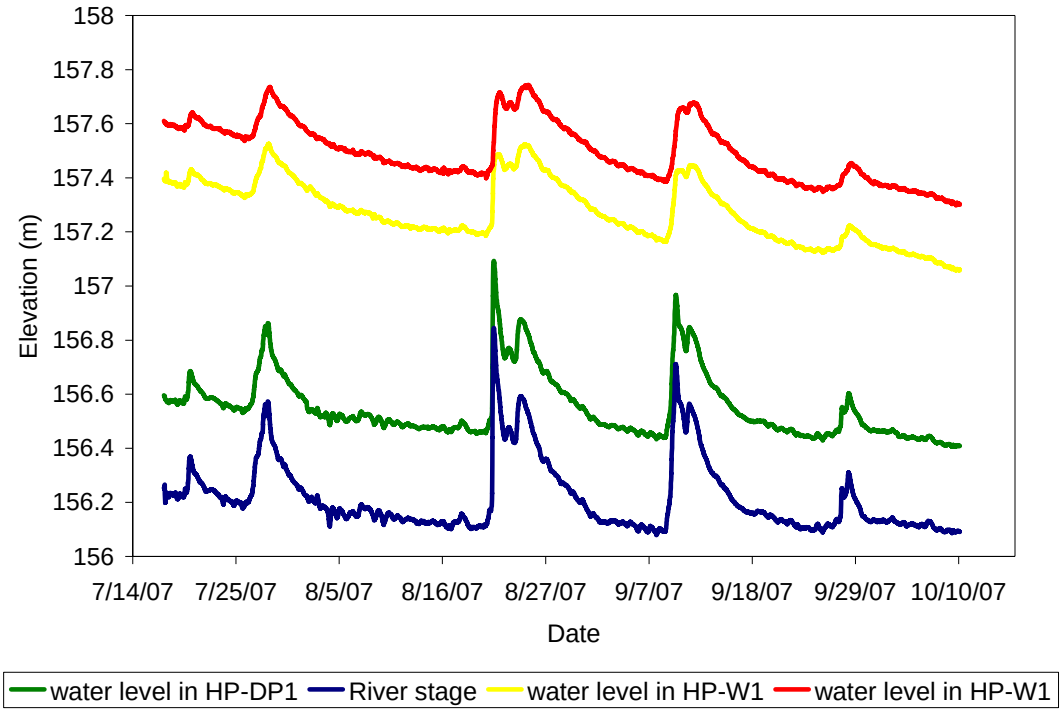

Figure B3. Water levels and river stage at the Heritage Park site

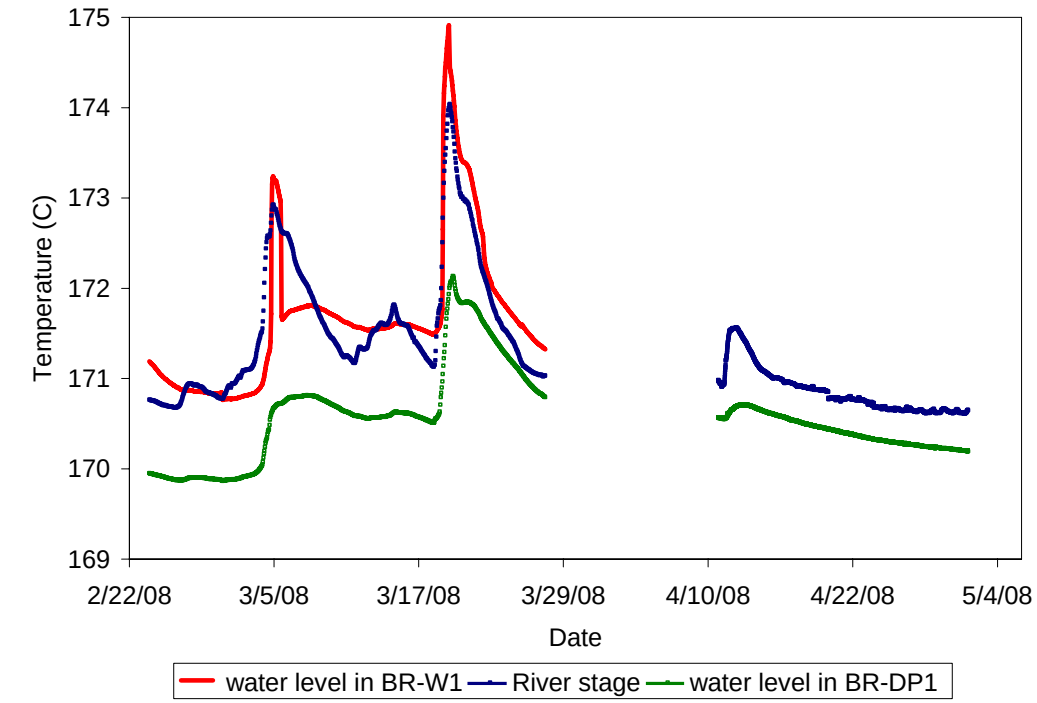

Figure B4: Water levels and river stage at the Boat Ramp site